Terms and Conditions of Use of Digitised Theses from Trinity College Library Dublin

Copyright statement

All material supplied by Trinity College Library is protected by copyright (under the Copyright and Related Rights Act, 2000 as amended) and other relevant Intellectual Property Rights. By accessing and using a Digitised Thesis from Trinity College Library you acknowledge that all Intellectual Property Rights in any Works supplied are the sole and exclusive property of the copyright and/or other IPR holder. Specific copyright holders may not be explicitly identified. Use of materials from other sources within a thesis should not be construed as a claim over them.

A non-exclusive, non-transferable licence is hereby granted to those using or reproducing, in whole or in part, the material for valid purposes, providing the copyright owners are acknowledged using the normal conventions. Where specific permission to use material is required, this is identified and such permission must be sought from the copyright holder or agency cited.

Liability statement

By using a Digitised Thesis, I accept that Trinity College Dublin bears no legal responsibility for the accuracy, legality or comprehensiveness of materials contained within the thesis, and that Trinity College Dublin accepts no liability for indirect, consequential, or incidental, damages or losses arising from use of the thesis for whatever reason. Information located in a thesis may be subject to specific use constraints, details of which may not be explicitly described. It is the responsibility of potential and actual users to be aware of such constraints and to abide by them. By making use of material from a digitised thesis, you accept these copyright and disclaimer provisions. Where it is brought to the attention of Trinity College Library that there may be a breach of copyright or other restraint, it is the policy to withdraw or take down access to a thesis while the issue is being resolved.

Access Agreement

By using a Digitised Thesis from Trinity College Library you are bound by the following Terms & Conditions. Please read them carefully.

I have read and I understand the following statement: All material supplied via a Digitised Thesis from Trinity College Library is protected by copyright and other intellectual property rights, and duplication or sale of all or part of any of a thesis is not permitted, except that material may be duplicated by you for your research use or for educational purposes in electronic or print form providing the copyright owners are acknowledged using the normal conventions. You must obtain permission for any other use. Electronic or print copies may not be offered, whether for sale or otherwise to anyone. This copy has been supplied on the understanding that it is copyright material and that no quotation from the thesis may be published without proper acknowledgement.

A Formulation of Discrete Differential Geometry Applied to Fermionic Lattice Field Theory and its Implications for Chiral Symmetry

Steven Watterson
MPhys (Hons) AMInstP

A Thesis submitted to
The University of Dublin
for the degree of

Doctor of Philosophy

Department of Mathematics
University of Dublin
Trinity College

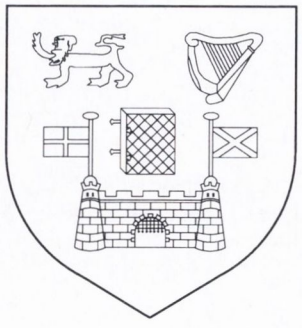

April, 2007

Declaration

This thesis has not been submitted as an exercise for a degree at any other University. Except where otherwise stated, the work described herein has been carried out by the author alone. This thesis may be borrowed or copied upon request with the permission of the Librarian, University of Dublin, Trinity College. The copyright belongs jointly to the University of Dublin and Steven Watterson.

Signature of Author .....

Steven Watterson
3rd April, 2007

Summary

In this thesis, we develop the Geometric Discretization formulation of Dirac-Kähler fermions.

We note that the naive definition of chiral symmetry is only approximately captured in the formulation. However, we show that we can use the two complexes associated with the definition of the Hodge star to construct chiral projection operators that exactly project a different chirality of field on to each complex. Similarly, we construct flavour projection operators that project a different flavour of field on to each complex. We also see that, in two space-time dimensions, we need four complexes to simultaneously separate the chiral and flavour components of the field.

We subsequently develop projection operators for four dimensional space-time. The flavour projection requires us to introduce a new operator by analogy to the Hodge star, that takes the complement of a form or cochain in the $\{1, 2\}$ subspace, but not the $\{3, 4\}$ subspace. Correspondingly, we define new complexes that complement the original complex in just one of the $\{1, 2\}$ or $\{3, 4\}$ subspaces. Using this operator and the Hodge star, we define flavour projection operators for the Dirac-Kähler fields. We find that to isolate both the chiral and flavour components of the fields simultaneously requires eight complexes in four space-time dimensions.

We also define an Abelian gauge theory for the Geometric Discretization and adapt the Hybrid Monte Carlo algorithm to it, using the algorithm to calculate the static potential between fermions. We find that the calculation is in agreement with analytical results. We additionally study topological gauge fields and show how their effects differ between the Geometric Discretization and standard lattice QED.

Acknowledgements

The list of all those to whom I am indebted for their help and support is a long and worthy collection of names. Without the help of each and every soul, I would never have reached the position from which I write this acknowledgement.

My Mother and Father's unwaivering support and faith in my abilities has been a constant source of comfort and reassurance and I hope they appreciate my gratitude. Elaine has shown the patience of a Saint and strength of Atlas and for her eternal smile I am grateful. To the men, women and children of DU Rifle Club thank you for the whiskey, Dutch Gold and occasional bit of sport. To John Butler: thank you for softening my landing in Irish society so well. To Eabhnat Ni Fhloinn and the cast and crew of G29 I am unspeakably grateful for the camaraderie and support. My fellow post-grads Francesca, Alan, Justin and Ritchie are also on my Christmas card list, having had to put up with my ignorant lattice questions over the past years, as are Don and Donie for sharing their wit and wisdom. Karen and Deborah deserve special praise for keeping the department afloat.

I would also like to thank Richard Timoney together with the members of the TrinLat group for being so friendly, approachable, helpful and supportive. In particular, I would like to thank Mike Peardon and Fermin Viniegra for sacrificing their time to work with me. I only hope that I prove worthy.

I owe a further debt of gratitude to Prof Peter Ghazal and the Division of Pathway Medicine at the University of Edinburgh, who have opened up a new world of possibilities.

This list barely scratches the surface of all those who have made a personal contribution to my progress. My deepest gratitude is extended to all of them.

Thanks also to Queens University for allowing me some time on their cluster [80] to support the work done on Trinity's HPC cluster.

Contents

List of Figures

1 Introduction and Motivation

Science is symbiotic. In every discipline, there are theoretical and experimental strands living side-by-side, each helping the other to progress.

In some disciplines, the dialogue between the strands can be qualitative, but in particle physics the phenomena of interest are impossible to observe directly. Instead, the dialogue must take the form of quantitative comparisons. Theoreticians calculate values from the theories. Experimentalists measure values from the experiments. If the comparison agrees, the theory is verified; if not, the theory is shown to be flawed and further study is needed.

The dialogue can be beneficial to both strands. A theory with a history of successful predictions can direct experimentalists towards more fruitful experimental set-ups. An experimental measurement can reduce the number of options available in the construction of a theory, when multiple possibilities present themselves.

The established theory for describing the quantum mechanical behaviour of particles is *Quantum Field Theory* and there are many ways of using it to calculate verifiable quantities. Which way we choose is determined by the quantity in question.

When we are studying the interaction between quarks, a successful approach is to pixellate space and time by replacing the four continuous dimensions with a four dimensional lattice of points. In most formulations, the fields that represent particles and their gauge fields are sampled at the points and the motion of the field is represented by a ripple across the lattice.

Unfortunately, the act of sampling the fields at the points of the lattice introduces problems. Fields that would have measurably different momenta in the continuum can have the same momenta when it is calculated from the sampled points. This problem is known as *fermion doubling* and it is so profound that an entire research field has grown up around it.

Resolving the problem is particularly difficult because removing the degeneracy between fields invariably breaks some of the symmetry of the equations. The symmetry is known as *chiral* symmetry and it is important for many reasons, including

the role it plays in the creation of pions.

Several schemes have been proposed that remove the degeneracy to varying degrees and each has a different consequence for the chiral symmetry. The Ginsparg-Wilson formulation [1], which encompasses the domain wall and overlap formulations, is the most successful scheme to date, but it is very computationally costly. It introduces many more fields which must be included in the calculations, making them considerably more time consuming.

One scheme achieves a trade off between removing the degeneracy and maintaining chiral symmetry. In four space-time dimensions, the *staggered* fermion formulation [2][3][4] reduces the sixteen degenerate fields to four and maintains a limited form of chiral symmetry.

This scheme is related to a continuum description of fermionic field theory that uses a basis of differential forms on a manifold, instead of vectors and that replaces matrix operators with the operators of differential geometry. The description is known as the Dirac-Kähler formulation and it has proven difficult to recreate on a complex. The difficulty comes with uniquely and locally defining certain operators so that they obey the algebra of differential geometry. In particular, it is difficult to define the Hodge star so that its square is proportional to the identity and to define the wedge product so that it is local and obeys Leibniz's rule.

One proposal that addresses these problems is that of David Adams [5][6]. He resolves the former problem by introducing a second complex, in parallel with the first, known as the *dual*, and by defining the Hodge star to be a 1-to-1 mapping between the two complexes. He resolves the latter problem by introducing a wedge product that is defined by applying the continuum wedge product to an interpolated space.

It has been shown by Rabin [7] that the Hodge star is related to the chiral symmetry of the theory, so it is natural to ask whether the doubling in the number of fields that is brought about by introducing the dual is related to the degeneracy of the fields.

The application of this scheme to the Dirac-Kähler formulation has been studied

before, in the PhD theses of Vivian de Beaucé [8] and Samik Sen [9]. However, both concentrated on the technical aspects of the formulation. Between them, they define the scheme and the operators for cubic lattices and tentatively study the gauge fields.

In this thesis, we will build on their work. We start by studying the theory as it stands and by looking into the technical details of how it addresses fermion doubling and how it closely it approximates the continuum theory.

Next, we consider the role of the dual and we show how it can be used to achieve exact chiral symmetry as well as how we can use it to isolate the degenerate fields from the theory. We start this work in two dimensional space-time. However, we also extend it to four space-time dimensions. In this case, we are required to introduce two more complexes, one of which is the dual in two of the four dimensions and the other is effectively the dual in the remaining two dimensions. We will see how we can use these complexes to isolate the four degenerate fields and separate the chiral components of each.

We will also explicitly construct an Abelian gauge theory for the formulation, as it is introduced. The description will be non-compact, requiring us to introduce gauge fixing terms for the action. We shall study this in some detail, including for topologically interesting field configurations.

With the Abelian gauge theory constructed, we describe how we use it to perform calculations. The basic algorithm that we use is the Hybrid Monte Carlo (*HMC*) algorithm [10] which is used widely in conventional lattice QCD calculations. We describe the discrete Dirac-Kähler scheme in a way that is suitable for lattice calculations and we show how the HMC algorithm is implemented for our scheme.

Finally, we will use the algorithm to calculate a selection of properties for the Abelian gauge field. In particular, we will study the topological charge and the static fermion potential of the gauge field, using Wilson loops [11].

Some of this work has appeared in the conference proceeding [12].

2 Thesis Structure

Before we enter into the study of a fermionic field theory using discrete differential geometry, we first must familiarize ourselves with the two ingredients. A background chapter is devoted to each subject. In the middle of the chapter on differential geometry the reader will find a small section of original work that modifies the definition of one of the operators used in one of the seminal papers in the area. Appendix A is also dedicated to this result.

We must also devote some time to getting up to speed with the work that has been done by my predecessors on this formulation of discrete differential geometry. A third background chapter is devoted to this.

With the background behind us, we will plunge into the original work proper. Chapter 6 contains three sections. The first contains observations on the discrete differential geometry formulation as it stands. Here, we will look at how it addresses the problem of fermion doubling. We will also see that some of the correspondences between the Dirac and Dirac-Kähler formulations that exist in the continuum, are only approximately recreated on the complex. We will see that this has implications for chiral symmetry. The second section introduces a formulation that takes advantage of the dual complex to produce an exact chiral symmetry that we can use to isolate the chiral components of the fermion fields. In 1+1 space-time dimensions, we shall see that this needs only a little modification to enable us to separate the flavour components, instead of the chiral components. To isolate both, simultaneously requires us to introduce two more complexes. We proceed to study this scheme in 3+1 space-time dimensions, for which some of the mathematical detail is relegated to Appendix B. This case follows a similar pattern to the 1+1 case, with the exception that we must introduce two more complexes just to isolate the flavour components of the fields. To isolate the chiral and flavour components, simultaneously requires eight complexes. The third section introduces an Abelian field theory for the discrete differential geometry and constructs all the terms that are necessary to complete calculations.

This leads us to Chapter 7, in which we construct a computing framework that

allows us to carry out calculations using the Abelian gauge theory described. The data types and algorithms are explained here along with the design considerations.

In Chapter 8, we review the Schwinger model, describing its formulation and some of the relevant results that can be obtained from it analytically. In particular, we review the analytical results that describe the static fermion potential in order to use this as a benchmark for the results of our calculations.

In the next chapter, we present the results of calculations obtained using the framework described in Chapter 7. We study the topological charge of the ensemble of gauge configurations that we generated and we plot the static potential between charges, attributable to the Abelian field. Here, we also mention the chiral condensate and some of the difficulties that this formulation faces in trying to calculate it.

Chapter 10 is the penultimate chapter and in it we discuss the possible future directions for the work.

In the final chapter, we bring together the conclusions from our work and assess the merit of our discrete Dirac-Kähler formulation.

Appendix A contains a modification to the wedge product defined by Becher and Joos. These details provide support for Section 4.3.2.

Appendix B contains the details of the correspondence between the Hodge star operator and γ_5, the generator of chiral symmetry in 3+1 space-time dimensions. This is the link that allows us to isolate the chiral components of the fermion fields on each complex. It also contributes to the understanding of how we can isolate the flavour components. To complete this understanding, we also need the details of the correspondences between the operators and complexes that complement forms in the $\{1, 2\}$ subspace, but not the $\{3, 4\}$ subspace. This is also contained in this appendix. This appendix supports Sections 6.2.4 and 6.2.5.

3 Background: Fermionic Lattice Field Theory

3.1 Fermionic Field Theory

Fermion behaviour is governed by the Dirac equation and its exact form depends on the space in which we work. We shall develop the theory with one space and one time dimension because this space is computationally simpler than and is a close analogue of 3+1 dimensional space-time. In this space, the Dirac equation uses the Pauli σ matrices, σ_1 and σ_2 to implement the anticommuting Clifford algebra.

After a Wick rotation, the space and time dimensions become two Euclidean space-time dimensions. This gives us an action that is wholly real allowing us to consider the path integral as a probability distribution, weighting the possible routes through the system that the quantum fields may take. In Minkowski space, the action is complex, so instead of a probability, each route has a phase associated with it; the route that incurs the least phase corresponding to the classical solution to the system. In Euclidean space, the classical solution corresponds to the route that maximizes the probability weight.

The 2D Euclidean Dirac equation is written as

$$[\sigma^\mu \partial^\mu + m]\,\psi = 0$$

where we have used the Einstein summation convention that repeated indices are summed over the number of dimensions of the space-time. The Pauli matrices are

$$\sigma_1 = \begin{pmatrix} 0 & 1 \\ 1 & 0 \end{pmatrix} \qquad \sigma_2 = \begin{pmatrix} 0 & -i \\ i & 0 \end{pmatrix} \qquad \sigma_3 = \begin{pmatrix} 1 & 0 \\ 0 & -1 \end{pmatrix}$$

In the next section, we will see what happens when we try to recreate this description on the lattice.

3.2 The Fermion Doubling Problem

The lattice formulation of field theory was first laid down by Ken Wilson, in 1974 [18]. We will only concern ourselves here with the bits needed to understand the problem of fermion doubling.

On the Euclidean lattice, continuous fields are replaced with discrete fields. $\psi(x)$, a field that has a value everywhere in space-time is replaced with ψ_j that only has values at the lattice points, j. In two dimensions, we can visualise ψ_j as a 2d histogram.

The derivative is replaced with a finite difference operator. There are several different choices for a difference operator. We could use any of the three following definitions for the derivative at site i,

$$\partial_\mu \psi_j = \begin{cases} \frac{1}{a}\left[\psi_{j+\hat{\mu}} - \psi_j\right] \\ \frac{1}{a}\left[\psi_j - \psi_{j-\hat{\mu}}\right] \\ \frac{1}{2a}\left[\psi_{j+\hat{\mu}} - \psi_{j-\hat{\mu}}\right] \end{cases}$$

However, the third definition has two advantages over the other candidates. It approximates the continuum derivative more accurately and has symmetry properties under spatial inversion. This is the conventional choice.

The fermion doubling problem arises because of this choice, but to see it, we must step into Fourier space and look at the definition from there. But before we do so, we shall look at the continuum Dirac equation in momentum space, so that we have a benchmark.

We write $\psi(x)$ in momentum space as $\psi(x) = \frac{1}{2\pi}\int dp^2 \tilde{\psi}(p) e^{-i\vec{p}\cdot\vec{x}}$. The Dirac equation has the following effect.

$$[\sigma_\mu \partial_\mu + m]\frac{1}{2\pi}\int dp^2 \tilde{\psi}(p) e^{-i\vec{p}\cdot\vec{x}} = \frac{1}{2\pi}\int dp^2 e^{-i\vec{p}\cdot\vec{x}}\left[-ip_\mu \sigma_\mu \tilde{\psi}(p) + m\tilde{\psi}(p)\right] = 0$$

If we specialise to the case where $m = 0$ and we take $\tilde{\psi}(p)$ to be a solution, we can see that $\tilde{\psi}(p)$ can only be nonzero when $p_\mu = 0$, because the σ_μ are linearly independent.

Now we will look at the lattice case and see how it compares. We write the field ψ_j as $\frac{1}{N}\sum_p \tilde{\psi}_p e^{-ia\vec{p}\cdot\vec{j}}$, where we have used the discrete Fourier transform and j is a dimensionless number labelling the lattice site. N is the extent of the square lattice. We write ∂_μ as $\frac{1}{2a}\left(T_\mu - T_{-\mu}\right)$, where T_μ is a translation operator that has the following effect: $T_\mu \psi_j = \psi_{j+\hat{\mu}}$. The lattice Dirac equation reads

$$\frac{1}{N}\left[\sigma_\mu \frac{T_\mu - T_{-\mu}}{2a} + m\right]\sum_p \tilde{\psi}_p e^{-ia\vec{p}\cdot\vec{j}} = \frac{1}{N}\sum_p e^{-ia\vec{p}\cdot\vec{j}}\left[-i\frac{\sin(p_\mu a)}{a}\sigma_\mu \tilde{\psi}_p + m\tilde{\psi}_p\right] = 0$$

This presents us with a problem. If we think about just one coordinate of p, then, when $m = 0$, the equation has two solutions: one at $p = 0$ and one at $p = \frac{\pi}{a}$. We know from the continuum expression that only the first solution is physical, but the second solution is as real as the first as far as the lattice Dirac equation is concerned.

The consequence of this phantom solution is seen in the Green's function that represents a fermion's propagation. For every dimension of space-time there are now two virtual fermions that can be exchanged, instead of one. In two dimensions, we have $2^2 = 4$ types of fermion.

The confusion arises because the definition for ∂_μ is unable to distinguish between the following two waves.

Figure 1: A 1d lattice at $p = 0$.

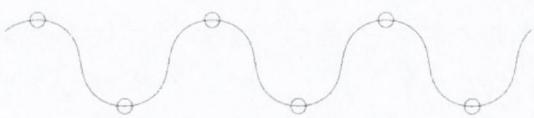

Figure 2: A 1d lattice at $p = \frac{\pi}{a}$.

∂_μ uses only every second lattice site, so both of the waves in Figures 1 and 2 appear flat.

This is the problem of *fermion doubling*, so named because the number of fermions has doubled in each dimension.

3.3 The Fermion Doubling Story

The problem of fermion doubling was recognized by Ken Wilson when he put forward the idea of a lattice field theory [18]. He also proposed a solution that, whilst effective, had the unfortunate side-effect of robbing the theory of chiral symmetry. Subsequently, others have proposed formulations that remove some of the phantom solution (known as *doublers*) and that impede the chiral symmetry, all to differing degrees.

After Wilson's suggestion, Kogut and Susskind proposed an idea that reduced the number of doublers (in four dimensions) to four and retained some degree of chiral symmetry [2][3][4]. About five years later, Nielsen and Ninomiya nailed down the relationship between the doublers and chirality in a theorem that showed that

doublers were necessary to maintain chiral symmetry on the lattice [24][25]. It took another ten years for anyone to make any significant ground, but it happened when David Kaplan added an extra spatial dimension to the lattice. In doing so he was able to remove all but one doubler, isolating the remaining doubler at the far end of the extra dimension [28]. This left the a single solution on a 4d space-time slice at the near end of the extra dimension. Kaplan took the idea from a paper by Callan and Harvey, published seven years before [29], who had done the same thing in the continuum, but were unaware of the implications for the lattice. Shortly after, another proposal came to light that had been worked on more or less at the same time. Neuberger and Narayanan introduced an infinite set of regulator fields to cancel the doublers [46][47][48][49][50]. This 'tower'of extra fields has since been shown to be equivalent to Kaplan's description, where the extra dimension is taken to be infinite.

Before we proceed, it is worth taking a moment to appreciate why it is that so many have dedicated themselves to preserving chiral symmetry. What does chiral symmetry give us that inspires such loyalty?

There are many answers. When continuum theories are renormalized they can in principle incur both additive and multiplicative changes to particle masses. However, when the theory has chiral symmetry, the particle mass must stay zero throughout, meaning that it can only incur multiplicative changes. To facilitate accurate renormalization on the lattice, the lattice description must respect chiral symmetry, too [20]. Chiral symmetry also provides the theoretical basis for the formulation of pions. When the theory respects chiral symmetry, but the vacuum state does not, the theory is said to have *spontaneous* symmetry breaking. The number of pions existing in the theory then corresponds to the number of independent symmetries that have been broken [21]. Other reasons are given in [23].

Many comprehensive texts and review articles exist on the subject of fermion doubling, (eg [19] [22] [23]). I shall précis the most relevant developments in the following sections.

3.3.1 Wilson Fermions

Wilson's solution to the problem of doublers was ingenious. He reasoned that we could add any non-divergent term to the lattice action as long as it was multiplied by a because this meant that it would go to zero in the continuum limit [18]. The term he chose to add was the lattice equivalent of the second derivative because, in Fourier space, it corresponds to $(1 - \cos(p_\mu a))$. This term breaks the degeneracy between $p = 0$ and $p = \frac{\pi}{a}$.

The drawback to this approach is that the extra term acts like a mass term, in the sense that it contributes a term bilinear in the fermionic fields that does not include a γ matrix. Consequently, it breaks the chiral symmetry of the action.

It is tempting to think that we could include a factor of γ in its definition, to retain the symmetry, but to do so would break the Lorentz invariance of the continuum limit of the action. The extra term is essentially an implementation of $\partial_\mu \partial^\mu$, which is a Lorentz invariant quantity. A term such as $\gamma_\mu \partial_\mu \partial^\mu$ would not be; it has one too many free indices.

3.3.2 Staggered Fermions

A few years after Wilson published his ideas, Kogut, Susskind and Banks suggested a variant that went some way to eliminating doublers, whilst maintaining an element of the chiral symmetry [2][3][4]. Their idea was to construct a description that only accessed the first half of the Brillouin zone, but that had the same continuum limit. By limiting the system to the first half of the Brillouin zone, the region in which doubling takes place is excluded, but the effective lattice spacing of the new description is now twice as long as that of the basic theory. To have the proper continuum behaviour, the basic spinors in each square of the effective lattice must be grouped together in such a way as to represent effective spinors.

The starting point is to diagonalize the Dirac equation because this will make the construction of the effective spinors easier. In two Euclidean dimensions, we can do this with the following substitution

$$\Psi_x \to \sigma_2^{x_2}\sigma_1^{x_1}\Psi_x \qquad\qquad \bar{\Psi}_x \to \bar{\Psi}_x\sigma_1^{x_1}\sigma_2^{x_2} \tag{1}$$

When we apply the derivative operator to this action, we can see how the Dirac equation emerges.

$$\bar{\Psi}_x\sigma_1^{x_1}\sigma_2^{x_2}\frac{1}{2a}\sum_\mu \left[T_\mu - T_{-\mu}\right]\sigma_2^{x_2}\sigma_1^{x_1}\Psi_x = \bar{\Psi}_x\frac{1}{2a}\sum_\mu l^x\sigma_\mu\left[\Psi_{x+\hat{\mu}} - \Psi_{x-\hat{\mu}}\right] \tag{2}$$

where $l^x = (-1)^{x_{\mu-1}+..+x_1}$. The next step is to group together the basic spinors so that the lattice spacing between each group is twice the basic lattice spacing. We can see how that is done in Figure 3.

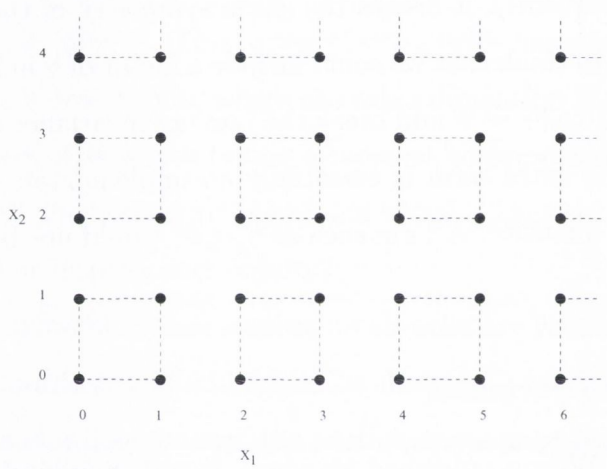

Figure 3: A 2D lattice. The squares correspond to sets of four linearly independent spinors, each of which are premultiplied by a different combination of σ matrices.

If each square is identified by its lower left corner, the effective spacing between squares will be $2a$ where a is the basic lattice spacing.

At this point, we still have too many degrees of freedom, so we jettison all but the one of the components of the transformed spinors from equation (1) and write the remaining component as χ_x. Which component we choose is arbitrary, although it is usual to keep the first.

The derivative in equation (2), which we have shown to correspond to the Dirac operator, does not mix the components of the spinors, so this is a valid procedure.

We can now construct an effective spinor belonging to a square as a combination of the χ_x fields within that square.

$$\hat{\Psi}_S = \sum_{c \in S} \sigma_1^{x_1^c} \sigma_2^{x_2^c} \chi_{x^c} \tag{3}$$

where the sum is over the corners, c in square S and $\hat{\Psi}_S$ is the effective spinor.

This prescription is completely effective in removing the doublers as we have defined them above. However, it has degeneracies of its own of which we must be mindful.

If we construct the effective fermion from the χ_x fields at all four corners of a single cell, we will have $\hat{\Psi}$ equal to a 2×2 matrix with four complex degrees of freedom. Each column of this matrix represents a degenerate effective fermion. This is perfect if we require a theory with two degenerate flavours of fermion, but is problematic if we require only one flavour.

The final feature worth noting about this formulation is the presence of chiral symmetry, although it is not in the form to which we are accustomed. Naturally, this formulation does not affect the vector symmetry of the action, but the axial symmetry comes intertwined with the symmetry of the degenerate flavours. The axial symmetry is generated by $\sigma_3 \otimes \sigma_3$, where the first σ_3 acts on the components of the spinor $\hat{\Psi}$ and the second σ_3 acts on the space of degenerate flavours, mixing them. Consequently, the chiral projection operators are $P_{R/L} = \frac{1}{2}(I \otimes I \pm \sigma_3 \otimes \sigma_3)$.

3.3.3 Nielsen and Ninomiya's Theorem

When it was first published, the staggered fermion formulation represented a small victory in the struggle to remove doublers whilst preserving chiral symmetry, but it was clear that it was a compromise of sorts. Degeneracy had been partially removed at a cost of part of the chiral symmetry. Its publication meant that there were three possibilities for lattice fermions.

The first was the original lattice theory, with full chiral symmetry and lots of degenerate doublers. The second was the staggered formulation with its reduced degeneracy and limited chiral symmetry. The third was the Wilson formulation with

no doublers, but no chiral symmetry. Between them, it was becoming clear that a trade off existed between maintaining the symmetry and removing the degeneracy.

It took five years for this relationship to be pinned down and that happened when Nielsen and Ninomiya published their "no-go" theorem in 1981 [24][25]. In it they state that, under some fairly mild conditions, the degeneracy is a consequence of having chiral symmetry on the lattice.

Their argument proceeded as follows. Each solution to the chiral lattice Dirac equation corresponds to a point where the momentum space lattice Hamiltonian goes to zero. On the lattice, momentum space is periodic, so providing the Hamiltonian is sufficiently smooth, every field that crosses the line $H(p) = 0$ once must do so again, in order to maintain periodicity. The second crossing is the degenerate doubler. There are implicit assumptions in this argument, but we will see that they correspond to very mild constraints in position space that nearly all useful Hamiltonians fulfil.

The first is that the Hamiltonian be translationally invariant, which means that momentum must be a conserved quantity. This stops us from crudely excluding the regions of momentum space in which the doubling occurs.

The second is that the Hamiltonian must be smooth in momentum space, in all derivatives of p. The consequence of smoothness is that the position space Hamiltonian is local to the corresponding degree. We can see this more easily if we start with the definition of locality and work backwards.

Locality is defined by the rate at which the Hamiltonian goes to zero as we separate the two points, on which it operates. We can quantify the degree of locality by insisting that $(x-y)^n H(x,y) \not\to \infty$ as $(x-y) \to \infty$. If the Hamiltonian is independent of position, it must depend only on the separation between x and y, so we can rewrite this condition as $z^n H(z) \not\to \infty$ as $z \to \infty$. Stepping into 1D momentum space, this becomes

$$\begin{aligned} z^n \tfrac{1}{\sqrt{2\pi}} \int dp \tilde{H}(p) e^{-ipz} &= \tfrac{1}{\sqrt{2\pi}} \int dp \tilde{H}(p) (i)^n \tfrac{\partial^n}{\partial p^n} e^{-ipz} \\ &= (-i)^n \tfrac{1}{\sqrt{2\pi}} \int dp e^{-ipz} \tfrac{\partial^n}{\partial p^n} \tilde{H}(p) \end{aligned}$$

For this expression to be non-divergent, the nth derivative of $\tilde{H}(p)$, at $p = 0$, must not diverge. An equivalent statement is that the $n-2$th derivative is smooth.

If $H(z)$ is more local than any power of z^n, then $H(p)$ must be smooth to all orders, which excludes the possibility of using piecewise functions to create a doubler-free Hamiltonian.

The next assumption is that the Hamiltonian must be chiral, which means that the terms must be proportional to the σ matrices. Because the σ matrices are linearly independent, chirality ensures that $H(p)$ only goes to zero when each of the p_μ go to zero, not when a combination of non-zero p_μ cancel.

The final assumption is that the charge is conserved and this is guaranteed through the hermiticity of the Hamiltonian.

These four assumptions are not very restrictive and most serious proposals up until this point in time had met them. One that had not is the SLAC derivative [26] in which the lattice derivative is replaced by a factor of p_μ in momentum space. This formulation is chiral and is doubler-free, but it can be shown that the position space representation is non-local [27].

Nielsen and Ninomiya's theorem shows that all proposals bound by the listed constraints suffer the trade off between chirality and uniqueness. It took over ten years for a description to be proposed that navigated its way around the assumptions in an attractive and viable fashion.

3.3.4 Domain Wall Fermions

In 1992, David Kaplan proposed a formulation that succeeded where others had failed. He put non-degenerate, chiral fermions on the lattice by introducing an extra dimension to the scheme [28]. By including a mass term that switched sign as it crosses the origin in the extra dimension, a single chiral solution fell out of the description that clung to the four dimensional slice at the origin of the extra dimension. The clinginess could be seen from its wave function which reached into the extra dimension, but was exponentially damped.

However, the doubling did not go away entirely. For a finite, periodic lattice, the sign of the mass term had to switch back somewhere along the length of the extra dimension and it was here that the doubler field could be found. When the lattice

was infinite, the exponential suppression ensured that the two solutions decouple. However, in the finite case, the situation was less perfect. The small overlap between the solutions acted as a mass term and so broke the symmetry.

A few years later Furman and Shamir refined the model by removing the requirements that the lattice be periodic and that the mass be a function of the extra dimension [30]. Providing the mass had a value between 0 and 2 lattice spacings, chiral solutions would appear on each wall. The advantage of making the lattice non-periodic was that the same physical lattice size resulted in greater exponential decoupling between the two solutions than in Kaplan's original formulation.

Furman and Shamir's formulation used the following action for four dimensions

$$S_F = \sum_{n,\mu=1..5} \bar{\psi}_n \frac{1}{2} \gamma_\mu \left[\psi_{n+\hat{\mu}} - \psi_{n-\hat{\mu}}\right] + \sum_{n,\mu=1..5} \bar{\psi}_n \frac{1}{2} \left[\psi_{n+\hat{\mu}} + \psi_{n-\hat{\mu}} - 2\psi_n\right] + m_0 \sum_n \bar{\psi}_n \psi_n$$

If we limit the extent of the lattice in the extra dimension to L_s and introduce a coupling between the two ends, m_f, we can rewrite S_F as

$$S_F = \sum_{x,x',s,s'} \bar{\psi}(x,s) D_F(x,s,x',s') \psi(x',s') \tag{4}$$

where

$$D_F(x,s,x',s') = \delta(s-s') \not{D}(x,x') + \delta(x-x') \not{D}^\perp(s,s')$$

$$\begin{aligned} \not{D}(x,x') &= \tfrac{1}{2} \textstyle\sum_{\mu=1..4} \left[(1+\gamma_\mu) U_\mu(x) \delta(x+\hat{\mu}-x') + (1-\gamma_\mu) U_\mu^\dagger(x') \delta(x'+\hat{\mu}-x)\right] \\ &+ (m_0 - 2n)\delta(x-x') \end{aligned}$$

$$\not{D}^\perp(s,s') = \begin{cases} P_R \delta(1-s') - m_f P_L \delta(L_s - 1 - s') - \delta(0-s') : \text{if } s = 0 \\ P_R \delta(s+1-s') + P_L \delta(s-1-s') - \delta(s-s') : \text{if } 0 < s < L_s - 1 \\ -m_f P_R \delta(0-s') + P_L \delta(L_s - 2 - s') - \delta(L_s - 1 - s') : \text{if } s = L_s - 1 \end{cases}$$

The $U_\mu(x)$ are the gauge links $U_\mu(x) = \exp(ieA_\mu(x))$ and $P_{R/L}$ are the chiral projection operators $P_{R/L} = \frac{1}{2}(1 \pm \gamma_5)$.

For an example of a recent calculation using this formalism, see [31].

3.3.5 Overlap Fermions

Around the same time, Narayanan and Neuberger proposed a subtly different formulation [46][47][48][49][50]. Starting with the same action as (4), but with the coupling

between the two walls zero (m_f), they rewrote the effective action as

$$e^{S_{eff}(U)} \propto < b- |\hat{D}_-(\hat{T}_-)^{s-1}(\hat{T}_+)^{s-1}\hat{D}_+^\dagger|b+ >$$

where s labels an extra coordinate, $|b\pm>$ are the states of the system at the infinite extremes of the extra coordinate and $\hat{D}_\pm$ and $\hat{T}_\pm$ are the many body operators

$$\hat{D}_\pm = e^{\hat{a}^\dagger Q_\pm \hat{a}} \qquad \hat{T}_\pm = e^{\hat{a}^\dagger H_\pm \hat{a}}$$

and $Q_\pm$ and $H_\pm$ are defined through

$$e^{Q_\pm} = \begin{pmatrix} \frac{1}{\sqrt{B^\pm}} & \frac{1}{\sqrt{B^\pm}}C \\ 0 & \sqrt{B^\pm} \end{pmatrix} \qquad e^{H_\pm} = \begin{pmatrix} \frac{1}{B^\pm} & \frac{1}{B^\pm}C \\ C^\dagger\frac{1}{B^\pm} & C^\dagger\frac{1}{\sqrt{B^\pm}}C + B^\pm \end{pmatrix}$$

The $B^\pm$ and C terms are:-

$$B^\pm_{n\alpha i,m\beta j} = (5 \mp m)\delta_{n\alpha i,m\beta j} - \frac{1}{2}\delta_{\alpha\beta}\sum_\mu \left[\delta_{m,n+\hat{\mu}}U^{ij}_{n,\mu} + \delta_{n,m+\hat{\mu}}U^{ji*}_{m,\mu}\right]$$

$$C_{n\alpha i,m\beta j} = \frac{1}{2}\sum_\mu \left[\delta_{m,n+\hat{\mu}}U^{ij}_{n,\mu} - \delta_{n,m+\hat{\mu}}U^{ji*}_{m,\mu}\right]\sigma^{\alpha\beta}_\mu$$

The $\hat{T}_\pm$ are transfer matrices along the extra dimension and by taking the infinite limit in the extra dimension, their ground states ($|0\pm, U>$) are the eigenstates that come to dominate. After some algebra, this leaves us with an overlap between ground states

$$e^{S(U)} =< 0-, U|O+, U >$$

from which the description gets its name. After further analysis, this can be shown to induce the chiral Dirac operator

$$D = \left(1 + \gamma_5 \frac{H}{\sqrt{H^\dagger H}}\right) \tag{5}$$

where H is the Hamiltonian. Although easy on the eye, this formula is tough to implement. The combination of Hs must be expanded as a series and the number of terms that must be taken is dependent on the application and the accuracy required, just as in the domain wall case. For an example of a contemporary calculation using this formulations, see [32].

3.3.6 Ginsparg-Wilson Fermions

Both the domain wall and overlap formulations achieve chiral symmetry in the limit of an infinite parameter. The test for lattice chiral symmetry is that the formulation must fulfil the Ginsparg-Wilson relation [33]:-

$$D\gamma_5 + \gamma_5 D = aD\gamma_5 D$$

which both these schemes do. In this expression a is the lattice spacing and D the Dirac operator.

The relationship between the two schemes has been established by Borici in his work on Truncated Overlap fermions [34][35].

3.3.7 The Fuzzy Sphere

A novel approach has been taken by the research group at the Dublin Institute for Advanced Studies, who study a formulation in which the manifold is replaced with a quantized phase space. The quantization leads to the space having toroidal properties and this geometry leads to a non-commutativity in the coordinates [36][37][38][39] .

4 Background: Differential Geometry

The premise of this thesis is to use a particular formulation of discrete differential geometry to study fermionic field theories. The formulation borrows finite element methods to define operators. Conventional lattice techniques, including all those seen in section 3, involve finite different methods, in which fields are sampled at the vertices of a lattice. Lattice operations process the sampled points to generate either scalar values or further fields valid only on the lattice vertices.

Finite element analysis uses the operators from the continuum on a finite data set. The fields at the vertices are linearly interpolated in the regions between vertices to give us a continuous field on which the operators are applied [40][41]. Integrals can also be approximated in the scheme by integrating over the links, faces, cubes and hypercubes of the lattice and by interpolating in the regions between neighbouring domains.

Before we introduce and extend the discrete differential geometry scheme, we shall first run through the necessary background material from continuum differential geometry. The following references are good supporting texts [42] [43].

4.1 Differential Geometry in the Continuum

The foundation for almost all differential geometry is the infinitesimal line element, dx. On a manifold, we have scalars, vectors and tensors of any degree, but in order for a vector or tensor at a point to have a direction, its components must reach another point on the manifold. However, if the point were a finite distance away, the vector or tensor would no longer be local and this would create problems when the local axes are coordinate dependent. Instead we define the vectors or tensors so that they point to a coordinate an infinitesimal distance away.

Vectors are represented as *differential forms* with one line element (known as *one-forms*): $v_\mu(x)dx^\mu$. Matrices are described by differential forms with two line elements (*two-forms*): $g_{\mu\nu}(x)dx^\mu dx^\nu$. Similarly, tensors of degree n are represented by differential forms with n line elements (n-*forms*): $\eta_{\mu_1\mu_2\ldots\mu_n}(x)dx^{\mu_1}dx^{\mu_2}\ldots dx^{\mu_n}$. We can define an orientation for the elements by incorporating the wedge product, $\wedge$.

An area element (a two-form) is the wedge product of two line element one-forms: $dx^\mu \wedge dx^\nu$. By wedging this against more one-forms, we can build forms of arbitrary dimension.

The wedge operation is antisymmetric: $dx^\mu \wedge dx^\nu = -dx^\nu \wedge dx^\mu$. Two consequences of this are that the product of a differential form with itself is always zero and that tensors symmetric in any two indices vanish.

An operator whose definition follows from that of $\wedge$ is the Hodge star. This is an operator that maps a p-form to the complementary $(n-p)$-form, in n dimensional space. For example, in 2d, it maps dx (a 1-form) to dy (a 1-form) and vice versa. It also maps $dx \wedge dy$ (a 2-form) to a scalar (a 0 form) and vice versa. Formally, it is defined as follows

$$*dx^H = \varepsilon^{H,\mathcal{C}H} dx^{\mathcal{C}H} \tag{6}$$

where dx^H is taken to mean a h-form, the ordered $\wedge$ product of h 1-forms and where the H denotes the ordered set of indices in the h-form. $\mathcal{C}H$ denotes the ordered complement of H, ie all the components in the space not belonging to H, and ε is the Levi-Civita tensor. With this definition, $dx^H \wedge *dx^H$ should always be equal to a positive n-form of the same dimension as the space.

The anticommuting behaviour of $\wedge$ is reminiscent of the γ and σ matrices. However, the algebra is slightly different. In Euclidean space-time, the γ and σ matrices obey the Clifford algebra: $\{\gamma^\mu, \gamma^\nu\} = 2\delta^{\mu\nu}$ and $\{\sigma^\mu, \sigma^\nu\} = 2\delta^{\mu\nu}$, in which $\{\cdot,\cdot\}$ denotes anticommutation. To continue the correspondence, we construct a Clifford product between the forms to recreate the Clifford algebra and we do this by combining the $\wedge$ with a new operator, the contraction operator.

Contraction is denoted $e^\mu \lrcorner$ and is defined through the Hodge star: $e^\mu \lrcorner = *dx^\mu \wedge *$. In practice, it has the effect of reducing the degree of a form, by removing an individual line element from an arbitrarily long differential form. However, it can only remove the element that is at the left end of the differential form, so to remove an element that is buried deep within an n-form, we must first use the anticommutation relation to shift it to the left end. For example

$$e^\mu \lrcorner dx^\nu \wedge dx^\mu = -e^\mu \lrcorner dx^\mu \wedge dx^\nu = -dx^\nu$$

This puts us in a position to define the Clifford product, $\vee$,

$$dx^\mu \vee dx^\nu = (dx^\mu \wedge + e^\mu \lrcorner)\, dx^\nu$$

and we can use it to define a Euclidean Clifford algebra for the differential forms:

$$\{dx^\mu, dx^\nu\}_\vee = 2\delta^{\mu\nu}$$

We can build algebraic objects as linear combinations of different forms and their tensor coefficients. When we do this, the various n-forms behave as bases for a local space. For example, in 2D Euclidean space, we can define an arbitrary function as $F(x) = f_0(x) + f_1(x)dx^1 + f_2(x)dx^2 + f_{12}(x)dx^1 \wedge dx^2$, which can be written more succinctly as $F(x) = f_0(x) + f_\mu(x)dx^\mu + f_{\mu\nu}(x)dx^\mu dx^\nu$ or $F(x) = \sum_H f_H(x)dx^H$. To construct an inner product between these objects, we use the Hodge star. If $F(x)$ and $G(x)$ represent $\sum_H f_H(x)dx^H$ and $G(x) = \sum_K g_K(x)dx^K$, respectively, we define the inner product to be

$$< F, G >= \int F \wedge (*G^*) \tag{7}$$

$F \wedge (*G^*)$ provides us with a measure of integration of the same dimension as the space and the integral sign is taken to mean integration over all space. Only the products between forms of identical dimension are non-zero.

When we take the Hodge star of a form twice in succession, we should recover the original form. However, along the way we may incur a minus sign, depending on both the dimension of the original form and the dimension of the space.

$$** dx^H = * \left(\varepsilon^{H,\mathcal{C}H} dx^{\mathcal{C}H}\right) = \varepsilon^{H,\mathcal{C}H}\varepsilon^{\mathcal{C}H,H} dx^H = (-1)^{h(n-h)} dx^H$$

We can refine the definition of the Hodge star to remove any ambiguity around the minus sign, by including another operator, $\mathcal{B}$, as Becher and Joos do [45]. We define $\mathcal{B}$ so that it has the following effect on dx^H

$$\mathcal{B}dx^H = (-1)^{\binom{h}{2}} dx^H$$

We can now create a new star operator, $\star = *\mathcal{B}$ that has the property: $\star\star = I$.

Another operator, defined in a similar fashion, is $\mathcal{A}$. $\mathcal{A}$ also operates on a form to generate a combination of minus signs, with the effect: $\mathcal{A}dx^H = (-1)^h dx^H$.

Finally, we must introduce the derivative operators. One of the most useful vectors, in field theories, is the derivative and in differential geometry it can take one of two forms. The exterior derivative is defined as an operator that acts upon a local field and increases the degree of its form: $d = dx^\mu \wedge \partial_\mu$. The adjoint derivative (sometimes known as the *coderivative*) also acts upon a local field, but reduces the degree of its form: $\delta = -(-1)^{nh+n} * d*$. It can be simplified to $\delta = -e^\mu \lrcorner \partial_\mu$.

The derivatives can be combined to construct the Dirac operator: $\not{D} \equiv (d - \delta)$, which is equivalent to $(dx^\mu \wedge + e^\mu \lrcorner)\partial_\mu = dx^\mu \vee \partial_\mu$. The Laplacian, which is the square of the Dirac operator, takes the form $(-d\delta - \delta d)$ because the antisymmetry of both d and δ ensure that $d^2 = \delta^2 = 0$.

This gives us all the tools we need to see how fermionic field theories can be represented using differential geometry, which is the theme of the next section.

4.2 The Dirac-Kähler Equation

The Dirac equation was first written in terms of differential geometry by Kähler and its new form was subsequently christened the Dirac-Kähler equation [44]. A review can be found in the paper by Becher and Joos [45].

Because of the correspondence between the Clifford algebras of the γ and σ matrices and the differential forms under $\vee$, we can write the Dirac-Kähler equation as

$$(dx^\mu \vee \partial_\mu + m)\Phi(x) = 0$$

where $\Phi(x)$ is a differential form. In 4D space-time, $\Phi(x)$ has sixteen independent components; in 2D, it has four:

$$\Phi(x) = \phi(x) + \phi_1(x)dx^1 + \phi_2(x)dx^2 + \phi_{12}(x)dx^1 \wedge dx^2$$

This raises a question about the equivalence of degrees of freedom. In 2D, we have four complex components of $\Phi(x)$, but just two complex components of $\Psi(x)$. This can be resolved by introducing a second spinor which we combine with the first to

turn $\psi(x)$ into a 2×2 matrix,

$$\psi_(x) = \begin{pmatrix} \psi_1^{(1)}(x) & \psi_1^{(2)}(x) \\ \psi_2^{(1)}(x) & \psi_2^{(2)}(x) \end{pmatrix}$$

We can relate the conventional Dirac basis to the Dirac-Kähler basis through the matrix Z, defined as

$$Z = 1 + \sigma_1^T dx^1 + \sigma_2^T dx^2 + \sigma_1^T \sigma_2^T dx^1 \wedge dx^2 = \sum_H (-1)^{\binom{h}{2}} \sigma_H^T dx^H$$

where the σ_μ are the Pauli matrices, H represent the product of ordered components and h is the number of components in H.

We use Z to relate $\Phi(x)$ to $\psi(x)$ as follows

$$\Phi(x) = \sum_H \phi(x, H) dx^H = \sum_{a,b} \psi_a^{(b)} Z_{ab}$$

where a denotes the row and (b) the column of ψ. Z has the useful property $dx^\alpha \vee Z = \sigma_\alpha^T Z$, which means that $dx^\alpha \vee \Phi(x) = \sum_{ab} (\sigma_\alpha \psi)_a^{(b)} Z_{ab}$. Using the following identities for the σ matrices, we can explicitly relate $\phi(x, H)$ to $\psi(x)$.

$$\text{Tr}\left(\sigma^H (\sigma^K)^\dagger\right) = 2\delta^{HK} \qquad \sum_H \sigma_{ab}^H \sigma_{cd}^{H*} = 2\delta_{ac}\delta_{bd} \tag{8}$$

$$\phi(x, H) = \text{Tr}\left(\sigma_H^\dagger \psi\right) \qquad \psi_a^{(b)} = \tfrac{1}{2} \sum_H \sigma_{ab}^H \phi(x, H) \tag{9}$$

When we introduce gauge fields, we must replace ∂_μ with $\partial_\mu - ieA_\mu$. We write the covariant Dirac-Kähler equation as

$$(d - \delta)\Phi(x) = ieA(x) \vee \Phi(x)$$

where $A(x)$ is a 1-form, $A(x) = A_\mu(x) dx^\mu$. The Abelian gauge transformation takes the form

$$\Phi(x) \to e^{i\theta(x)} \Phi(x) \qquad A_\mu(x) \to A_\mu(x) + \tfrac{1}{e} \partial_\mu \theta(x) \tag{10}$$

In order to construct a useful action, we must also introduce source terms. In the Dirac basis, we would use the spinors η and $\bar{\eta}$ as sources to construct a covariant action that looks like

$$\bar{\psi} \left(\not{D} - ie\not{A} + m\right) \psi + \bar{\eta}\psi + \bar{\psi}\eta$$

In the Dirac-Kähler basis, we construct the counterpart to η and $\bar{\eta}$, which we shall denote $\Theta(x) = \sum_{ab} \eta_a^{(b)}(x) Z_{ab}$ and $\bar{\Theta}(x) = \sum_{ab} \bar{\eta}_a^{(b)}(x) Z_{ab}$. The fermionic contribution to the action is now

$$S_F = < \bar{\Phi}, (d - \delta - ieA + m)\, \Phi > + < \bar{\Theta}, \Phi > + < \bar{\Phi}, \Theta >$$

We must also include the gauge action and a source for the gauge field. In the Dirac basis the action is defined to be $-\frac{1}{4} F_{\mu\nu} F^{\mu\nu}$, where $F_{\mu\nu} = \partial_\mu A_\nu - \partial_\nu A_\mu$. The Dirac-Kähler representation of $F_{\mu\nu}$ is dA, where d is the exterior derivative mentioned earlier. The anticommuting properties of the dx provide the antisymmetry that accounts for the two terms in $F_{\mu\nu}$ and the gauge action is a product of two of these terms.

$$S_G = < dA, dA >$$

The source field must have the same dimension as the gauge field, so we add the term $< \rho, A >$ to the action, defining ρ to be $\rho = \rho_\mu(x) dx^\mu$.

There is one more family of features of the Dirac-Kähler description that we must see before we are done. It centres around the operation that corresponds to the σ_3 matrix. This will give us the set of projection operators that isolate the chiral components of $\Phi(x)$ and also the projection operators that separate the columns of ψ, allowing us to single out the degenerate spinor fields.

Given that $\sum_{ab} (\sigma_\mu \psi)_a^{(b)} Z_{ab} = \sum_{ab} \psi_a^{(b)} \left(\sigma_\mu^T Z\right)_{ab}$, we can use the definition $\sigma_3 = -i\sigma_1\sigma_2$ and write

$$\sum_{ab} (\sigma_3 \psi)_a^{(b)} Z_{ab} = -i \sum_{ab} \psi_a^{(b)} \left((\sigma_1\sigma_2)^T Z\right)_{ab} = -i dx^1 \vee dx^2 \vee \sum_{ab} \psi_a^{(b)} Z_{ab}$$

However, there is some ambiguity here, because we can achieve a similar result using the Hodge star operator. We can show that, in even dimensions, $\sigma_3^T Z = -i * \mathcal{B}\mathcal{A} Z$. In odd dimensions, the relationship lacks the $\mathcal{A}$: $\sigma_3^T Z = -i * \mathcal{B} Z$.

Using the familiar projection operators, $P_{R/L} = \frac{1}{2}(1 \pm \sigma_3)$, we can project $\Psi(x)$ into its positive and negative chiral components with $P_{R/L} = \frac{1}{2}(1 \mp i * \mathcal{B}\mathcal{A}) = \frac{1}{2}(1 \mp i dx^1 \vee dx^2 \vee)$.

We can also use these operators to isolate the columns of ψ through right multiplication. In the Dirac basis, $\psi P_{R/L}$ projects out the first/second column of ψ. In

this context, we relabel $P_{R/L}$ as $P_{1/2}$ to distinguish its function. Returning to Z, we can see that its right multiplication properties are $Z\sigma_\mu^T = Z \vee dx^\mu$. We can also show that $Z\sigma_3^T = -i * \mathcal{B}Z$, which means that we can isolate the degenerate fields by using the flavour projection operator $P_{1/2} = (1 \mp i * \mathcal{B})$.

4.3 The Discrete Dirac-Kähler Equation

A number of attempts have been made to put the Dirac-Kähler equation on the lattice. One of the reasons for such interest is that it provides the continuum limit for the staggered fermion formulation. A recent review has been provided by Scott Wilson [51].

One of the first attempts was by Becher and Joos [45] and we will briefly outline their approach.

We divide the lattice into squares, as in Figure 4.

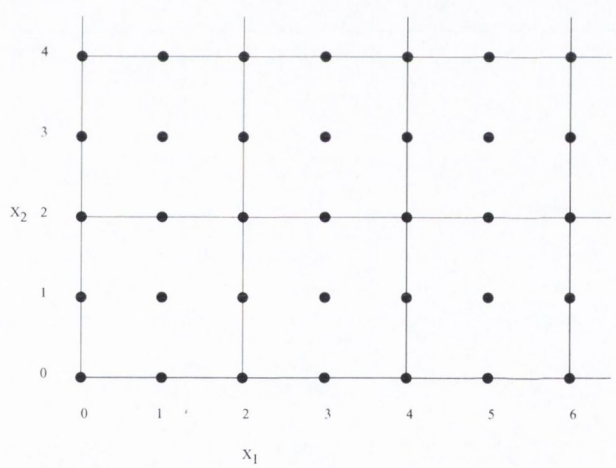

Figure 4: A 2D lattice for the Becher and Joos model. Each square represents four differential forms.

The discretization is done so that to each square four discrete differential forms are associated. The four differential forms correspond to the simplices at the bottom left corner, the left and bottom edges and the whole square and all four take as their coordinate the location of the point at the bottom left corner of the square. The bottom edge corresponds to $d^{x,1}$ and the left edge to $d^{x,2}$. The form $d^{x,1} \wedge d^{x,2}$

(denoted $d^{x,12}$) corresponds to the whole square and the zero form $d^{x,\emptyset}$ corresponds to the bottom left corner. In the centre of each of these objects is a lattice site. Using (9), we put the value of $\phi(x,H) = \mathrm{Tr}\left(\sigma_H^\dagger \psi(x,H)\right)$ on these sites, where $\psi(x,H)$ is sampled at the site.

The Clifford algebra for the theory is not straightforward. The contraction operator is similar to that of the continuum: $e^\mu \lrcorner d^{x,H} = \epsilon_{\mu,H/\mu} d^{x,H/\mu}$. However, the wedge product is defined by

$$d^{x,H} \wedge d^{y,K} = \epsilon_{H,K} d^{x,H\cup K} \delta^{y,x+e_H} \tag{11}$$

(provided $H \cap K = \emptyset$; otherwise it is zero). Here, $H \cup K$ is an ordered expression; the minus signs are accounted for by $\epsilon_{H,K}$. The interesting feature of this definition is the δ-function. It tells us that the product will only be non-zero if the simplices, corresponding to the forms on either side of the wedge, share a common point. Specifically, it says that the simplex corresponding to the form on the right hand side of the wedge must start from the point where the simplex, corresponding to the form on the left, ends. If this is not the case, the product is zero. If we write a general 1-form as $d^\mu = \sum_x d^{x,\mu}$, we can see that this has the undesirable consequence that: $e^\mu \lrcorner d^\mu \wedge d^{y,H} \neq d^{y,H}$, when $\mu \notin H$ and $d^\mu \wedge e^\mu \lrcorner d^{y,H} \neq d^{y,H}$, when $\mu \in H$. Instead, we have $e^\mu \lrcorner d^\mu \wedge d^{y,H} = d^{y-e_\mu,H}$, when $\mu \notin H$ and $d^\mu \wedge e^\mu \lrcorner d^{y,H} = d^{y-e_\mu,H}$, when $\mu \in H$. With this definition, the exterior derivative, d, is defined as

$$d = d^\mu \wedge \partial_\mu = d^\mu \wedge (1 - T_{-\mu}) \tag{12}$$

where we have the operators, $T_{\pm\mu}$ that sample a field from one square in the direction $\pm\mu$: $T_{\pm\mu}\phi(x,H) = \phi(x \pm e_\mu, H)$.

With this definition, the Clifford product is non-local. The Clifford algebra is

$$\{d^\mu, d^\nu\}_\vee = d^\mu \vee d^\nu \vee + d^\nu \vee d^\mu \vee = 2\delta^{\mu\nu} T_{-\mu}$$

and the non-locality of the Clifford product has the consequence of making both the Dirac-Kähler and Laplacian operators non-local.

4.3.1 Locality vs Leibniz

It is reasonable to ask why Becher and Joos did not choose a simpler definition for the wedge product. The definition

$$d^{x,H} \wedge d^{y,K} = \epsilon_{H,K} \delta^{x,y} d^{x,H \cup K} \tag{13}$$

gives $e^{\mu} \lrcorner d^{\mu} \wedge d^{y,H} = d^{y,H}$, when $\mu \notin H$ and $d^{\mu} \wedge e^{\mu} \lrcorner d^{y,H} = d^{y,H}$, when $\mu \in H$. This means that it has a local Clifford algebra

$$\{d^{\mu}, d^{\nu}\}_{\vee} = d^{\mu} \vee d^{\nu} \vee + d^{\nu} \vee d^{\mu} \vee = 2\delta^{\mu\nu}$$

which would seem to make it preferable to the definition of equation (11).

However, they had a very good reason for not choosing this definition. Leibnitz' rule is the rule governing the differentiation of products. In the continuum, it is

$$d(\Phi \wedge \Theta) = (d\Phi) \wedge \Theta + (\mathcal{A}\Phi) \wedge (d\Theta) \tag{14}$$

and it is desirable to have the same relation on the complex.

The definition in equation (13) leads to a forwardly defined exterior derivative

$$d = d^{\mu} \wedge \partial_{\mu} = d^{\mu} \wedge (T_{\mu} - 1)$$

which violates equation (14). However, the exterior derivative in equation (12), fulfils Leibnitz' rule and it is for this reason that Becher and Joos chose the wedge definition of equation (11).

4.3.2 An Alternative Definition for the Wedge Product

Whilst studying the work of Becher and Joos, we constructed an alternative definition for the wedge product that has interesting properties. It is possible to define a wedge product, within the framework that Becher and Joos use, that satisfies Leibnitz' rule and has a local Clifford algebra. However, this definition does not lead to local action because the Hodge star cannot be defined to be local.

The definition of the wedge product is critical in the product between fields and in the application of the exterior derivative. In both cases, its definition determines

which terms go to zero and which terms remain non-zero. In Appendix A, we derive a definition for the wedge product by starting with an undefined wedge product and asking what form it must take in order to be local and permit Leibnitz' rule. The definition we arrive at is subtly different to both Becher and Joos definition and to the naive local definition: $d^{x,H} \wedge d^{y,K} = \epsilon_{HK} d^{x,H\cup K}\delta^{x,y}$ for $H \cap K = \emptyset$.

To describe the effect of our alternative definition on the lattice in the Dirac basis, we would have to introduce subtle and non-trivial Dirac delta functions between lattice sites in both the definitions of the product between fields and the lattice derivative because, on the complex, the wedge product affects both these definitions.

We discuss the alternative definition in depth in Appendix A. Here we shall introduce the definition and demonstrate that it satisfies Leibnitz' rule for the simplest case of a one dimensional complex. A two dimensional example is provided in Appendix A.

If we introduce the following definition for the wedge product

$$\begin{array}{rcll} d^{x,H}\tilde{\wedge}d^{y,K} & = & \epsilon_{H,K} d^{y,H\cup K}\delta^{x,y+e_K} & \text{for } H \cap K = \emptyset \\ & & 0 & \text{otherwise} \end{array} \tag{15}$$

we can see that this has the properties

$$\begin{aligned} e^\mu \lrcorner d^\mu \tilde{\wedge} d^{y,H} &= d^{y,H} && \text{when } \mu \notin H \\ d^\mu \tilde{\wedge} e^\mu \lrcorner d^{y,H} &= d^{y,H} && \text{when } \mu \in H \end{aligned}$$

which lead to the local Clifford algebra

$$\{d^\mu, d^\nu\}_{\tilde{\vee}} = d^\mu \tilde{\vee} d^\nu \tilde{\vee} + d^\nu \tilde{\vee} d^\mu \tilde{\vee} = 2\delta^{\mu\nu}$$

In Appendix A, we arrive at the definition in equation (15) by considering Leibnitz' rule for an arbitrary definition of wedge product. If the wedge is to have a local Clifford product, the exterior derivative must be forwardly defined, so we use this as a constraint. By demanding that Leibnitz' rule be satisfied, we show that this is sufficient to derive the definition in equation (15). In doing so, we show that the following definition for the exterior derivative

$$d = d^\mu \tilde{\wedge} \partial_\mu = d^\mu \tilde{\wedge} (T_\mu - 1) \tag{16}$$

is local and satisfies Leibnitz' rule in the general case.

As an example, we shall show here that Leibnitz' rule is satisfied for the simplest case of a 1d complex.

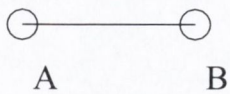

Figure 5: A one dimensional complex.

In Figure 5, we have three simplices: $[A]$, $[B]$ and $[AB]$ corresponding to $d^{A,\emptyset}$, $d^{B,\emptyset}$ and $d^{A,1}$, respectively. We define two fields on this complex with

$$\begin{aligned}\Phi &= \phi(A,\emptyset)d^{A,\emptyset} + \phi(B,\emptyset)d^{B,\emptyset} + \phi(A,1)d^{A,1} \\ \Theta &= \theta(A,\emptyset)d^{A,\emptyset} + \theta(B,\emptyset)d^{B,\emptyset} + \theta(A,1)d^{A,1}\end{aligned}$$

Using the wedge product of equation (15), the product between these fields is

$$\Phi\tilde{\wedge}\Theta = \phi(A,\emptyset)\theta(A,\emptyset)d^{A,\emptyset} + \phi(B,\emptyset)\theta(B,\emptyset)d^{B\emptyset} + \phi(B,\emptyset)\theta(A,1)d^{A,1}$$

The exterior derivative of this expression is

$$\begin{aligned}d(\Phi\tilde{\wedge}\Theta) &= \textstyle\sum_{y,\mu} d^{y,\mu}\tilde{\wedge}(T_{e_\mu} - 1)(\Phi\tilde{\wedge}\Theta) \\ &= d^{A,1}\tilde{\wedge}(T_{e_1} - 1)(\Phi\tilde{\wedge}\Theta) \\ &= \Big(\phi(B,\emptyset)\theta(B,\emptyset) - \phi(A,\emptyset)\theta(A,\emptyset)\Big)d^{A,1}\tilde{\wedge}d^{A,\emptyset} \\ &= \Big(\phi(B,\emptyset)\theta(B,\emptyset) - \phi(A,\emptyset)\theta(A,\emptyset)\Big)d^{A,1}\end{aligned} \tag{17}$$

with all other terms going to zero.

Now we look at the two terms $(d\Phi)\tilde{\wedge}\Theta$ and $(\mathcal{A}\Phi)\tilde{\wedge}(d\Theta)$.

$$\begin{aligned}d\Phi &= \textstyle\sum_{y,\mu} d^{y,\mu}\tilde{\wedge}(T_{e_\mu} - 1)\Phi \\ &= d^{A,1}\tilde{\wedge}(T_{e_1} - 1)\Phi \\ &= \Big(\phi(B,\emptyset) - \phi(A,\emptyset)\Big)d^{A,1}\tilde{\wedge}d^{A,\emptyset} \\ &= \Big(\phi(B,\emptyset) - \phi(A,\emptyset)\Big)d^{A,1} \\ d\Theta &= \Big(\theta(B,\emptyset) - \theta(A,\emptyset)\Big)d^{A,1}\end{aligned}$$

For the first of the two terms, we have

$$\begin{aligned}(d\Phi)\tilde{\wedge}\Theta &= \Big(\Big(\phi(B,\emptyset)-\phi(A,\emptyset)\Big)d^{A,1}\Big)\\ &\quad \tilde{\wedge}\Big(\theta(A,\emptyset)d^{A,\emptyset}+\theta(B,\emptyset)d^{B,\emptyset}+\theta(A,1)d^{A,1}\Big)\\ &= \Big(\phi(B,\emptyset)\theta(A,\emptyset)-\phi(A,\emptyset)\theta(A,\emptyset)\Big)d^{A,1}\end{aligned}$$

For the second of the two terms, we have

$$\begin{aligned}(\mathcal{A}\Phi)\tilde{\wedge}(d\Theta) &= \mathcal{A}\Big(\phi(A,\emptyset)d^{A,\emptyset}+\phi(B,\emptyset)d^{B,\emptyset}+\phi(A,1)d^{A,1}\Big)\\ &\quad \tilde{\wedge}\Big(\theta(B,\emptyset)-\theta(A,\emptyset)\Big)d^{A,1}\\ &= \Big(\phi(A,\emptyset)d^{A,\emptyset}+\phi(B,\emptyset)d^{B,\emptyset}-\phi(A,1)d^{A,1}\Big)\\ &\quad \tilde{\wedge}\Big(\theta(B,\emptyset)-\theta(A,\emptyset)\Big)d^{A,1}\\ &= \Big(\phi(B,\emptyset)\theta(B,\emptyset)-\phi(B,\emptyset)\theta(A,\emptyset)\Big)d^{A,1}\end{aligned}$$

Combining these terms, we have

$$\begin{aligned}(d\Phi)\tilde{\wedge}\Theta+(\mathcal{A}\Phi)\tilde{\wedge}(d\Theta) &= \Big(\phi(B,\emptyset)\theta(A,\emptyset)-\phi(A,\emptyset)\theta(A,\emptyset)\Big)d^{A,1}\\ &+ \Big(\phi(B,\emptyset)\theta(B,\emptyset)-\phi(B,\emptyset)\theta(A,\emptyset)\Big)d^{A,1}\\ &= \Big(\phi(B,\emptyset)\theta(B,\emptyset)-\phi(A,\emptyset)\theta(A,\emptyset)\Big)d^{A,1}\end{aligned}$$

which is the same as the last line of equation (17).

4.3.3 The Non-Local Commutator

Another formulation that accepts and works within these limitations is that proposed by Kanamori and Kawamoto [52] [53] [54]. Their formulation both achieves locality and permits Leibnitz's rule to be enforced, but they achieve this by making a very unorthodox sacrifice. They introduce a non-commutativity between fields and discrete differential forms.

$$g(x+\hat{\mu})d^{x,\mu}=d^{x,\mu}g(x)$$

which ensures that $d(f(x)g(x))=(df(x))g(x)+f(x)(dg(x))$.

To construct both a Clifford product that respects this result and gives a Hermitian action, they find it necessary to introduce two orientations of the lattice. One

orientation is for line elements lying in the positive μ direction and one for line elements lying in the negative μ direction. The line element that points from x to $x+\hat{\mu}$ is labelled $\theta^{+\mu}$ The line element that points from $x+\hat{\mu}$ to x is labelled $\theta^{-\mu}$. With these objects, their exterior derivative is defined to be

$$df = \sum_{\mu} \{(\partial_{+\mu} f)\theta^{+\mu} - (\partial_{-\mu} f)\theta^{-\mu}\}$$

where $\partial_{\pm\mu} f(x) = \pm(f(x \pm \hat{\mu}) - f(x))$.

Their formulation naturally includes a doubling of fields, which they have speculated lends itself to the representation of bosonic and fermionic fields in a supersymmetric theory.

The non-locality has received more theoretical treatment elsewhere [55][56][57], where it is studied in the context of a differential calculus on a finite set.

5 Background: Geometric Discretization

All the formulations that we have considered so far come up against the locality-Leibnitz problem which they each address in their own way with their own limitations.

However, the ideas that we have seen are all immersed in a finite difference formulation of field theory. Perhaps if we take a different approach at this level, we might be able to make more progress.

Geometric discretization is a formulation that does offer something different. It uses finite element methods to create interpolated, continuous fields on which we can use the operators from the continuum, but that have only a finite number of degrees of freedom. It doesn't solve the problem entirely, as we shall see, but it reduces it to a lattice approximation which is controllable by adjusting the lattice spacing.

The foundation for Geometric discretization was built by David Adams in his PhD thesis [58]. It has since been added to by Samik Sen [9] and Vivien de Beaucé [8] in their theses. Some of the details have been published in the papers [59] [60] [61] [62] [63] [64] [65] [66] [67] [68]. Work has also been done by Bartlomiej Czech at the University of Pennsylvania [69].

5.1 Geometric Discretization

To construct the geometric discretization, we start with the same lattice structure as in the Becher and Joos method (see Figure 4).

In 2D, the simplices are the points and the lines and squares that lie between points. In higher dimensions, the list would include cubes and hypercubes.

We can use the simplices as building blocks to construct a topological model of a given space. The collection of simplices together is known as a *complex* and we can use the simplices to construct complexes that are isomorphic to arbitrary topological spaces.

To introduce our notation, we will use the reference square from Figure 6.

In this example, the complex comprises nine simplices. Four are the points at the corners of the square: $[A]$, $[B]$, $[C]$ and $[D]$. Four are the edges: $[AB]$, $[BC]$, $[DC]$ and $[AD]$ and one is the square $[ABCD]$.

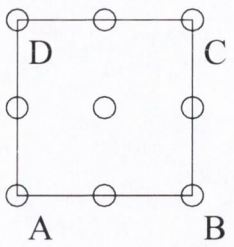

Figure 6: A sample square from the GD lattice.

5.1.1 The De Rham and Whitney Maps

We use the De Rham operator to discretize continuous fields. If $\Phi(x) = \phi(x, H)dx^H$ is an arbitrary, continuous differential form, $R\Phi(x)$ would generate nine separate terms. The first four would comprise the field of the zero-forms sampled at the corners of the square: $\phi(A, \emptyset)[A]$, $\phi(B, \emptyset)[B]$, $\phi(C, \emptyset)[C]$ and $\phi(D, \emptyset)[D]$. The second four would be the integrals of the 1-forms along the edges:-

$$\begin{aligned}
\tilde{\phi}([AB])[AB] &= (\textstyle\int_{[AB]} dx^1 \phi(x, 1))[AB] \\
\tilde{\phi}([DC])[DC] &= (\textstyle\int_{[DC]} dx^1 \phi(x, 1))[DC] \\
\tilde{\phi}([AD])[AD] &= (\textstyle\int_{[AD]} dx^2 \phi(x, 2))[AD] \\
\tilde{\phi}([BC])[BC] &= (\textstyle\int_{[BC]} dx^2 \phi(x, 2))[BC]
\end{aligned}$$

Finally, we also have the effect of R on the two-form:-

$$\tilde{\phi}([ABCD])[ABCD] = (\int_{[ABCD]} dx^1 dx^2 \phi(x, 12))[ABCD]$$

For the purposes of consistency, we shall also use the $\tilde{\phi}$ notation to denote the mapped zero forms: $\tilde{\phi}([A])[A]$, $\tilde{\phi}([B])[B]$, $\tilde{\phi}([C])[C]$, and $\tilde{\phi}([C])[C]$. We have chosen this notation because it underlines the property that the effect of R is to map continuous fields to a linear combination of the simplices with field values as their coefficients. The general linear combination of these elements is the Geometric Discretization representation of a general *cochain*.

To map the opposite way, from discrete to continuous fields, we use the Whitney map. This acts on a general cochain to generate continuous terms containing two factors. One is a differential form that reflects the space that the simplex covered.

The other is a set of functions that interpolate in the regions between neighbouring simplices.

To illustrate this, we look again at the complex in Figure 6. The bottom left and top right corners of the square are taken to have the coordinates (a_1, a_2) and (b_1, b_2). We must introduce the generalised coordinates as tools to interpolation.

$$\mu_1 = \frac{b_1 - x_1}{b_1 - a_1} \qquad \mu_2 = \frac{b_2 - x_2}{b_2 - a_2}$$

These coordinates are only valid within cells on whose boundary can be found the simplices between which we are to interpolate. Outside of that cell they are zero. For the zero-simplices above, we have

$$\begin{aligned} W[A] &= \mu_1\mu_2 & W[B] &= \mu_2(1-\mu_1) \\ W[C] &= (1-\mu_1)(1-\mu_2) & W[D] &= \mu_1(1-\mu_2) \end{aligned}$$

Applying W to the cochain $\tilde{\Phi} = \tilde{\phi}([A])[A] + \tilde{\phi}([B])[B] + \tilde{\phi}([C])[C] + \tilde{\phi}([D])[D]$ gives $\tilde{\phi}([A])\mu_1\mu_2 + \tilde{\phi}([B])\mu_2(1-\mu_1) + \tilde{\phi}([C])(1-\mu_1)(1-\mu_2) + \tilde{\phi}([D])\mu_1(1-\mu_2)$ which is a function that interpolates between the four corners.

The one-simplices are a little trickier. On $[AB]$, we have two coordinates, one relative to $[A]$ denoted μ_1 and one relative to $[B]$, denoted $(1-\mu_1)$. If we rewrite the former as ν_1 and the latter as ν_2, the Whitney map of $[AB]$ is $\mu_2(\nu_1 d\nu_2 - \nu_2 d\nu_1)$. This reduces to $-\mu_2 d\mu_1$. The four one-simplices are mapped to

$$\begin{aligned} W[AB] &= -\mu_2 d\mu_1 & W[BC] &= -(1-\mu_1)d\mu_2 \\ W[DC] &= -(1-\mu_2)d\mu_1 & W[AD] &= -\mu_1 d\mu_2 \end{aligned}$$

The two-simplex $[ABCD]$ is mapped to $d\mu_1 \wedge d\mu_2$. This set of forms and coordinates are collectively known as the *Whitney elements.*

In cases where we are dealing with the unit square, they become very simple. $\mu_1 = 1 - x_1$, $\mu_2 = 1 - x_2$, $d\mu_1 = -dx_1$ and $d\mu_2 = -dx_2$. Because we will be using these objects a great deal, to keep the notation simple and intuitive, we will always assume that the simplex in question has been mapped to a unit square.

In discretizing a continuous space, much information is lost about its structure, so it is unsurprising that $WR \neq I$. However, when we start with a discretized space it is reassuring to see that $RW = I$.

5.1.2 The Exterior Derivative

In this framework, the discrete exterior derivative can be obtained by interpreting the behaviour of the continuous derivative operator on the Whitney elements. We denote the geometrically discretized derivative as D with $DR = Rd$. In the simple example of a single one-simplex $[AB]$, the coordinates are $(1-x)\tilde{\phi}([A]) + x\tilde{\phi}([B])$ and applying d gives $\tilde{\phi}([B])dx - \tilde{\phi}([A])dx$. R maps this back to $\left(\tilde{\phi}([B]) - \tilde{\phi}([A])\right)[AB]$.

5.1.3 The Discrete Wedge

The wedge product of two discrete forms is similarly defined by the behaviour of the continuous wedge on the Whitney elements. We use the Whitney map to map each simplex to the continuum, apply the continuum wedge and then map back to the complex with the de Rham map.

$$\tilde{\phi}\tilde{\wedge}\tilde{\theta} = R\left[W\left(\tilde{\phi}\right) \wedge W\left(\tilde{\theta}\right)\right]$$

5.1.4 The Hodge Star and the Dual Complex

In equation (6), we saw that the continuum Hodge star is defined to be a local operator that uniquely maps a form to its complement. On the lattice this is harder to define. Referring once again to Figure (6), if we want to map $[AB]$ to its complement, the only simplices available of the proper dimension are $[BC]$ and $[AD]$, so we must define the Hodge star to map to either or both. However, when we apply the same definition a second time, the result will not be proportional to I, because it must include $[CD]$. This makes the definition of $*$ non-local.

David Adams proposed a solution to this difficulty [5][6] by introducing a second lattice in the same physical space as the first, but distinct from it. The dual complex has the same dimension as the original, but is off-set as shown in Figure 7.

Simplices from the original and dual complexes are related by their midpoints. In 2D, a zero simplex from one complex is mapped to the 2-simplex from the other whose centre coincides with the original zero-simplex. A one-simplex in the $\hat{x}_1$ direction is mapped to the one-simplex in the x_2 direction that intersects it. The 2-simplex is mapped to the point at its centre. When the correct sign factors are

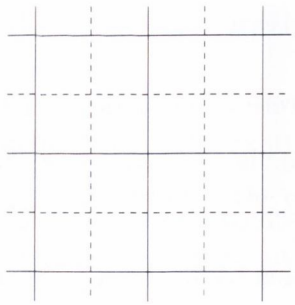

Figure 7: The original complex (solid lines) and the dual (dashed) superimposed.

included, this gives a 1-to-1 mapping that enjoys the continuum locality property: $** = (-1)^{h(n-h)}I$, where n is the dimension of the space and h the degree of the simplex.

5.1.5 The Adjoint Derivative and Contraction Operator

With the Hodge Star in place, we can define an adjoint derivative: $\delta = -(-1)^{nh+n} * D*$, where D is the discrete exterior derivative of section (5.1.2), acting in the space of the dual complex.

The contraction operator also follows neatly. $e^\mu \lrcorner = *Rdx^\mu \wedge W*$, where W and R are the Whitney and De Rham transforms.

5.1.6 The Inner Product and the Barycentric Subdivided Lattice

In his thesis, Samik Sen, detailed this extensively [9]. We shall briefly summarize his idea.

To define a product between two discrete cochains we start from the continuum definition, equation (7). Straight away, we see that there is an obstacle for GD. The definition wedges two cochains, one of which will have been mapped to the dual complex. This is not possible using the definition for the discrete wedge that we gave earlier, so we must construct a new definition for use in the inner product.

We introduce a new lattice, the Barycentric Subdivided Lattice that is defined by the union of both the original lattice and the dual, but with an extra feature. Vertices are introduced at the centre of each simplex (the *barycentres*) and the set of

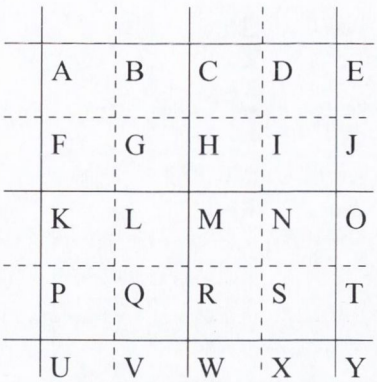

Figure 8: The Barycentric lattice.

simplices on the new lattice is defined from the union of the vertices of the original lattice, the dual lattice and the barycentres. The set of 25 vertices, corresponding to Figure 7, is shown in Figure 8.

On this lattice we use a special Whitney transform, W^B, that provides interpolation between the new set of vertices. These Whitney elements have a smaller range of support than those on the original and dual lattices alone.

We now define the inner product of $< F, G >$ as follows.

$$< \sigma, \eta >= \int_M W^B(B\sigma) \wedge W^B(B * \eta)$$

where $B\sigma$ is the Barycentric representation of σ and W^B is the Whitney map to the barycentric subdivided lattice.

5.1.7 Flavour Projection Operators

In the Dirac basis, the Dirac spinor is a 2×2 matrix, whose columns represent degenerate spinors. In the continuum, the columns can be isolated using projection operators, $P^{(b)}$ because the Clifford product is associative: $dx^\mu \vee \partial_\mu(\Phi \vee P^{(b)}) = (dx^\mu \vee \partial_\mu \Phi) \vee P^{(b)} = 0$, where b labels the column of ψ. This idea transfers to GD, but the correspondence is not simple. In his thesis, Vivien de Beaucé showed that the flavours could be isolated both in the case of cubic complexess and, with more difficulty, in triangular complexes [8].

In the Dirac basis, we use the operators $P^{(b)}$ to isolate the columns of ψ through

right application: $\psi^{(b)} = \psi \vee P^{(b)}$. In 4D, the $P^{(b)}$ are defined as

$$P^{(b))} = \frac{1}{4}(1 + i\alpha_b\gamma_1\gamma_2)(1 + \beta_b\gamma_1\gamma_2\gamma_3\gamma_4) \tag{18}$$

where

b	α_b	β_b
1	-1	-1
2	$+1$	-1
3	-1	$+1$
4	$+1$	$+1$

In section 4.2, we showed how the Dirac chiral projection operators, $P_{R/L}$, were related to their Dirac-Kähler counterparts. We can use the same logic and the identity $Z \vee dx^\alpha = Z\gamma_\alpha^T$ to obtain

$$P^{(b)} = \frac{1}{4}(1 + i\alpha_b dx^1 \vee dx^2)(1 + \beta_b dx^1 \vee dx^2 \vee dx^3 \vee dx^4)$$

In 2D, the equivalent operators are $P^{(b)} = \frac{1}{2}(1 + \alpha_b i\sigma_1\sigma_2) = \frac{1}{2}(1 + \alpha_b i dx^2 \vee dx^1)$, where

$$\alpha_b = \begin{cases} -1 & \text{for} \quad b = 1 \\ +1 & \text{for} \quad b = 2 \end{cases}$$

6 Principal Research

This chapter comprises three sections and each section represents an independent set of observations on or developments of the geometric discretization. In the first, 6.1, we discuss the geometric discretization as it has so far been laid out, which is consistent with how it has been described in [8][9][58][63]. In the first subsection, 6.1.1, we look at how it addresses the issues of fermion doubling, comparing this to the staggered fermion formulation. In subsection 6.1.2, we compare $dx^\mu\vee$, from the continuum, to its discrete counterpart. In the latter case, we find that the correspondence between $dx^\mu \vee \Phi(x)$ and $\sigma^\mu\psi(x)$ from the continuum in two space-time dimensions is made approximate by the spatial discretization. Whilst this has implications for the discrete differential geometry, it does not affect the correspondence between the Dirac-Kähler operator and the staggered Dirac operator. It does, however, have implications for the naive discrete definition of chiral symmetry which is proportional to the discrete counterpart of $(dx^1 \wedge dx^2)\vee$ and this is discussed in subsection 6.1.3.

In the second section 6.2, we see how we can use the dual complex to implement an exact chiral symmetry. Subsections 6.2.1 – 6.2.3 are dedicated to this result. We also see how we can use the dual to implement flavour symmetry. This naturally raises the question of how we can simultaneously implement both symmetries. We see in subsection 6.2.4 that to achieve this we must introduce two more complexes, one analogous to the original complex and one analogous to the dual and that we must carefully define our operators to map between the four complexes.

We extend this idea to four dimensional space-time in subsection 6.2.5, introducing a new operator and new complexes to facilitate flavour symmetry. To simultaneously maintain the chiral and flavour symmetry requires eight complexes in total, in analogy to the four complexes required in two space-time dimensions.

In the third section, 6.3, we return to the established formulation of geometric discretization [8][9][58][63] and develop an Abelian field theory for it, introducing the elements necessary to perform a discrete field theory calculation (subsections 6.3.1 – 6.3.4). In subsections 6.3.5 – 6.3.7, we consider topological gauge configurations, highlighting some of the differences between their treatment within the geometric

discretization and standard lattice QED.

6.1 Observations on Geometric Discretization

Before we proceed to develop the Geometric Discretization, we shall first highlight some of its interesting features.

6.1.1 Fermion Degeneracy

As we saw in section 3.2, fermion doubling arises in the lattice Dirac equation, the Green's function for which provides the propagator for the lattice fermion field. It is interesting to see exactly how the geometric discretization removes the doublers in momentum space and how this compares with the staggered fermion formulation.

We mentioned in section 3.3.2, that the staggered fermion formulation removes the degeneracy by reducing the extent of the Brillouin zone, whilst maintaining the continuum limit of the Dirac operator. By halving the zone, it excludes the regions in which the doubling solutions exist. This approach has its own degeneracy because, in two space-time dimensions, two spinor fields simultaneously and independently share the same lattice.

In the geometric discretization, two spinors also share the same space, but the mechanism is subtly different. To see this, we must analyse the formulation in momentum space. Each component of the differential field represents a separate degree of freedom, so, in the continuum, we must transform each field to momentum space separately.

$$\phi_H(x))dx^H = \frac{1}{2\pi}\int d^2p\hat{\phi}_H(p)e^{i\vec{p}\cdot\vec{x}}dx^H$$

When we apply the De Rham map, we integrate this over a finite region. The discrete fields are

$$\tilde{\phi}([H])[H] = \int_{[H]} dx^H \frac{1}{2\pi}\int d^2p\hat{\phi}_H(p)e^{i\vec{p}\cdot\vec{x}}[H] = \frac{1}{2\pi}\int d^2p\frac{1}{(ip)^h}\hat{\phi}_H(p)e^{i\vec{p}\cdot\vec{x}}|_{x=\partial H}[H]$$

where (∂H) denotes the boundary of H. The factor of $\frac{1}{(ip)^h}$ is the the unique feature here that removes the doublers from the discrete Dirac-Kähler operator. The discrete adjoint field is similarly defined from the continuum.

In the context of the action, there are two types of term to consider. The first is where δ reduces the degree of a form, before its inner product is taken with a simplex from the adjoint field of the same, lower dimension. The second is where D increases the dimension of the simplex before the inner product is taken with the adjoint field.

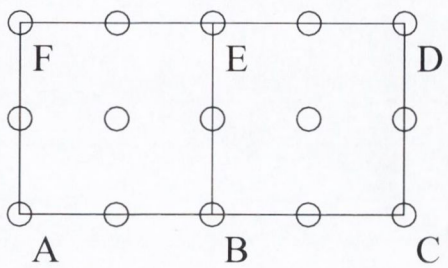

Figure 9: Two squares from the GD complex.

To provide a specific example of each, we use the square in Figure 9. In the first case, one of the terms to contribute to the action is

$$< \tilde{\bar{\phi}}([B])[B], -\delta\left(\tilde{\phi}([BC])[BC] + \tilde{\phi}([AB])[AB]\right) >$$

Replacing $\tilde{\phi}([BC])$ and $\tilde{\phi}([AB])$ with their momentum space counterparts, we have

$$< \tilde{\bar{\phi}}([B])[B], -\delta\left(\frac{1}{2\pi}\int d^2p\hat{\phi}_1(p)\frac{\left(e^{ip_1[C]_1} - e^{ip_1[B]_1}\right)}{ip_1}e^{ip_2[B]_2}[BC]\right.$$

$$\left. +\frac{1}{2\pi}\int d^2p\hat{\phi}_1(p)\frac{\left(e^{ip_1[B]_1} - e^{ip_1[A]_1}\right)}{ip_1}e^{ip_2[B]_2}[AB]\right) >$$

$$=< \tilde{\bar{\phi}}([B])[B], \frac{1}{2\pi}\int d^2p\hat{\phi}_1(p)\frac{\left(e^{ip_1[C]_1} + e^{ip_1[A]_1} - 2e^{ip_1[B]_1}\right)}{ip_1a}e^{ip_2[B]_2}[B] >$$

In this expression $[A]_1$ denotes the coordinate in the x_1 direction of the point $[A]$. If the distance BC is a, this can be rewritten as

$$< \tilde{\bar{\phi}}([B])[B], \frac{1}{2\pi}\int d^2p\hat{\phi}_1(p)\frac{4i\sin^2(\frac{p_1a}{2})}{p_1a}e^{i\vec{p}\cdot[\vec{B}]}[B] > \tag{19}$$

which is a definition that is free of doublers.

When we look at the second type of term in the action, we have

$$< \tilde{\bar{\phi}}([AB]), D\left(\tilde{\phi}([B])[B] + \tilde{\phi}([A])[A]\right) > \tag{20}$$

In this case, we must write both the fermion field and the adjoint field in momentum space.

$$\tilde{\bar{\phi}}([AB])[AB] = \int_{[AB]} dx^1 \frac{1}{2\pi} \int d^2p \hat{\bar{\phi}}_1(p) e^{i\vec{p}\cdot\vec{x}}[AB]$$
$$= \frac{1}{2\pi} \int d^2p \hat{\bar{\phi}}_1(p) \frac{\left(e^{ip_1[B]_1} - e^{ip_1[A]_1}\right)}{ip_1} e^{ip_2[B]_2}[AB]$$

Expanding this around the mid point of $[AB]$, we have

$$\frac{1}{2\pi} \int d^2p \hat{\bar{\phi}}_1(p) \left(\frac{2i\sin(\frac{p_1 a}{2})}{ip_1}\right) e^{ip_1[AB]_1} e^{ip_2[B]_2}[AB]$$

When we calculate the right hand part of equation (20), we have

$$\frac{1}{2\pi} \int d^2p \hat{\phi}_1(p) \left(\frac{e^{ip_1[B]_1} - e^{ip_1[A]_1}}{a}\right) e^{ip_2[B]_2}[AB]$$

Doing the same expansion, this becomes

$$\frac{1}{2\pi} \int d^2p \hat{\phi}_1(p) \left(\frac{2i\sin(\frac{p_1 a}{2})}{a}\right) e^{ip_1[AB]_1} e^{ip_2[B]_2}[AB]$$

The product of the momentum space factors is

$$\frac{4i\sin^2(\frac{p_1 a}{2})}{p_1 a}$$

which, reassuringly, gives us the same expression as equation (19) for the momentum space Dirac-Kähler operator.

From these derivations, we can see that the Dirac-Kähler operator explores half of the Brillouin zone, just as in the staggered fermion case. However, the momentum space representation of the operator does look different. In the staggered fermion formulation, the Dirac operator is proportional to $i\sin(\frac{p_\mu a}{2})$ [19]. In our case, it is proportional to $i\frac{\sin^2(\frac{p_\mu a}{2})}{p_\mu a}$, which has the same continuum limit.

6.1.2 The Correspondence Between $dx^\mu \vee \Phi$ and $\sigma^\mu \Psi$

The crux of the relationship between the Dirac basis and the Dirac-Kähler basis is provided by the matrix Z, which was described in section 4.2. In continuous two dimensional space-time, it has the properties $dx^\mu \vee Z = \sigma^T Z$ and $Z \vee dx^\mu = Z\sigma^T$. This leads to the correspondence

$$dx^\mu \vee \Phi(x) \quad \Leftrightarrow \quad \sigma\psi(x) \tag{21}$$

On the complex this relationship does not hold exactly, which has consequences for the naive definition of both chiral and flavour symmetry.

We can see that it exists approximately if we look at how a typical field is constructed within the geometric discretization. In two space-time dimensions, the continuous Dirac-Kähler field is

$$\text{Tr } [\psi(x)] + \text{Tr } [\sigma_1\psi(x)]\, dx^1 + \text{Tr } [\sigma_2\psi(x)]\, dx^2 + \text{Tr } [\sigma_2\sigma_1\psi(x)]\, dx^1 \wedge dx^2$$

If we limit our complex to the following square,

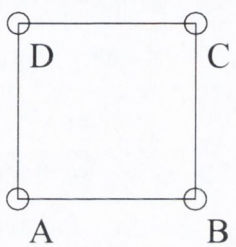

Figure 10: A square from the complex.

then our discrete fields are defined as

$$\begin{aligned}
\tilde{\phi}([A]) &= \text{Tr } [\psi(x)]\Big|_{x=A} & \tilde{\phi}([B]) &= \text{Tr } [\psi(x)]\Big|_{x=B} \\
\tilde{\phi}([C]) &= \text{Tr } [\psi(x)]\Big|_{x=C} & \tilde{\phi}([D]) &= \text{Tr } [\psi(x)]\Big|_{x=D} \\
\tilde{\phi}([AB]) &= \textstyle\int_{[AB]} \text{Tr } [\sigma_1\psi(x)]\, dx^1 & \tilde{\phi}([DC]) &= \textstyle\int_{[DC]} \text{Tr } [\sigma_1\psi(x)]\, dx^1 \\
\tilde{\phi}([AD]) &= \textstyle\int_{[AD]} \text{Tr } [\sigma_2\psi(x)]\, dx^2 & \tilde{\phi}([BC]) &= \textstyle\int_{[BC]} \text{Tr } [\sigma_2\psi(x)]\, dx^2
\end{aligned}$$

$$\tilde{\phi}([ABCD]) = \textstyle\int_{[ABCD]} \text{Tr } [\sigma_2\sigma_1\psi(x)]\, dx^1 \wedge dx^2$$

and $\tilde{\Phi}$ is the sum of these terms after each is multiplied by the appropriate simplex. When we apply $dx^\mu\vee$ to $W(\tilde{\Phi})$ and subsequently apply R, we would like to see something representing the correspondence in equation (21). However, instead we obtain an approximation to it.

By applying $dx^1\wedge$ to the Whitney map of $\tilde{\phi}([AD])[AD] + \tilde{\phi}([BC])[BC]$ and then applying R, we have $\frac{1}{2}\left(\tilde{\phi}([AD]) + \tilde{\phi}([BC])\right)[ABCD]$. We write this explicitly as

$$\frac{1}{2}\left(\int_{[AB]} \text{Tr } [\sigma_2\psi(x)]\, dx^2 + \int_{[BC]} \text{Tr } [\sigma_2\psi(x)]\, dx^2\right)[ABCD] \tag{22}$$

If the correspondence existed on the complex as it does in the continuum, we would instead expect to see

$$\left(\int_{[A}\mathrm{Tr}\,[\sigma_2\psi(x)]\,dx^1\wedge dx^2\right)[ABCD] \qquad (23)$$

Alas this term is not defined in the discretization, so we must make do with the approximation to it represented by equation (22). The only case in which equations (22) and (23) agree is when the field $\psi(x)$ is linear in x_1. We can generalize this statement to say that the correspondence in equation (21) only holds for linear fields.

This does not affect the relationship between the Dirac-Kähler operator and the staggered Dirac operator. In this case, the combination of R, $dx^1\wedge$ and W map both $\tilde{\phi}([AD])$ and $\tilde{\phi}([BC])$ on to $[ABCD]$, but ∂_1 introduces the correct sign between them giving a derivative of the correct form and that is consistent with what we would expect from the staggered fermion description.

6.1.3 Chiral Symmetry

In section 4.2, we saw that, in the continuum, $\sigma_3\psi(x)$ corresponded to $-i*\mathcal{BA}\Phi(x) = -idx^1\vee dx^2\vee\Phi(x)$. For the reasons explained in section 6.1.2, the discrete counterpart of $-idx^1\vee dx^2\vee$ acting on $\tilde{\Phi}$ only exactly represents $\psi(x)\rightarrow\sigma_3\psi(x)$ when the $\psi(x)$ fields are linear.

In GD, $*$ maps between the original and dual complexes and in the next section, we shall see how we can take advantage of the correspondence between $\sigma_3\psi(x)$ and $-i*\mathcal{BA}\Phi$ from the continuum and the definition of $*$ on the complex to construct chiral and flavour projection operators that isolate different chiral or flavour components on each complex.

6.2 The Role of the Dual Complex

Our goal is to isolate select components of the fields on each complex. We want to construct projection operators that project different flavours or chiralities of fermion on to each of the original and dual complexes. We shall see that this requires us to construct a field to place on the dual that adequately cancels with the fields on the original when we apply the projection operators.

6.2.1 The Projection Operators

To construct the projection operators, we resolve the Hodge star into two separate operators, just as de Beaucé and Sen did [64]: one that acts on the original complex and maps to the dual ($*_O$) and one that maps the other way ($*_D$).

$$* = *_O + *_D$$

Both $*_O$ and $*_D$ are defined so as to be consistent with section 5.1.4. All that differs are their domain and range. The square of this definition is $** = *_O *_D + *_D *_O$, which respects all the desirable properties of the theory.

We want to build our chiral projection operators so that they project a field of one chirality on to one complex and a field of the other chirality on to the other complex.

We define our chiral projection operator to be

$$P_{R/L} = \frac{1}{2}\left(1 \mp i *_d \mathcal{BA} \pm i *_o \mathcal{BA}\right)$$

Application of P_R leaves the right handed components of $\tilde{\Phi}$ on the original complex and the left handed components of $\tilde{\Phi}$ on the dual complex.

Just as there is a relationship between $\sigma_3\psi(x)$ and $-i * \mathcal{BA}\tilde{\Phi}$, there is also a relationship between $\psi(x)\sigma_3$ and $-i * \mathcal{B}\tilde{\Phi}$, as we saw in section 4.2. We can use this to construct flavour projection operators that leave one flavour of field on one complex and the other flavour on the other complex.

We define our flavour projection operators to be

$$P^{(b)} = \frac{1}{2}\left(1 \mp i *_d \mathcal{B} \pm i *_o \mathcal{B}\right)$$

Application of $P^{(1)}$ leaves the first flavour of field on the original complex and the second flavour of field on the dual.

6.2.2 The Field on the Dual Complex

Unfortunately, it is not enough to just place normal geometrically discretized fermion fields on the dual complex, if we want the components to cancel correctly when we

apply these projection operators. Although the fields will have the right structure in terms of the trace of the σ matrices and ψ, the domains of integration will be different.

Instead, for the dual complex, we use $\tilde{\phi}([..]_D, [..]_O)$ to denote a field associated with the simplex $[..]_D$ and whose value in terms of the σ_i and ψ is associated with the simplex $[..]_D$, but whose domain of integration is the simplex $[..]_O$ from the original complex. This enables us to write the field for the dual as

$$\sum_{[H]} \tilde{\phi}([H]_D, [\mathcal{C}H]_O)[H]$$

where $[\mathcal{C}H]$ denotes the simplex of complementary dimension, but same barycentre as the simplex $[H]$. We can write down the term $\tilde{\phi}([..]_D, [..]_O)$ explicitly as

$$\tilde{\phi}\left([H]_D, [\mathcal{C}H]_O\right) = \int_{[\mathcal{C}H]_O} \mathrm{Tr}\left[\sigma_H^\dagger \psi\right] dx^{\mathcal{C}H}$$

The changes to the domain are implemented so as to affect only the initial discretization of the fields. They do not apply to the De Rham used in the definition of the discrete operators. As such, they allow the proper cancellation without changing the algebra of the geometric discretization.

6.2.3 Commutation Relations

In the Dirac basis, the requirement for chiral symmetry is $\{\sigma_3, \partial\!\!\!/\} = 0$. The equivalent statement in the Dirac-Kähler basis is $\{-i * \mathcal{BA}, d - \delta\} = 0$ and it follows that this is true for the geometric discretization: $\{-i * \mathcal{BA}, D - \delta\} = 0$.

Flavour symmetry follows from the associativity of matrix multiplication, in the Dirac basis: $(\partial\!\!\!/\psi(x))\sigma_3 = \partial\!\!\!/(\psi(x)\sigma_3)$. As we saw in 4.2, $\psi(x)\sigma_3 \Leftrightarrow -i * \mathcal{B}\Phi(x)$, so the equivalent statement in the Dirac-Kähler basis is $[-i * \mathcal{B}, d - \delta] = 0$. It follows that this is also true for the geometric discretization: $[-i * \mathcal{B}, D - \delta] = 0$.

6.2.4 Simultaneously Isolating Chiral and Flavour Components

Before we proceed, it will be best for us to briefly review what we have achieved so far in the context of staggered fermions.

Essentially, we have used two staggered fermion formulations with one on the original complex and one on the dual. The discrete differential geometry has ensured that the incarnation on the dual is similar to that on the original, except that it is already multiplied by σ_3. The $P_{R/L}$ operator leaves $\frac{1}{2}(1+\sigma_3)\psi$ on one complex and $\frac{1}{2}(1-\sigma_3)\psi$ on the other. The $P^{(b)}$ operator leaves $\psi\frac{1}{2}(1+\sigma_3)$ on one complex and $\psi\frac{1}{2}(1+\sigma_3)$ on the other.

This gives us a way to isolate the flavours or chiral components of the spinors, but we cannot isolate both simultaneously. For example, we can use $P_{R/L}$ so that one complex will have the upper components from the spinors and the other will have the lower components. However, this makes the system unsuitable for separating the flavour components. If we apply $P^{(b)}$ now, we will reintroduce negative chiral components on to the complex containing just the positive components and vice versa.

To project out the chiral and flavour components simultaneously, we must introduce another pair of complexes: another original complex and another dual. If we denote the first set of original and dual as A and the additional set as B, then we can modify the flavour projection operators, $P^{(b)}$ so that they map between original and dual complexes from different sets, whilst $P_{R/L}$ map between complexes in the same set. This is illustrated in Figure 11.

With these operators, we apply P_R to the A set, so that it leaves the right components of ψ on the original of A and the left components on the dual of A. We apply P_L to the B set, so that it leaves the left components of ψ on the original complex of B and the right components on the dual of B.

Next we apply $P^{(b)}$. Using $P^{(1)}$, we combine the right components of ψ on the original of A and the right components of ψ on the dual of B to leave the right components of flavour 1 on the original of A and the right components of flavour 2 on the dual of B. We use $P^{(2)}$ to combine the left components of ψ on the dual complex of A and the left components on the original complex of B to leave the left components of flavour 1 on the dual complex of A and the left components of flavour 2 on the original complex of B.

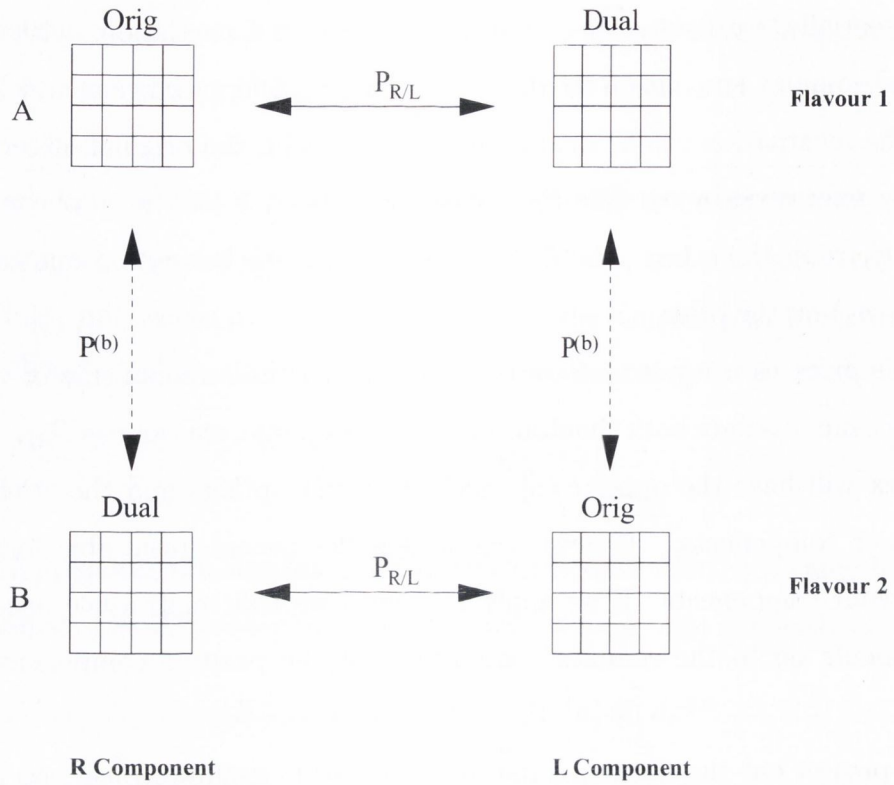

Figure 11: How we isolate the four chiral and flavour components.

We now have four independent non-degenerate, chiral fields, each of which respect the Dirac-Kähler algebra.

After this projection, the contributions from all four complexes must be included in the action

$$S = S_O^A + S_D^A + S_O^B + S_D^B$$

6.2.5 In Four Dimensions

It is interesting to extend these ideas to four dimensions because the flavour symmetry becomes more involved.

The structure of the chiral projection operator remains the same, although the details differ. Instead of the relationship $\sigma_3\psi \Leftrightarrow -i*\mathcal{BA}\Phi$, we have $\gamma_5\psi \Leftrightarrow -*\mathcal{BA}\Phi$ and the chiral projection operators become

$$P_{R/L} = \frac{1}{2}\left(1 \mp *\mathcal{BA}\right)$$

For the right multiplication of γ_5 to ψ we have $\psi\gamma_5 \Leftrightarrow -*\mathcal{B}\Phi$. However, in four dimensions, there are four columns of ψ which means that we have four flavours to separate. Consequently, in order to separate the four flavours, we need a second projection operator and we can see this in equation (18) where the flavour projection operator $P^{(b)}$ comprises two projections: $\frac{1}{2}(1+i\alpha_b\gamma_1\gamma_2)$ and $\frac{1}{2}(1+\beta_b\gamma_1\gamma_2\gamma_3\gamma_4)$. The second projection that we need corresponds to the factor of $\frac{1}{2}(1+i\alpha_b\gamma_1\gamma_2)$.

It is apparent from the preceding sections that when we apply $\sigma_3(=-i\sigma_1\sigma_2)$ to ψ in two space-time dimensions, the corresponding action in differential geometry is to map each form to its complement in both the 1 and 2 dimensions. In four space-time dimensions, when we apply $\gamma_1\gamma_2\gamma_3\gamma_4$ to ψ, the corresponding action in differential geometry is to map each form to its complement in all four space-time dimensions. In the same way, we translate the application of $\gamma_1\gamma_2$ to ψ in terms of differential geometry by identifying it with mapping a form to its complement in the 1 and 2 directions, but not in the 3 and 4 directions. As in the case of the Hodge star, to capture this property discretely, we must introduce another complex, ensuring that the map to and from this extra complex is local and that its square is proportional to the identity.

We cannot draw a 4D picture of how this extra complex relates to the original and the dual, but we can draw its analogue in two dimensions. In Figure 12, we have the original 2D complex, drawn with a black continuous line. The dual complex is drawn with a black dashed line. A complex that is complementary to the original in the 1 direction, but not the 2, is shown in red. Its 1-direction lines lie on top of the original complex and its 2-direction lines lie on top of the dual complex. We have shown the lines of this complex slightly offset in order to make them easier to distinguish.

To put this on a mathematical footing, we define the operator ♠ that maps a differential form to its complement in the 1 and 2 dimensions, leaving the 3 and 4 dimensions untouched.

$$\spadesuit dx^H = \rho_{H_{12},\mathcal{C}H_{12}} dx^{(\mathcal{C}H_{12})H_{34}}$$

Here $\mathcal{C}$ is the complement in the $\{1,2\}$ dimensions. We can show (see Appendix B)

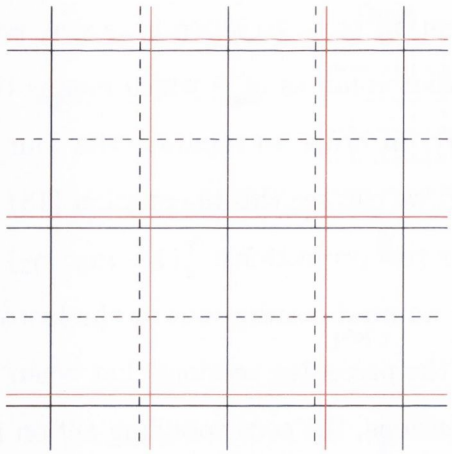

Figure 12: The 2D complex. Black continuous lines denote the original complex, black dashed lines denote the dual and red lines denote the complex that is complementary to the original in the 1 direction, but not in the 2 direction.

that

$$\psi\gamma_1\gamma_2 \quad \Leftrightarrow \quad \spadesuit\mathcal{B}_{12}\Phi$$

where $\mathcal{B}_{12}$ is defined to be consistent with the previous definition, but is limited to the $\{1,2\}$ subspace:-

$$\mathcal{B}_{12}dx^H = \binom{h_{12}}{2}dx^H$$

where h_{12} is the number of components of H in the subspace $\{1,2\}$.

Alas, this is not the complete picture. The extra complex that we have introduced also has a dual. These four complexes enable us to separate all four flavours of field so that each goes on a unique complex. Figure 13 shows the analogues of all four complexes in two dimensions. The fourth complex can be interpreted either as the dual to the extra complex or as the complement in the 1 dimension of the dual complex. Which way we describe it is only a matter of the order in which we apply the $*$ and $\spadesuit$ operators, starting from the original complex.

To separate the flavour components we take a similar approach to the previous 2D case.

In Appendix B, we see that $\psi\gamma_5 \Rightarrow Z\gamma_5^T \Leftrightarrow -*\mathcal{B}\Phi$, so we write the factor from the flavour projection operator involving $\gamma_1\gamma_2\gamma_3\gamma_4$ as $\frac{1}{2}(1+\beta_b * \mathcal{B})$. We also see in

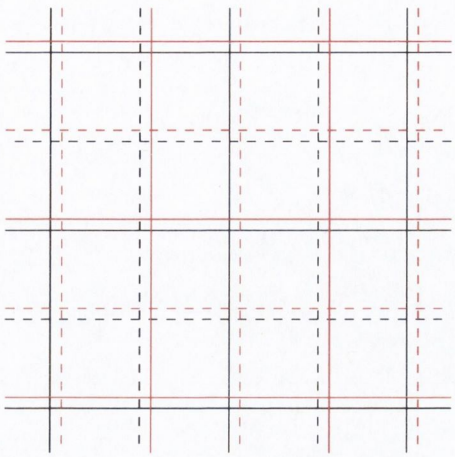

Figure 13: The 2D complex. In addition to the lines in Figure 12, we have included the dual to the extra complex in dashed red lines.

Appendix B the correspondence between right multiplication of ψ by $\gamma_1\gamma_2$ and $\spadesuit\mathcal{B}_{12}\Phi$. We write the other factor in the flavour projection operator as $\frac{1}{2}(1 + i\alpha_b\spadesuit\mathcal{B}_{12})$

As in the 2D case, we separate the Hodge star into maps between the complexes: $* = *_{od} + *_{do} + *_{et} + *_{te}$. In addition to labelling the original and dual complexes by o and d, we introduce labels here for the other two complexes. e denotes the *extra* complex related to the original by $\{1, 2\}$ complementarity. We shall christen this complex, the *12c* complex. t denotes the final complex: the dual of the 12c complex (or the 12 complement of the dual, depending on how you choose to look at it). We shall name this complex the *12cd* (12-complement's dual) and the reason for labelling t becomes apparent when we look at Figure 13. With the 12c and 12cd complexes, the complete pattern looks like tartan.

$*_{od}$ maps from the original complex to the dual and $*_{do}$ maps the other way. $*_{et}$ maps from the 12c complex to the 12cd complex and $*_{te}$ maps the other way. If we take the square of $*$, we have $** = *_{od}\,*_{do} + *_{do}\,*_{od} + *_{et}\,*_{te} + *_{te}\,*_{et}$. All other terms are zero because of the lack of continuity between their range and domain.

We rewrite the factor containing $\gamma_1\gamma_2\gamma_3\gamma_4$, from the flavour projection operator, as

$$P_{\beta_b} = \frac{1}{2}\left(1 + \beta_b *_{do} \mathcal{B} - \beta_b *_{od} \mathcal{B} + \beta_b *_{et} \mathcal{B} - \beta_b *_{te} \mathcal{B}\right)$$

For the other projection, we follow the same logic. We write $\spadesuit$ as $\spadesuit = \spadesuit_{oe} + \spadesuit_{eo} + \spadesuit_{dt} + \spadesuit_{td}$. The square of this is $\spadesuit\spadesuit = \spadesuit_{oe}\spadesuit_{eo} + \spadesuit_{eo}\spadesuit_{oe} + \spadesuit_{dt}\spadesuit_{td} + \spadesuit_{td}\spadesuit_{dt}$. As in the previous case, all other terms go to zero because of their lack of continuity between the domain and range.

Here, $\spadesuit_{oe}$ maps from the original complex to the 12c complex and $\spadesuit_{eo}$ maps the other way. $\spadesuit_{dt}$ maps from the dual complex to the 12cd complex and $\spadesuit_{td}$ maps the other way.

We construct the projection operator as

$$P_{\alpha_b} = \frac{1}{2}\left(1 + i\alpha_b\spadesuit_{eo}\mathcal{B}_{12} - i\alpha_b\spadesuit_{oe}\mathcal{B}_{12} + i\alpha_b\spadesuit_{td}\mathcal{B}_{12} - i\alpha_b\spadesuit_{dt}\mathcal{B}_{12}\right)$$

To resolve the flavour components on each complex under the application of the complete projection operator, we must first decide what fields to put on the dual, 12c and 12cd complexes. As in two space-time dimensions, the consideration is the domain of integration. The fields on all four complexes must be discretized using the same domains of integration so that, after projection, the correct cancellation occurs.

We shall choose the domains to be consistent with the simplices of the original complex, although the choice is arbitrary. Naturally, the fields that go on the original complex are the normal fields that are discretized in accordance with section 5.1.1. On the dual, we put the fields

$$\sum_H \tilde{\phi}\left([H]_d, [\mathcal{C}H]_o\right)[H]_d$$

where each field is associated with the simplex $[H]_d$, but is initially integrated over the region $[\mathcal{C}H]_o$ from the original complex. In this instance $\mathcal{C}$ denotes complementarity in all 4 dimensions. On the 12c complex, we put

$$\sum_H \tilde{\phi}([H]_{12c}, [\mathcal{C}_{12}H]_o)[H]_{12c}$$

Finally, on the 12cd complex, we put

$$\sum_H \tilde{\phi}([H]_{12cd}, [\mathcal{C}_{34}H]_o)[H]_{12cd}$$

In each instance of $\tilde{\phi}([A],[B])$, $[A]$ indicates the simplex associated with the field: the simplex that defines the field structure in terms of σ and ψ and is used to implement

the Dirac-Kähler algebra. The second simplex, $[B]$, indicates the initial domain of integration. For the formulation that we have discussed here, the regions always correspond to simplices from the original complex. The operations $\mathcal{C}_{12}$ and $\mathcal{C}_{34}$ denote complementarity in just the $\{1,2\}$ and $\{3,4\}$ subspaces, respectively.

The projection operations commute with the discrete Dirac-Kähler equation, which means that the Dirac-Kähler algebra does not mix these flavours (see Appendix B.3).

As in the 2D case, we cannot simultaneously isolate the chiral and flavour components of the fields using just one set of complexes, so we must introduce a second set.

In the 2D case, we chose to separate the chiral components within the same set and then isolate the flavours by projecting between the sets. However, this was an arbitrary choice. We could equally as well have chosen to separate the flavours within the sets and isolate the chiral components by projecting between the sets. In 4D, it makes much more sense to use the latter arrangement. This will give us two sets of complexes, A and B, each containing the four complexes: original, dual, 12-complement and 12-complement-dual. In total we now have eight complexes.

Firstly, we will look at how the flavours separate within each set. To this end, we write the flavour projection operator as $P^{(b)} = P_{\beta_b} P_{\alpha_b}$.

On set A, we apply $P^{(1)}$. The first projection is P_{α_1} and this puts columns 1 and 3 of ψ on the original complex and columns 2 and 4 of ψ on the 12c complex. It also puts columns 1 and 3 of ψ on the dual complex and columns 2 and 4 on the 12cd complex.

The second projection is P_{β_1} and this takes columns 1 and 3 from both the original and dual complexes and leaves just column 1 on the original complex and just column 3 on the dual. It also takes columns 2 and 4 from the 12c and 12cd complexes and leaves column 4 on the 12c complex and column 2 on the 12cd complex. Figure 14 illustrates how P_{α_i} and P_{β_i} act within the set.

On set B, we apply $P^{(3)}$. The first projection, P_{α_3}, leaves columns 1 and 3 of ψ on the original and dual complexes and leaves columns 2 and 4 on the 12c and 12cd

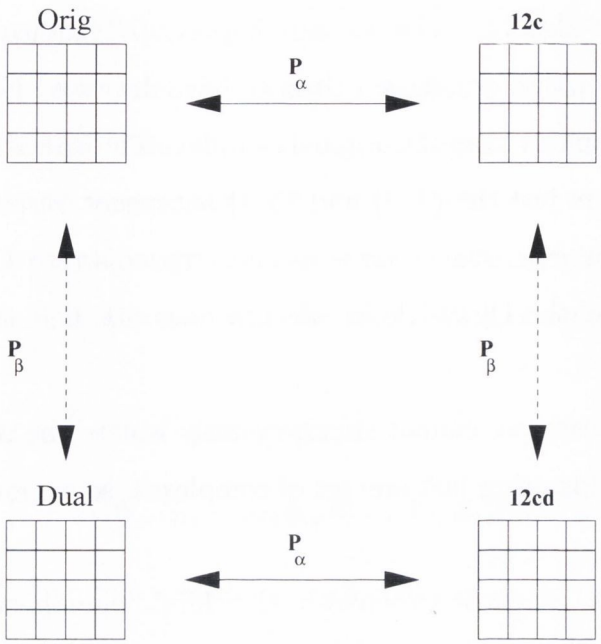

Figure 14: The complexes of 4D. P_α and P_β denote the parts of the flavour projection operator.

complexes. The second projection, P_{β_3}, leaves column 3 on the original complex and column 1 on the dual, as well as leaving column 2 on the 12c complex and column 4 on the 12cd complex.

We project between the sets to separate the chiral components and this is illustrated in Figure 15. We define the Hodge star so that it maps between the following pairs of complexes: (original of A, dual of B), (12c of A, 12cd of B), (12cd of A, 12c of B) and (dual of A, original of B). $P_{R/L}$ takes the form

$$\begin{aligned} P_{R/L} \;=\; & \tfrac{1}{2}\left(1 \pm *_{do}^{BA}\mathcal{BA} \mp *_{od}^{AB}\mathcal{BA} \pm *_{od}^{BA}\mathcal{BA} \mp *_{do}^{AB}\mathcal{BA}\right. \\ & \left. \pm *_{et}^{BA}\mathcal{BA} \mp *_{te}^{AB}\mathcal{BA} \pm *_{te}^{BA}\mathcal{BA} \mp *_{et}^{AB}\mathcal{BA}\right) \end{aligned}$$

and by applying P_R, we leave the positive chiral components of column 1 of ψ on the original complex of set A and the negative chiral components of column 1 on the dual of set B. It also leaves the positive chiral components of column 3 on the dual of A and the negative chiral components on the original of B. It leaves the positive chiral components of column 2 on the 12cd complex of A and the negative chiral components on the 12c complex of set B. It also leaves the positive chiral

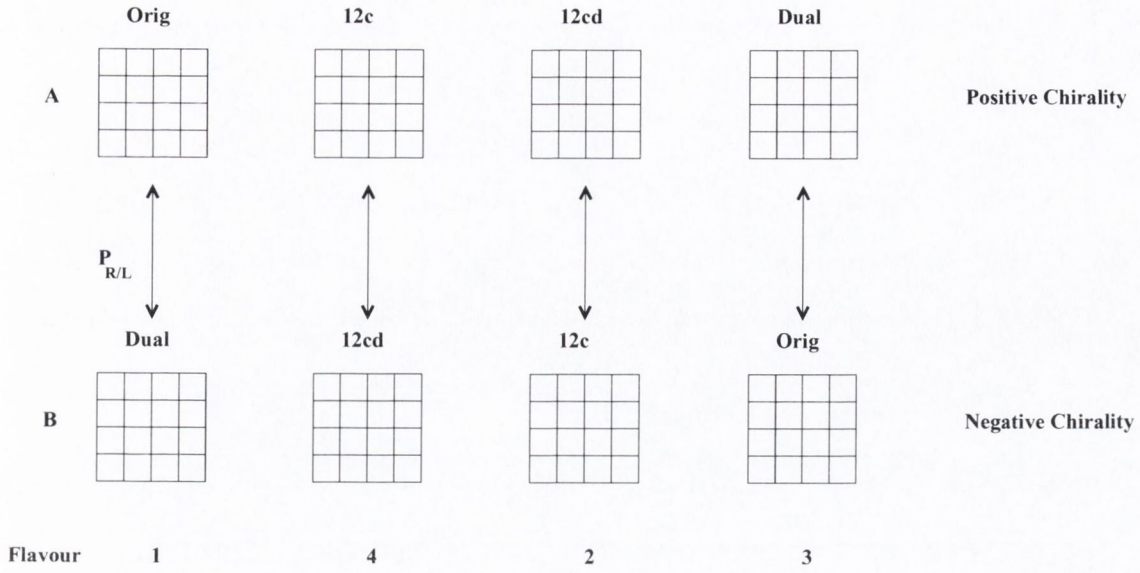

Figure 15: The two sets of complex in 4D. $P_{R/L}$ combines complexes from different sets to isolate the chiral components of each flavour.

components of column 4 on the 12c complex of A and the negative components on the 12cd complex of B.

6.3 Abelian Field Theory

In this description we now have several complexes. However, the formulation of the gauge theory is the same on each complex, so it only needs to be described once. The same formulation will generalise to higher dimensions and to more complexes in a very straight forward manner. In this section, we shall describe the gauge field formulation for the established geometric discretization, described in section 5.

In section 4.2, we saw that the continuum construction of the covariant Dirac-Kähler equation is $(d-\delta)\Phi(x) = iA(x) \vee \Phi(x)$, where $A(x)$ is a one-form. This is our starting point for constructing an Abelian field theory for the geometric discretization.

We discretize the fields by using the De Rham map. The $A(x)$, being one-forms, are discretized only over the one-simplices. Their discrete counterparts are denoted $\tilde{A}([..])$

Interestingly, even at this early stage, the dual complex starts to make its presence

felt. The definition of the adjoint derivative is proportional to $*D*$, in which D is the derivative operating on the dual complex. As a result, the Dirac-Kähler operator differentiates on both complexes. Hence, in order for it to be covariant, there must be a gauge field contribution to the Dirac-Kähler equation from both complexes. To achieve this we replace, $\tilde{A}\vee$ with $\tilde{A}_o \wedge + * \tilde{A}_d \wedge *$. We use the suffixes o and d to indicate whether the fields are on the original or dual complexes, respectively.

6.3.1 The Gauge Transformation

In the continuum, an Abelian gauge transform is a zero-form. To discretize this, we sample the continuous function at the vertices of the complex. If G denotes the continuous gauge transform: $e^{i\theta(x)}$, the discretized version is $\tilde{G} = \sum_Z e^{i\tilde{\theta}([Z])}$, where the $\tilde{\theta}([Z])$ are the fields $\theta(x)$ sampled at the zero-simplices $[Z]$.

We define the Abelian gauge transformation to be

$$\tilde{\Phi} \rightarrow R\left[W\left(e^{i\tilde{\theta}}\right) W\left(\tilde{\Phi}\right)\right]$$

If we use the reference square in Figure 6, we can illustrate this transform with the following examples.

$$\tilde{\phi}([A])[A] \rightarrow e^{i\tilde{\theta}([A])}\tilde{\phi}([A])[A]$$

$$\tilde{\phi}([AB])[AB] \rightarrow \frac{1}{2}\left(e^{i\tilde{\theta}([A])} + e^{i\tilde{\theta}([B])}\right)\tilde{\phi}([AB])[AB]$$

$$\tilde{\phi}([ABCD])[ABCD] \rightarrow \frac{1}{4}\left(e^{i\tilde{\theta}([A])} + e^{i\tilde{\theta}([B])} + e^{i\tilde{\theta}([C])} + e^{i\tilde{\theta}([D])}\right)\tilde{\phi}([ABCD])[ABCD]$$

We infer that the conjugate field must transform as follows, in order to keep the bilinear, $< \bar{\tilde{\Phi}}, \tilde{\Phi} >$, invariant,

$$\bar{\tilde{\phi}}([A])[A] \rightarrow \bar{\tilde{\phi}}([A])\left[e^{i\tilde{\theta}([A])}\right]^{-1}[A]$$

$$\bar{\tilde{\phi}}([AB])[AB] \rightarrow \bar{\tilde{\phi}}([AB])\left[\frac{1}{2}\left(e^{i\tilde{\theta}([A])} + e^{i\tilde{\theta}([B])}\right)\right]^{-1}[AB]$$

$$\bar{\tilde{\phi}}([ABCD])[ABCD] \rightarrow \bar{\tilde{\phi}}([ABCD])\left[\frac{1}{4}\left(e^{i\tilde{\theta}([A])} + e^{i\tilde{\theta}([B])} + e^{i\tilde{\theta}([C])} + e^{i\tilde{\theta}([D])}\right)\right]^{-1}[ABCD]$$

Now that we know how the fields transform, we can look at how the gauge fields must transform, in order for the action to remain invariant. The Dirac-Kähler equation with transformed spinor fields looks like

$$(D-\delta)R\left[W\left(e^{i\tilde{\theta}}\right)W\left(\tilde{\phi}\right)\right] = ie\left(\tilde{A}_o\wedge + * \tilde{A}_d \wedge *\right) R\left[W\left(e^{i\tilde{\theta}}\right)W\left(\tilde{\Phi}\right)\right] \qquad (24)$$

To analyse this, we break it into two parts. The first contains the D and $\tilde{A}_o$ terms and concerns the original complex. The second contains the δ and $\tilde{A}_d$ terms and concerns the dual.

For the first, we have

$$(D)R\left[W\left(e^{i\tilde{\theta}}\right)W\left(\tilde{\Phi}\right)\right] = ie\tilde{A}_o\wedge R\left[W\left(e^{i\tilde{\theta}}\right)W\left(\tilde{\Phi}\right)\right]$$

D obeys Leibnitz's rule, which means that we can write

$$(D)R\left[W\left(e^{i\tilde{\theta}}\right)W\left(\tilde{\Phi}\right)\right] = R\left[\left\{dW\left(e^{i\tilde{\theta}}\right)\right\}\wedge\left\{W\left(\tilde{\Phi}\right)\right\}+\left\{W\left(e^{i\tilde{\theta}}\right)\right\}\left\{dW\left(\tilde{\Phi}\right)\right\}\right]$$

We must introduce a transformation rule for the field $\tilde{A}_o\wedge$ so that it cancels with the first term on the right hand side. At this stage it is fairly arbitrary how we distribute the transform about a transforming wedge and a transforming field. One way would be to define the wedge to transform as $[H]\wedge[K]\rightarrow[H]G([H\cup M])\wedge[G(M)]^{-1}[M]$ and the $\tilde{A}_o$ to transform as $\tilde{A}_o\rightarrow\tilde{A}_o-\frac{i}{e}[G([..])]^{-1}R[dW(e^{i\tilde{\theta}})]$, where in the wedge expression the $G[([..])]$ are the gauge transforms on the simplex $[H]$ (defined as $G([H])=R\left[W(e^{i\tilde{\theta}})W([H])\right]$) and in the $\tilde{A}_o$ expression, the $G([..])$ is the gauge transform on the simplex to which $\tilde{A}_o$ is wedged. However, a simpler description would be to eliminate the transformation for $\wedge$ and instead use

$$\tilde{A}_o\rightarrow\tilde{A}_o-\frac{i}{e}R\left[dW(e^{i\tilde{\theta}})\right][G([..])]^{-1}$$

where $G([..])$ is the gauge transform on the simplex to which $\tilde{A}_o$ is being applied. In either case, $\tilde{A}_o$ is forced to become an operator because its transformations depends on context. Ultimately, it will not matter which definition we choose because they will amount to the same computational algorithms. However, the former would require $\wedge$ to be a context dependent operator, so the latter is preferred.

The second part of equation (24) gives

$$-\delta R\left[W\left(e^{i\tilde{\theta}}\right)W\left(\tilde{\Phi}\right)\right] = ie * \tilde{A}_d \wedge *R\left[W\left(e^{i\tilde{\theta}}\right)W\left(\tilde{\Phi}\right)\right] \tag{25}$$

In this case, $\delta = - * D*$, so we must apply the Hodge star before we can address the covariance. In order for Leibnitz's rule to hold on the dual complex, the gauge transformation term must be defined on the same complex as the Dirac-Kähler fields. This means that the Hodge star must transform in a way that replaces the gauge transformation on the original complex with that on the dual. This makes the Hodge star transformation context dependent. For the case where $*$ maps between the simplices $[H]$ and $[M]$ as $*[M] = \pm[K]$, we must have the following transformation

$$* \rightarrow G([H]) * [G([M])]^{-1}$$

where $G([H])$ and $G([M])$ are the gauge transforms on the simplices $[H]$ and $[M]$, respectively.

We can use this to simplify equation (25) to

$$*dR\left[W\left(e^{i\tilde{\theta}}\right)W\left(*\tilde{\Phi}\right)\right] = ie * \tilde{A}_d \wedge R\left[W\left(e^{i\tilde{\theta}}\right)W\left(*\tilde{\Phi}\right)\right]$$

and we can use Leibnitz's rule on this expression to obtain a similar transformation law as for the original complex

$$\tilde{A}_d \rightarrow \tilde{A}_d - \frac{i}{e}R\left[dW(e^{i\tilde{\theta}})\right][G([..])]^{-1}$$

The last operator that we must consider is the 12 complement operator, introduced in the last chapter as $\spadesuit$. Although this is a similar operator to the Hodge star and will have similar transformation properties, the reasons for defining the transformation are slightly different. In this case, we want $\spadesuit$ to transform so that the projection operators P_{α_B} maintain gauge invariance. The transformation law that we have defined above for $*$ guarantees that this is the case for the P_{β_b} projection operator.

The transformation law we require is

$$\text{If } \spadesuit[H] = \rho_{H_{12},\mathcal{C}H_{12}}[(\mathcal{C}H_{12})H_{34}]: \qquad \spadesuit \rightarrow G([(\mathcal{C}H_{12})H_{34}])\spadesuit[G([H])]^{-1}$$

where $G([H])$ is the gauge transform factor on the simplex that $\spadesuit$ is applied to and $G([(\mathcal{C}H_{12})H_{34}])$ is the simplex to which $[H]$ is mapped.

This completes the transformations necessary for our discrete Dirac-Kähler to be covariant. For later convenience, we summarize the transformation rules here

$$\begin{aligned}
\tilde{\phi} &\to R\left[W\left(e^{i\tilde{\theta}}\right)W\left(\tilde{\phi}\right)\right] \\
\bar{\tilde{\phi}}([..]) &\to \bar{\tilde{\phi}}([..])\left[R\left\{W(e^{i\tilde{\theta}})W([..])\right\}\right]^{-1} \\
\text{For } *[M] = \pm[K] \quad &: \quad * \to G([H]) * [G([M])]^{-1} \\
\text{For } \spadesuit[H] = \pm[(\mathcal{C}H_{12})H_{34}] : \quad &\spadesuit \to G([(\mathcal{C}H_{12})H_{34}])\spadesuit\,[G([H])]^{-1} \\
\tilde{A}_o &\to \tilde{A}_o - \tfrac{i}{e}R\left[dW(e^{i\tilde{\theta}})\right][G([..])]^{-1} \\
\tilde{A}_d &\to \tilde{A}_d - \tfrac{i}{e}R\left[dW(e^{i\tilde{\theta}})\right][G([..])]^{-1}
\end{aligned} \tag{26}$$

6.3.2 The Gauge Action

In the continuum, the differential geometry description of the gauge action is $-\frac{1}{2} < dA, dA >$, where dA corresponds to $F_{\mu\nu}$. The factor of $\frac{1}{2}$ replaces the conventional $\frac{1}{4}$ because the sums over indices are ordered and the antisymmetry of the differential forms accounts for the antisymmetry of the indices μ and ν. Within our geometric discretization, the gauge action has the corresponding definition: $S_G = -\frac{1}{2} < D\tilde{A}_o, D\tilde{A}_o > -\frac{1}{2} < D\tilde{A}_d, D\tilde{A}_d >$.

This expression is invariant under the gauge transformations (26). In the definition S_G, the $\tilde{A}$ are not wedged to other simplices, outside the mechanism of the inner product. Consequently, the factors of $[G([..])]^{-1}$ are equal to the identity. This leaves us with only the part of the gauge transform that involves the derivative of the field $e^{i\tilde{\theta}}$ to consider. In this case, we can rewrite the last two lines of equation (26) as

$$\begin{aligned}
\tilde{A}_o &\to \tilde{A}_o - \frac{i}{e}D\left[e^{i\tilde{\theta}}\right] \\
\tilde{A}_d &\to \tilde{A}_d - \frac{i}{e}D\left[e^{i\tilde{\theta}}\right]
\end{aligned}$$

The terms $D\tilde{A}_o$ and $D\tilde{A}_d$ then transform as $D\tilde{A}_o \to D\tilde{A}_o - \frac{i}{e}D^2\left[e^{i\tilde{\theta}}\right]$ and $D\tilde{A}_d \to D\tilde{A}_d - \frac{i}{e}D^2\left[e^{i\tilde{\theta}}\right]$. One of the properties of the exterior derivative is that $D^2 = 0$, both in the continuum and in our geometric discretization and this makes the gauge action invariant.

6.3.3 The Lorentz Gauge

The configuration space of the gauge field can be classified into groups of field configurations that are related by a transformation. We can span the space by taking a sample element from each group and using the transformation rules. When we define a gauge invariant observable and naively integrate it over the configuration space, we end up over counting the configurations that the observable would consider indistinguishable. The value of the observable is then ill defined, so we must pick a representative configuration from each group. A gauge fixing condition achieves this.

In the continuum, the Lorentz gauge fixing condition is $\partial_\mu A^\mu(x) = 0$. Within an action, the gauge fixing contribution is $S_{GF} = -\frac{1}{2\xi}\int dx^2 \left(\partial_\mu A^\mu(x)\right)^2$ and this term cancels with part of the gauge action. We can see this if we use integration by parts to rewrite $-\frac{1}{4}F_{\mu\nu}F^{\mu\nu}$ as

$$S_G = -\frac{1}{4}F^{\mu\nu}F_{\mu\nu} = -\frac{1}{2}\left(A^\mu \partial^\nu \partial_\mu A_\nu - A^\mu \partial^\nu \partial_\nu A_\mu\right)$$

We can rewrite the gauge fixing condition as

$$S_{GF} = -\frac{1}{2\xi}\left(\partial^\mu A^\mu\right)^2 = \frac{1}{2\xi}A^\mu \partial_\mu \partial^\nu A_\nu$$

When $\xi = 1$, this term cancels with the first term in S_G. For the geometric discretization we use $-\frac{1}{2\xi} < \delta A, \delta A >$ for S_{GF}. If we expand the definition of S_G, we have

$$\begin{aligned} S_G &= -\frac{1}{2} < D\tilde{A}_1, D\tilde{A}_1 > -\frac{1}{2} < D\tilde{A}_2, D\tilde{A}_2 > \\ &\quad -\frac{1}{2} < D\tilde{A}_1, D\tilde{A}_2 > -\frac{1}{2} < D\tilde{A}_2, D\tilde{A}_1 > \end{aligned}$$

Expanding S_{GF} similarly, we have

$$\begin{aligned} S_{GF} &= -\frac{1}{2\xi} < \delta\tilde{A}_1, \delta\tilde{A}_1 > -\frac{1}{2\xi} < \delta\tilde{A}_2, \delta\tilde{A}_2 > \\ &\quad -\frac{1}{2\xi} < \delta\tilde{A}_1, \delta\tilde{A}_2 > -\frac{1}{2\xi} < \delta\tilde{A}_2, \delta\tilde{A}_1 > \end{aligned}$$

Because of the inclusion of the dual complex, we have Stokes law: $< DP, Q > = < P, \delta Q >$, for two discrete fields P and Q. For the definition of δ in section 5.1.5, we

can rewrite S_G and S_{GF} as

$$\begin{aligned} S_G &= -\frac{1}{2} < \tilde{A}_1, \delta D \tilde{A}_1 > -\frac{1}{2} < \tilde{A}_2, \delta D \tilde{A}_2 > \\ &\quad -\frac{1}{2} < \tilde{A}_1, \delta D \tilde{A}_2 > -\frac{1}{2} < \tilde{A}_2, \delta D \tilde{A}_1 > \end{aligned}$$

$$\begin{aligned} S_{GF} &= -\frac{1}{2\xi} < \tilde{A}_1, D\delta \tilde{A}_1 > -\frac{1}{2\xi} < \tilde{A}_2, D\delta \tilde{A}_2 > \\ &\quad -\frac{1}{2\xi} < \tilde{A}_1, D\delta \tilde{A}_2 > -\frac{1}{2\xi} < \tilde{A}_2, D\delta \tilde{A}_1 > \end{aligned}$$

When we add these two terms and set $\xi = 1$, we see some interesting differences between the geometric discretization and the continuum. In the continuum, we have $d\delta = -\delta d$ when the directions of $dx^\mu \wedge \partial_\mu$ and $e^\nu \lrcorner \partial_\nu$ are different and $d\delta = \delta d$ when they are the same. As a result, in the continuum, we could cancel the bottom line from each term and combine the top lines. Combining the top lines would give us a term proportional to the second derivative, which is what we see in the Dirac basis description. However in the geometric discretization, the identity $D\delta = -\delta D$ only holds when the fields are perpendicular to each other. When they are parallel, there is no equivalence. This means that the two bottom lines can successfully cancel and the two top lines cannot be combined. This leaves us with

$$\begin{aligned} S_G + S_{GF} &= -\frac{1}{2} < D\tilde{A}_1, D\tilde{A}_1 > -\frac{1}{2} < D\tilde{A}_2, D\tilde{A}_2 > \\ &\quad -\frac{1}{2\xi} < \delta\tilde{A}_1, \delta\tilde{A}_1 > -\frac{1}{2} < \delta\tilde{A}_2, \delta\tilde{A}_2 > \\ &\quad -\frac{1}{2}\left(1 - \frac{1}{\xi}\right) < D\tilde{A}_1, D\tilde{A}_2 > -\frac{1}{2}\left(1 - \frac{1}{\xi}\right) < D\tilde{A}_2, D\tilde{A}_1 > \end{aligned}$$

When $\xi = 1$, we are left with terms that can be rearranged to make

$$S_G + S_{GF} = -\frac{1}{2} < \tilde{A}_\mu, -(D\delta + \delta D)\tilde{A}_\mu >$$

where $-(D\delta + \delta D)$ is the definition of the Laplacian operator seen in section 4.1.

6.3.4 The Path Integral Measure

It is not always straight forward to show that the measure of integration for a path integral respects the gauge transformations of the action. The revelation that the

fermion measure of continuum gauge theory did not respect axial symmetry led to the discovery of the axial anomaly [70].

For our purposes, we must be sure that the measures of integration of the fermion and gauge fields respects the transformation of equation (26).

For a given transformation, $\tilde{\phi} \rightarrow R\left[W\left(e^{i\tilde{\theta}}\right) W\left(\tilde{\phi}\right)\right]$, the result is a term that resembles $\frac{1}{N}\left[e^{i\tilde{\theta}([A_1])} + e^{i\tilde{\theta}([A_2])} + ... + e^{i\tilde{\theta}([A_N])}\right]\tilde{\phi}$. The term $\frac{1}{N}$ [..] only provides a phase, so we can say that

$$d\tilde{\phi} \rightarrow R\left[W\left(e^{i\tilde{\theta}}\right) W\left(d\tilde{\phi}\right)\right]$$

where $d\tilde{\phi}$ represent the measure of integration. By the same reasoning, we can say that

$$d\bar{\tilde{\phi}}([..]) \rightarrow d\bar{\tilde{\phi}}([..])\left[R\left\{W(e^{i\tilde{\theta}})W([..])\right\}\right]^{-1}$$

For these transformations, the product of the measures, $d\bar{\tilde{\phi}}d\tilde{\phi}$, is invariant, just as in the continuum case for $U(1)_v$.

The gauge field transforms as $\tilde{A} \rightarrow \tilde{A} - \frac{i}{e}R\left[dW(e^{i\tilde{\theta}})\right][G([..])]^{-1}$. Under this transformation, the measure of integration, $d\tilde{A}$, transforms so that the correction is proportional to $D^2\tilde{A}$. D^2 of any field is zero, so the measure of integration for the gauge field is also invariant.

6.3.5 Topological Fields and Charge

In two continuous space-time dimensions, a topologically interesting gauge field trajectory is provided by

$$A_1(x) = 0 \qquad\qquad A_2(x) = -\omega x_1 \tag{27}$$

where ω is proportional to the field strength, F_{12}, and is constant across the manifold. The manifold itself is a 2D torus, with $x_\mu \in [0, L_\mu]$. The gauge fields are not periodic in the x_1 direction, but their value at $x_1 = 0$ and $x_1 = L_1$ can be related by a gauge transform. Consequently, any function or action that is gauge invariant will see this field as periodic in both directions. This configuration has previously been discussed in [71] and we use a similar description, but with the discontinuity along a different boundary.

In the Dirac basis, the gauge transform that we use at the boundary between $x_1 = 0$ and $x_1 = L_1$ is $U(x) = e^{iwL_1x_2}$, so that, with a unit coupling constant,

$$A_2(x_1 = 0) = A_2(x_1 = L_1) - i\Big(\partial_2 U(x)\Big)U^{-1}(x) = A_2(x_1 = L_1) + \omega L_1 \tag{28}$$

In this expression, $\omega = \frac{2\pi Q}{L_1 L_2}$, where Q is the topological charge, $Q = \frac{1}{2\pi}\int dx^2 F_{12}$. If we substitute for ω in U, we have $U = e^{i2\pi Q x_2/L_2}$ and for this to be periodic in x_2, Q must be an integer.

In the lattice description of this gauge trajectory there are complications. There is no true topology because lattice fields are comparable to multidimensional histograms and, as such, any field can be smoothly deformed into any other field. Nonetheless, we can follow the same strategy as in the continuum, replacing the topological charge with a parameter, τ, that admits non-integer values.

In standard lattice gauge theory, the topologically interesting gauge field trajectory is represented by [71] [72]

$$U_1(n_1, n_2) = \begin{cases} 1 & \text{if } n_1 \neq L-1 \\ \exp[\frac{2\pi i n_2 \tau}{L}] & \text{if } n_1 = L-1 \end{cases} \tag{29}$$

$$U_2(n_1, n_2) = \exp[\frac{-2\pi i n_1 \tau}{L^2}] \tag{30}$$

where we have taken $L_1 = L_2 = L$. The topological charge can be calculated as,

$$Q = \sum_P \frac{\ln[U_P]}{2\pi i} \tag{31}$$

There is some subtlety to this expression. U_P is the ordered product of the gauge links around a plaquette and it is a complex quantity. When we take the log of a complex quantity, we have to introduce branch cuts to remove the ambiguity associated with the periodicity of the exponential function. Any complex expression can be written as $z = re^{i\theta}$ and clearly $z = re^{i\theta} = re^{i(\theta+n2\pi)}$. Taking the log, we have that $\ln(z) = \ln(r) + i\theta = \ln(r) + i(\theta + n2\pi)$. To remove the confusion between $i\theta$ and $i(\theta + n2\pi)$, the coordinate space is divided into different patches by branch cuts. Branch cuts in general run between the singularities of a function. In the case of $\ln(z)$ the singularities are at $z = 1$, where $\ln(1) = 0$ and at infinity at some direction. We

choose the branch cut to lie along the negative real axis up to the point $z = 1$ and this means that when we take the log of U_P, the exponent stays in the region $[-\pi, \pi]$.

We can calculate Q analytically for the above gauge field. Doing so, we see that we have $L(L-1)$ plaquettes for which $U_P = e^{2\pi i\tau/L^2}$, $(L-1)$ plaquettes for which $U_P = e^{2\pi i\tau/L^2}$ and one plaquette for which $U_P = e^{-2\pi i\tau(L^2-1)/L^2}$. Applying the log, with the branch cuts, this gives us

$$Q = \frac{1}{2\pi}\left((L^2-1)\left|\frac{2\pi\tau}{L^2}\right|_{-\pi}^{\pi} - \left|(L^2-1)\frac{2\pi\tau}{L^2}\right|_{-\pi}^{\pi}\right)$$

where $|..|_{-\pi}^{\pi}$ denotes 2π modulation in the interval $[-\pi, \pi]$. As τ increases from zero, both terms cancel each other. However, the contents of the $|..|$ of the second term rises more quickly than the contents of the $|..|$ of the first term. As the contents of the $|..|$ of the second term reaches π, it crosses the branch cut and has 2π subtracted from its value, allowing Q to increment. This process continues until we reach the point were the contents of the $|..|$ of the first term approaches π. At this point, the definition breaks down because as the contents increase through π, Q becomes negative. For a lattice where $L_1 = L_2 = L = 6$, as studied in [72], $Q = 0$ in the interval $\tau \in [-\frac{36}{2(35)}, \frac{36}{2(35)}]$. $Q = 1$ in the interval $\tau \in [\frac{36}{2(35)}, \frac{3(36)}{2(35)}]$ and $Q = -1$ when $\tau \in [-\frac{3(36)}{2(35)}, -\frac{36}{2(35)}]$.

The Geometrically discretized description of Q must be consistent with this description. To achieve this, we have to recreate the behaviour of the branch cut. Applying D to the cochains $\tilde{A}$ gives us the GD equivalent of F_{12} over a plaquette. By using the mod operation and then summing over all plaquettes, we are able to define an appropriate expression for Q.

We have

$$Q = \sum_P \frac{1}{2\pi}\left|eD\tilde{A}\right|_{-\pi}^{\pi} \tag{32}$$

where the $\sum_P$ denotes a sum over the orientated plaquettes.

6.3.6 Implementing Topological Fields in GD

Equation (27) describes continuous gauge fields with a discontinuity across one of the boundaries. The gauge fields across the boundary are related by a gauge transform. In this section, we shall apply the geometric discretization to this situation.

To discretize the gauge fields, we apply the de Rham map. This gives us the following discrete fields

$$\tilde{A}_1(n_1, n_2) = 0 \qquad \tilde{A}_2(n_1, n_2) = -\omega n_1$$

where the (n_1, n_2) are dimensionless coordinates, $\omega = \frac{2\pi\tau}{L^2}$ with L the dimensionless length of the complex and τ is the topological parameter. We have temporarily chosen not to use the notation $\tilde{A}([..])$ for the time being, as we feel that notation of the form $\tilde{A}(n_1, n_2)$ better expresses the coordinate dependence of the fields.

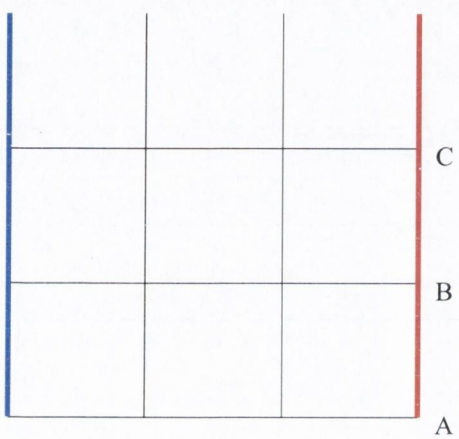

Figure 16: The periodic complex. The red and blue boundaries are identified as the same and it is across this boundary that the gauge field is discontinuous.

We proceed by explicitly constructing the gauge transform across the discontinuity. In Figure 16, we identify the red and blue boundaries as the same and we proceed by discretizing the gauge transform that relates the continuous fields $A_2(x_1 = 0)$ (blue) to $A_2(x_1 = L)$ (red).

In the continuum the transform is

$$U(x) = e^{\frac{2\pi i x_2 \tau}{L}}$$

This is a zero-form and applying the De Rham map, on the boundary, acts to sample $U(x)$ at the vertices of the discontinuity, yielding

$$\tilde{U}([A]) = e^{\frac{2\pi i n_2^A \tau}{L}} \qquad \tilde{U}([B]) = e^{\frac{2\pi i n_2^B \tau}{L}} \qquad \tilde{U}([C]) = e^{\frac{2\pi i n_2^C \tau}{L}} \tag{33}$$

Considering only the original complex for the moment and taking the simplex $[BC]$ as an example, we see that, using equation (26), it will transform as =

$$\begin{aligned}\tilde{A}_o^{\text{blue}}([BC]) &= \tilde{A}_o^{\text{red}}([BC]) - iR\left[dW\left(\tilde{U}([B])[B] + \tilde{U}([C])[C]\right)\right][G([B])]^{-1} \\ &\quad -iR\left[dW\left(\tilde{U}([B])[B] + \tilde{U}([C])[C]\right)\right][G([C])]^{-1}\end{aligned} \tag{34}$$

where $G([..])$ is the gauge transform on a fermion field belonging to simplex $[..]$. We have dropped a factor of $\frac{1}{e}$ from equation (26) because e is not included in equation (33). In this expression, we can make the following substitutions because the gauge simplices are wedged with zero-simplices and because we can explicitly substitute for the $\tilde{U}$ at the zero-simplices

$$G([B]) = \tilde{U}([B]) = e^{\frac{2\pi i n_2^B \tau}{L}} \qquad G([C]) = \tilde{U}([C]) = e^{\frac{2\pi i n_2^C \tau}{L}} = e^{\frac{2\pi i (n_2^B+1)\tau}{L}}$$
$$G([B])^{-1} = e^{\frac{-2\pi i n_2^B \tau}{L}} \qquad G([C])^{-1} = e^{\frac{-2\pi i (n_2^B+1)\tau}{L}}$$

and

$$\begin{aligned}R\left[dW\left(\tilde{U}([B])[B] + \tilde{U}([C])[C]\right)\right] &= \left[\tilde{U}([C]) - \tilde{U}([B])\right][BC] \\ &= \left(e^{\frac{2\pi i (n_2^B+1)\tau}{L}} - e^{\frac{2\pi i n_2^B \tau}{L}}\right)[BC] \\ &= \left(e^{\frac{2\pi i \tau}{L}} - 1\right) e^{\frac{2\pi i n_2^B \tau}{L}}[BC]\end{aligned}$$

The discrete wedge operations between $[BC]$ and the $[B]$ and $[C]$ simplices in the last two terms of equation (34) contribute the following factors of $\frac{1}{2}$

$$[BC]\tilde{\wedge}[B] = \tfrac{1}{2}[BC] \qquad [BC]\tilde{\wedge}[C] = \tfrac{1}{2}[BC]$$

All this gives, for equation (34),

$$\begin{aligned}\tilde{A}_o^{\text{blue}}([BC]) &= \tilde{A}_o^{\text{red}}([BC]) - \tfrac{i}{2}\left(e^{\frac{2\pi i \tau}{L}} - 1\right) - \tfrac{i}{2}\left(1 - e^{-\frac{2\pi i \tau}{L}}\right) \\ &= \tilde{A}_o^{\text{red}}([BC]) + \sin\left(\tfrac{2\pi\tau}{L}\right)\end{aligned} \tag{35}$$

Interestingly, we see here a consequence of the finite lattice size. In the limit of an infinitely large complex $\sin(\frac{2\pi\tau}{L})$ has the following behaviour

$$\lim_{L\to\infty} \sin\left(\frac{2\pi\tau}{L}\right) = \left(\frac{2\pi\tau}{L}\right) - O(L^{-3})$$

To first order this gives

$$\tilde{A}_o^{\text{blue}}([BC]) = \tilde{A}_o^{\text{red}}([BC]) = \tilde{A}_o^{\text{red}}([BC]) + \left(\frac{2\pi\tau}{L}\right)$$

which is the same as in the continuum (equation 28).

However, for finite extent, this transformation only approximates the continuum. To assess the accuracy of this approximation, we can calculate the fraction $\sin\left(\frac{2\pi\tau}{L}\right) / \left(\frac{2\pi\tau}{L}\right)$. The closer this is to 1, the better the approximation. For the values, $\tau = 1$ and for an extent $L = 6$ (the size used in [72] and which we will use later on), we see that $\sin\left(\frac{2\pi\tau}{L}\right) / \left(\frac{2\pi\tau}{L}\right) = 0.83$.

To complete the description of this gauge transformation, we would also have to consider for the dual complex. However, it provides such a poor approximation to the continuum transformation that we shall instead look for a better way to represent the transformation.

We proceed by extracting a set of gauge fields from the link variables in equations (29) and (30). For example, if we write the link variable between $[B]$ and $[C]$ as $U([BC]) = e^{ie\tilde{A}([BC])}$, we have that $\tilde{A}([BC]) = -\frac{2\pi n_1^B \tau}{L^2 e}$.

This gives

$$\tilde{A}_1(n_1, n_2) = \begin{cases} 0 & \text{if } n_1 \neq L-1 \\ \frac{2\pi n_2 \tau}{Le} & \text{if } n_1 = L-1 \end{cases} \tag{36}$$

$$\tilde{A}_2(n_1, n_2) = -\frac{2\pi n_1 \tau}{L^2 e} \tag{37}$$

6.3.7 Topological Fields in the Action

Applying the definition for the topological charge in equation (32) to the gauge field trajectory defined by equations (36) and (37), we obtain the plot in Figure 17, which is in agreement with Vranas' plot for the topological charge, calculated using equations (29), (30) and (31) (top left plot of Figure 1, page 26 of [72]).

When we study the gauge action associated with this field trajectory, we find a pronounced difference between the geometric discretization and the standard lattice description. To see this, we proceed by constructing explicit expressions for the gauge action in both the descriptions.

The lattice has $L(L-1)$ plaquettes that avoid the discontinuity altogether, each with $e^{ie\frac{2\pi\tau}{L^2 e}}$ as a product of gauge links. $(L-1)$ plaquettes cross the discontinu-

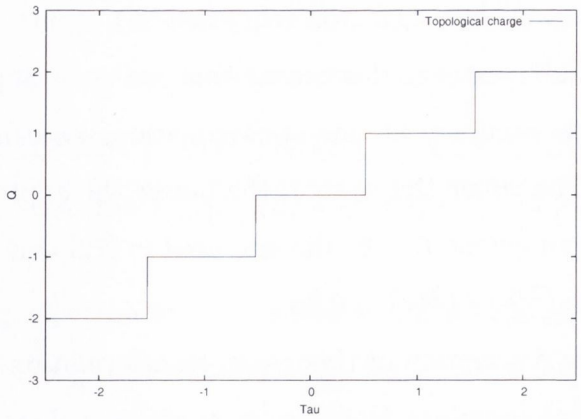

Figure 17: The topological charge.

ity, without crossing the boundary in the n_2 direction, each with a product $e^{ie\frac{2\pi\tau}{L^2e}}$. There is one plaquette around which the links cross both the n_2 boundary and the discontinuity, with a product $e^{ie\frac{2\pi\tau(1-L^2)}{L^2e}}$.

For standard lattice field theory, the gauge action is

$$S_G = \frac{1}{e^2}\sum_P \left[1 - \frac{1}{2}\left(U_P + U_P^\dagger\right)\right]$$

where P denotes a plaquette and U_P the product of link variables around it. This gives

$$S_G^{stand} = \frac{1}{e^2}\left[L^2 - (L^2-1)\cos(e\left(\frac{2\pi\tau}{L^2e}\right)) - \cos(e\left(\frac{2\pi\tau(1-L^2)}{L^2e}\right))\right] \qquad (38)$$

A plot of this expression can be found in Figure 18 and this agrees with the plot in Vranas' paper (top right plot of Figure 1, page 26 of [72]). There is a difference in the absolute value of S_G between the two plots, but, in his analysis, Vranas states that, "The absolute scale in these figures is of course irrelevant" (penultimate paragraph of page 13, [72]), making it plausible that his scale may have been adjusted. The relative scale is the same for both.

In the geometric discretization, we have $S_G = \frac{1}{2} < DA, DA >$ (from 6.3.2) and to calculate this we divide the complex up into the same three groups of plaquettes. The $L(L-1)$ plaquettes away from the discontinuity each contribute $\frac{2\pi^2\tau^2}{L^4e^2}$ to S_G. The $(L-1)$ plaquettes that cross the discontinuity, but not n_2 boundary each contribute

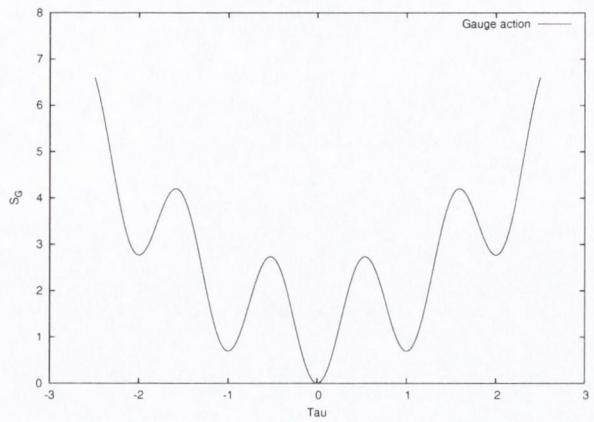

Figure 18: The gauge action for the trajectory described by equations (29) and (30) at $e = 0.89$ and $L = 6$.

$\frac{2\pi^2\tau^2}{L^4e^2}$ to S_G. The plaquette that crosses both the discontinuity and the n_2 boundary contributes $\frac{2\pi^2\tau^2(L^2-1)^2}{L^4e^2}$ to S_G. Summing these terms, we have

$$S_G^{GD} = L(L-1)\frac{2\pi^2\tau^2}{L^4e^2} + (L-1)\frac{2\pi^2\tau^2}{L^4e^2} + \frac{2\pi^2\tau^2(L^2-1)^2}{L^4e^2} = \frac{2\pi^2\tau^2(L^2-1)}{L^2e^2}$$

We can show that these two expressions are consistent, by expanding the cosine functions in S_G^{stand}. For small values of τ, we see that

$$S_G^{stand} = \frac{2\pi^2\tau^2(L^2-1)}{L^2e^2} + O(\tau^4)$$

which agrees with the expression for S_G^{GD}.

In the general expression for S_G^{stand}, the two cosine terms contribute the two periodicities that we see in Figure 18. The low frequency term provides the dominant 'U' shape and the higher frequency term provides the potential barriers between different topological regions, disfavouring the regions that are between integer topological charge. The local minima occur in regions of integer topological charge, giving these regions a degree of stability. The potential barriers can hamper calculations because once the system arrives in a topologically non-trivial minima, during a hybrid Monte Carlo calculation, for example, the barrier will impede its return to the topologically trivial state represented by the global minimum.

In the geometric discretization, S_G^{GD} has no comparable barriers between the different topological regions, as can be seen in Figure 19. S_G^{GD} is quadratic in the $\tilde{A}_\mu$,

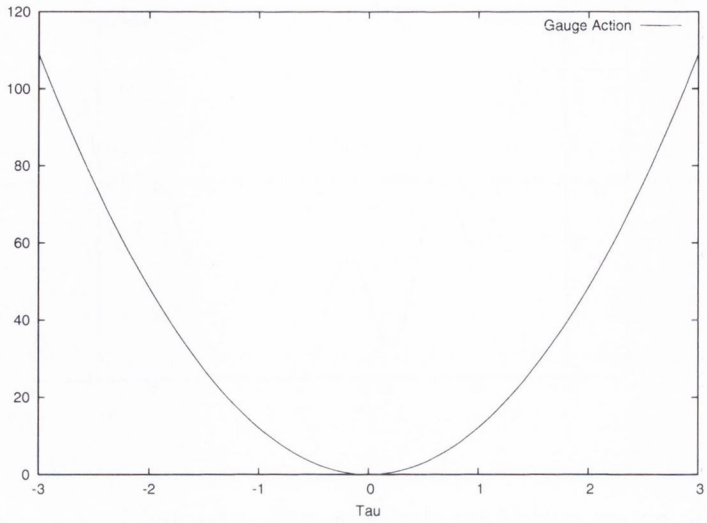

Figure 19: S_G vs τ using the GD action at $e = 0.89$ and $L = 6$.

so it describes the dominant 'U'shape, but is not of high enough order to describe the barriers. This is consistent with the continuum, in which the gauge action is also quadratic in A_μ.

Several other field theories have been developed that use similar non-compact definitions for the gauge links. Cahill uses such a formulation as a tool for calculating a range of phenomenological quantities [74] [75]. Gockeler *et al* have studied the equation of state for $U(1)$ gauge fields [76]. Fiore *et al* complete a range of calculations that allows them to explicitly compare compact and non-compact formulations [77] [78].

All these studies have used gauge actions similar to ours and they are quadratic in form. It is clear that the barriers between topological regions are an artifact of the compact description of gauge links. As such, we would expect that the non-compact descriptions offer the advantage of allowing the system to move more freely between regions of differing topological charge than the standard description.

7 Computational Implementation

In this chapter we describe the objects and algorithms used to implement the calculations described in chapter 9. We will also discuss some of the considerations for the implementation.

7.1 The Formulation

We have chosen to work in two space-time dimensions because this is a simpler and computationally cheaper environment than four space-time dimensions, in which to develop and test the formulation.

We have taken as our starting point the geometric discretization scheme as we originally introduced in section 5 together with the gauge theory we developed in section 6.3. The scheme is restricted to one original complex and one dual. The fermion fields exist on the original complex.

This formulation presented here is in keeping with the published formulation described in de Beaucé and Sen's work [8][9][58][63].

7.2 General Details

The algorithms have been implemented in 'C' using gcc to compile the code to a maximal level of optimization.

The code has been divided between five files:-

- `def.h` contains all the global parameters, set using the `#define` command
- `types.h` contains the user defined objects
- `global.h` contains the function prototypes for the `global.c` file
- `global.c` contains the all functions required by the Hybrid Monte Carlo algorithm and needed to calculate the value of the observables
- `hmc.c` implements the Hybrid Monte Carlo algorithm and measures the observables

Our complex is periodic. Although its size is adjustable, in the calculations, it is generally set as a 6x6, but we shall use Figure 20 as a reference complex for the

purposes of the following discussions.

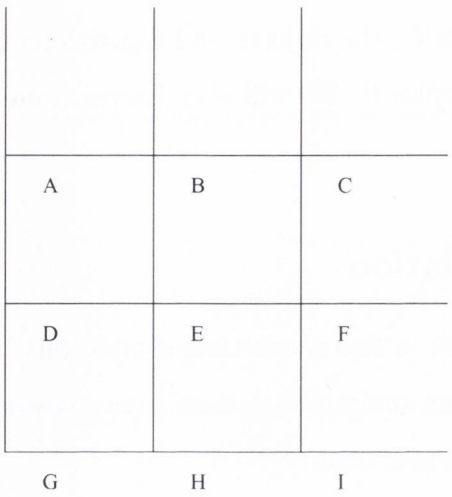

Figure 20: A periodic 2D complex.

7.3 Complex Numbers

Our most fundamental object is the complex number, which is defined in `types.h`. We define it as a pair of long doubles. It forms the basic unit of the fermion fields. In `global.c` we include the functions that perform standard complex arithmetic.

The gauge fields are parameterized using real numbers, so the complex numbers only entered the implementation through the fermion fields.

7.4 The Fields

To construct a vector representing all the degrees of freedom of the fermion fields, we need to know which components correspond to which simplices. The order we use is to start with the field belonging to the vertex nearest the top left corner of the complex. This will be the first component. We will treat it as part of a cell comprising the fields belonging to the x_1-direction one-simplex to its right, the x_2 direction one-simplex above it and the 2-simplex to the top right. These three values will then appear next in the vector, in the order given. We then proceed down the complex until we reach the bottom of that complex column. Then we move to the

column to the right and repeat the process. As a single vector for the complex in Figure 20, this is too long to fit on a single page, but if we break it into two, with the top portion on the left and the bottom portion on the right, then we have

$$\begin{pmatrix} [A] \\ [AB] \\ [AG] \\ [ABHG] \\ [D] \\ [DE] \\ [DA] \\ [DEBA] \\ [G] \\ [GH] \\ [GD] \\ [GHED] \\ [B] \\ [BC] \\ [BH] \\ [BCIH] \\ [E] \\ [EF] \\ [EB] \\ [EFCB] \end{pmatrix} \qquad \begin{pmatrix} [H] \\ [HI] \\ [HE] \\ [HIFE] \\ [C] \\ [CA] \\ [CI] \\ [CAGI] \\ [F] \\ [FD] \\ [FC] \\ [FDAC] \\ [I] \\ [IG] \\ [IF] \\ [IGDF] \end{pmatrix}$$

This is a fermion vector which we define in `types.h` as an array of $4 * N1 * N2$ complex numbers, where $N1$ and $N2$ are the dimensions of the complex.

The gauge field is a 1-form in the continuum and within the geometric discretization it exists only on the 1-simplices, so we only need to include the 1-simplices in its vector type, which is defined in `types.h`. For the gauge vector, we use a $2 * N1 * N2$ array of long doubles with the following basis for the complex shown in Figure 20:-

$$\begin{pmatrix} [AB] \\ [AG] \\ [DE] \\ [DA] \\ [GH] \\ [GD] \\ [BC] \\ [BH] \\ [EF] \\ [EB] \\ [HI] \\ [HE] \\ [CA] \\ [CI] \\ [FD] \\ [FC] \\ [IG] \\ [IF] \end{pmatrix}$$

For the purposes of our calculations, we must also include the gauge field on the dual complex.

To describe the dual gauge field, we follow the same approach but start with the dual cell that lies to the top right of the first original complex cell (shown in Figure 21). The basis for this vector is:-

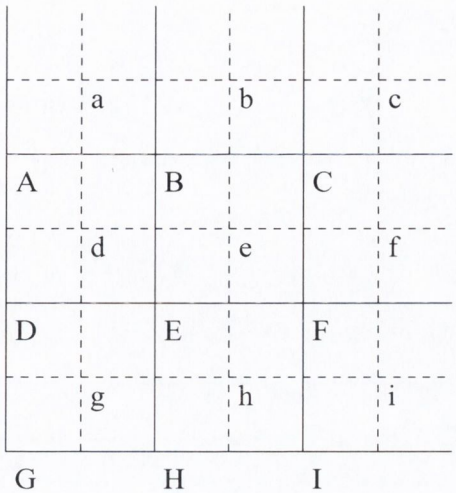

Figure 21: A periodic 2D complex plus its dual.

$$\begin{pmatrix} [ab] \\ [ag] \\ [de] \\ [da] \\ [gh] \\ [gd] \\ [bc] \\ [bh] \\ [ef] \\ [eb] \\ [hi] \\ [he] \\ [ca] \\ [ci] \\ [fd] \\ [fc] \\ [ig] \\ [if] \end{pmatrix}$$

7.5 The Operators

The operators are $(4 * N1 * N2)$x$(4 * N1 * N2)$ matrices that operate on the fermion vectors. They are constructed as an array of $16 * N1^2 * N2^2$ complex numbers. We store the elements of the matrix in a one dimensional array in much the same way that we store the fields of the complex. We start with the top left element of the matrix and proceed downward until we reach the bottom. The next array item is the first element of the second column and down the column we go and so on.

Principally, there are two types of operator. The first is the free field Dirac-Kähler operator, which is antisymmetric. The second is the interaction term, whose symmetries are harder to define.

We define the Dirac-Kähler operator, starting from a null matrix. In section 7.4, we grouped together simplices into cells and we can see that each row of the matrix corresponds to a cell of the complex defined through the fermion vector basis. We find the four columns that correspond to the same cell and define our changes to the null matrix around those.

If the row corresponds to a 0-simplex, the four elements in the columns corresponding to the same cell are

$$(0, 1, 1, 0)$$

We denote the elements belonging to the next four columns of the same row with $T(1)$. These columns belong to the next cell on the complex. These elements contribute

$$T(1)(0, 0, -1, 0)$$

We also have a contribution from the cell immediately to the left of the one corresponding to the row. We indicate the set of columns belonging to this cell with $T(-N2)$. Their contribution to the row is

$$T(-N2)(0, -1, 0, 0)$$

All other elements on that row remain equal to zero.

In this notation $T(X)$ indicates the number of cells we must move over from the cell corresponding to the row. The contents of the brackets are the elements in that

cell, for that row.

The other rules are:-

For a row corresponding to a 1-simplex in the 1-direction

$$(-1,0,0,-1)+T(1)(0,0,0,1)+T(N2)(1,0,0,0)$$

For a row corresponding to a 1-simplex in the 2-direction

$$(-1,0,0,1)+T(-1)(1,0,0,0)+T(-N2)(0,0,0,-1)$$

For a row corresponding to a 2-simplex

$$(0,1,-1,0)+T(-1)(0,-1,0,0)+T(N2)(0,0,1,0)$$

This prescription doesn't specify the changes that must be made near the boundary of the complex. These changes are implemented as conditional statements in the routines that generate the Dirac-Kähler matrix. The conditional changes are:-

If the row corresponds to a cell in the far right column of the complex,

- $T(N2)$ must be replaced with $T(-N2(N1-1))$.

If the row corresponds to a cell in the far left column of the complex,

- $T(-N2)$ must be replaced with $T(N2(N1-1))$.

If the row corresponds to a cell on the top row of the complex,

- $T(-1)$ must be replaced with $T(N2-1)$.

If the row corresponds to a cell on the bottom row of the complex,

- $T(1)$ must be replaced with $T(-(N2-1))$.

For the interaction term, we start with two four component arrays that tell us where, in a matrix of the same dimensions as the Dirac-Kähler operator, the gauge fields should appear and what coefficient they should have, depending on the discrete geometry involved. There is one array for each complex and we have a program function that constructs the interaction matrix from the two arrays.

Writing out these rules becomes more complicated than for the free field Dirac-Kähler operator because in addition to specifying where on each line the non-zero entries are to be found, we must also specify which gauge fields are required.

To this end, we necessarily extend our notation. We identify the columns of a row with cells, in the same way as for the Dirac-Kähler operator. However, we also use the $T(X)$ notation to indicate on which gauge simplex the appropriate gauge field can be found. $T(X)$ describes a cell relative to the one identified by the outer set of brackets. For example, $T(1)(0, A[T(-1)(0,1,0,0)], 0, 0)$ would indicate the 1-direction gauge simplex from the current cell, placed in the column corresponding to the 1-direction simplex of the next cell. o and d indicate whether the field is from the original complex or dual. As mentioned in section 7.4, we associate a cell from the dual complex to one from the original if the barycentre of the dual 0-simplex and the original 2-simplex coincide: $A \Leftrightarrow a$, $B \Leftrightarrow b$, etc. When we use $T(N)$ to indicate a gauge simplex from the dual complex, it is this dual cell that we take as the starting point.

The rules are:-

For a row corresponding to a 0-simplex

$$(0, \frac{1}{4}\tilde{A}_d[T(-N2)(0,1,0,0)] + \frac{1}{4}\tilde{A}_d[T(-N2+1)(0,1,0,0)],$$
$$\frac{1}{4}\tilde{A}_d[T(1)(0,0,1,0)] + \frac{1}{4}\tilde{A}_d[T(-N2+1)(0,0,1,0)], 0)$$
$$+T(-N2)(0, \frac{1}{4}\tilde{A}_d[(0,1,0,0)] + \frac{1}{4}\tilde{A}_d[T(1)(0,1,0,0)], 0, 0)$$
$$+T(1)(0,0,+\frac{1}{4}\tilde{A}_d[(0,0,1,0)] + \frac{1}{4}\tilde{A}_d[T(-N2)(0,0,1,0)], 0)$$

For a row corresponding to a 1-simplex in the 1-direction

$$(\frac{1}{2}\tilde{A}_o[(0,1,0,0)], 0, 0, -\frac{1}{2}\tilde{A}_d[T(1)(0,0,1,0)])$$
$$+T(1)(0,0,0,-\frac{1}{2}\tilde{A}_d[(0,0,1,0)]) + T(N2)(\frac{1}{2}\tilde{A}_d[T(-N2)(0,1,0,0)], 0, 0, 0)$$

For a row corresponding to a 1-simplex in the 2-direction

$$(\frac{1}{2}\tilde{A}_o[(0,0,1,0)], 0, 0 + \frac{1}{2}\tilde{A}_d[T(-N2)(0,1,0,0)])$$
$$+T(-1)(\frac{1}{2}\tilde{A}_o[T(1)(0,0,1,0)], 0, 0, 0) + T(-N2)(0,0,0,\frac{1}{2}\tilde{A}_d[(0,1,0,0)])$$

For a row corresponding to a 2-simplex

$$(0, -\frac{1}{4}\tilde{A}_o[(0,0,1,0)] - \frac{1}{4}\tilde{A}_o[T(N2)(0,0,1,0)],$$

$$+\frac{1}{4}\tilde{A}_o[(0,1,0,0)] + \frac{1}{4}\tilde{A}_o[T(-1)(0,1,0,0)],0)$$

$$T(-1)(0,-\frac{1}{4}\tilde{A}_o[T(1)(0,0,1,0)] - \frac{1}{4}\tilde{A}_o[T(N2+1)(0,0,1,0)],0,0).$$

$$+T(N2)(0,0,+\frac{1}{4}\tilde{A}_o[T(-N2)(0,1,0,0)] + \frac{1}{4}\tilde{A}_o[T(-N2-1)(0,1,0,0)],0)$$

We have to include corrections to these rules because of the periodic boundary conditions of the complex. The corrections apply to the $T(X)$ indicating the location of the gauge simplex as well as the $T(X)$ indicating the location of the cell within the row.

With these two matrices, we can construct the covariant Dirac-Kähler operator as: (the first matrix) - ie(the second matrix). The symmetry properties of this operator are discussed in section 7.7.

There is one other type of operator that we define in the file `types.h`. We define an operator for gauge fields that we use in the definition of $D\tilde{A}$ which is required for S_G and in $\delta\tilde{A}$ which is used in S_{GF}.

This operator is a subset of the lines from the free field Dirac-Kähler operator. For $D\tilde{A}$, we only need the lines that correspond to 2-simplices. For the $\delta\tilde{A}$ operator, we only need the lines that correspond to 0-simplices.

7.6 The Algorithm

We use the Hybrid Monte Carlo algorithm [10][19] to generate a succession of gauge field configurations on which we calculate the observables. The most computationally demanding parts of the Hybrid Monte Carlo algorithm are the matrix inversions and the calculations of the matrix determinant. For reasons of computational efficiency, I wrote the determinant function in such a way that it performs Gaussian elimination to make the matrix upper diagonal and then calculates the determinant as the product of the diagonal elements.

The inversion routine I wrote in two ways. One routine used Gaussian elimination with pivoting to calculate the inverse. I wrote another routine that used the conjugate gradient algorithm to solve for the inverse column by column. However,

after comparing both algorithms in identical circumstances, I found that the conjugate gradient algorithm was slower on both 3*3 and 6*6 complexes, although in both cases it was only by about 10%. Clearly, the reason that conjugate gradient is popular is not just its efficiency, but also that it can be implemented with lower memory requirements for large matrices.

7.7 Hermiticity Issues

One difficulty with this formulation comes from the symmetry properties of the covariant Dirac-Kähler operator.

In the continuum, the Dirac-Kähler operator is antisymmetric and the gauge field term is anti-hermitian, so the overall formulation is also anti-hermitian. In our formulation, the free field Dirac-Kähler operator is still antisymmetric. However, the gauge field term has no comparable properties.

This is a consequence of the role of the gauge fields in the inner product. In standard lattice gauge field theory, the inner product between a spinor and adjoint spinor on neighbouring lattice sites contains a parallel transporter. This transporter is involved in both the terms $\bar{\psi}(n)U(n)\psi(n+1)$ and $\bar{\psi}(n+1)U^{\dagger}(n+1)\psi(n)$ and so is involved in both forward and backward propagation of the fermion field along the lattice. However, in the case of GD, the fermion field is propagated backwards and forward by gauge fields from different complexes and these fields have been discretized by integrating over different domains. As we saw in section 6.3.1, it was fundamentally necessary to define the gauge fields in this way so as to ensure that the gauge fields transform to maintain the invariance of the derivative on each complex.

For example, referring to Figure 21, the fermion field on the simplex $[BE]$ is mapped to the simplex $[ABED]$ by the derivative D and by the two gauge simplices $[AB]$ and $[DE]$. However, the field on the simplex $[ABED]$ is mapped back to the simplex $[BE]$ by the adjoint derivative and by the gauge simplex $[de]$. The De Rham map that discretizes the gauge field belonging to $[de]$ has a different domain of integration to the De Rham map that discretizes the gauge fields belonging to the $[AB]$ and $[DE]$ simplices.

In taking the transpose, $\tilde{A}_d([de])$ and $\frac{1}{2}(\tilde{A}_o([AB]) + \tilde{A}_o([DE]))$ are interchanged, but they only approximate each other to the zeroth order.

If we were to demand the desired hermiticity properties of the gauge fields, this would define a relationship between the gauge fields on each complex. However, because each gauge field is involved in the propagation of the fermion fields on several simplices, the only case in which this could be realised is when the value of the gauge fields are a linear function of position. For example, referring again to Figure 21, if we were to constrain $\tilde{A}_d([de])$ to be equal to $\frac{1}{2}(\tilde{A}_o([AB]) + \tilde{A}_o([DE]))$, we would also have to constrain $\tilde{A}_d([de])$ to be equal to $\frac{1}{2}(\tilde{A}_o([BC]) + \tilde{A}_o([EF]))$ because the field on $[BE]$ will also propagate on to $[BCFE]$. Similarly, we would have to define $\tilde{A}_o([BC])$ to be equal to $\frac{1}{2}(\tilde{A}_d([ab]) + \tilde{A}_d([de]))$ and $\frac{1}{2}(\tilde{A}_d([bc]) + \tilde{A}_d([ef]))$. This could only be achieved if gauge fields parallel to the 1 direction were linear in the n_2 coordinate and independent of n_1. A similar analysis also applies to the fields parallel to the 2 direction. They would have to be a linear function of the n_1 coordinate alone. As we shall see, we cannot constrain the gauge fields to be linear in the coordinates in a HMC calculation, so we must obtain hermiticity properties by other means.

The hermiticity is necessary to ensure that the determinant of the covariant Dirac-Kähler operator is always real and positive. This is required for the action to be bounded and stable.

The solution that we have adopted to this problem has been to replace the determinant of the covariant Dirac-Kähler operator, $\det(M)$, with $\sqrt{\det(M)^\dagger \det(M)}$, which is similar to the quarter-root trick commonly used in staggered fermion calculations [73].

7.8 Hybrid Monte Carlo Algorithm

The HMC algorithm [10] that we used for generating the gauge field configurations is well understood. However our implementation is quite unusual, so it is necessary to describe it in detail.

We start by choosing random gauge field configurations for each of the two complexes. We use a Gaussian function to populate the gauge fields from the distribution

$e^{-\frac{1}{2}\tilde{A}^2}$. Starting with a configuration populated by a Gaussian function allows us to clearly see thermalization using the gauge action. We also choose a set of momenta for the gauge fields on both complexes, from the distribution $e^{-\frac{1}{2}\tilde{P}^2}$.

We construct the Dirac-Kähler operator as the sum $M = D - \delta + m - ie\tilde{A}_o - ie\tilde{A}_d$, and we invert this using Gaussian elimination, where necessary.

The Hamiltonian for this system is

$$H = S_G^o + S_G^d + S_{GF}^o + S_{GF}^d + \frac{1}{2}\sum_l \tilde{P}_o^2(l,\tau) + \frac{1}{2}\sum_l \tilde{P}_d^2(l,\tau) + \ln\sqrt{\det(M^\dagger M)}$$

where l labels a simplex and τ is the simulation time. S_G is the gauge action from Section 6.3.2 and S_{GF} is the gauge fixing term from Section 6.3.3.

We derive an update scheme, with which to evolve the system, from the equations of motion $\dot{\tilde{A}}(l,\tau) = \frac{\partial H}{\partial \tilde{P}(l,\tau)}$ and $\dot{\tilde{P}}(l,\tau) = -\frac{\partial H}{\partial \tilde{A}(l,\tau)}$, where the dot denotes the derivative with respect to simulation time.

Taking advantage of the identity

$$\frac{\partial}{\partial \tilde{A}(l,\tau)} \ln\sqrt{\det(M^\dagger M)} = Re\left(\mathrm{Tr}\left(M^{-1}\frac{\partial M}{\partial \tilde{A}(l,\tau)}\right)\right) \tag{39}$$

which is shown in Appendix C, we arrive at the following update scheme, using the leapfrog method and a simulation time step of $\Delta\tau$.

$$\begin{aligned}
\tilde{A}_o(l,\tau+\Delta\tau) &= \tilde{A}_o(l,\tau) + \Delta\tau\tilde{P}_o(l,\tau+\tfrac{\Delta\tau}{2}) \\
\tilde{A}_d(l,\tau+\Delta\tau) &= \tilde{A}_d(l,\tau) + \Delta\tau\tilde{P}_d(l,\tau+\tfrac{\Delta\tau}{2}) \\
\tilde{P}_o(l,\tau+\tfrac{\Delta\tau}{2}) &= \tilde{P}_o(l,\tau-\tfrac{\Delta\tau}{2}) + \Delta\tau\left[-\frac{\partial S_G}{\partial \tilde{A}_o(l,\tau)} - \frac{\partial S_{GF}}{\partial \tilde{A}_o(l,\tau)} - Re\left(\mathrm{Tr}\left(M^{-1}\frac{\partial M}{\partial \tilde{A}_o(l,\tau)}\right)\right)\right] \\
\tilde{P}_d(l,\tau+\tfrac{\Delta\tau}{2}) &= \tilde{P}_d(l,\tau-\tfrac{\Delta\tau}{2}) + \Delta\tau\left[-\frac{\partial S_G}{\partial \tilde{A}_d(l,\tau)} - \frac{\partial S_{GF}}{\partial \tilde{A}_d(l,\tau)} - Re\left(\mathrm{Tr}\left(M^{-1}\frac{\partial M}{\partial \tilde{A}_d(l,\tau)}\right)\right)\right]
\end{aligned} \tag{40}$$

As vectors of the type described in Section 7.4, $\frac{\partial S_G}{\partial \tilde{A}}$ and $\frac{\partial S_G}{\partial \tilde{A}}$ are calculated using $D^T D\tilde{A}$ and $\delta^T\delta\tilde{A}$, respectively. The $\tilde{A}_o(l,\tau)$, $\tilde{A}_d(l,\tau)$, $\tilde{P}_o(l,\tau)$ and $\tilde{P}_d(l,\tau)$ are purely real quantities.

To facilitate the use of the leapfrog scheme, we first need to evolve the momenta of the gauge fields by a half step using the gauge force term

$$\begin{aligned}
\tilde{P}_o(l,\tfrac{\Delta\tau}{2}) &= \tilde{P}_o(l,0) + \tfrac{\Delta\tau}{2}\left[-\frac{\partial S_G}{\partial \tilde{A}_o(l,0)} - \frac{\partial S_{GF}}{\partial \tilde{A}_o(l,0)} - Re\left(\mathrm{Tr}\left(M^{-1}\frac{\partial M}{\partial \tilde{A}_o(l,0)}\right)\right)\right] \\
\tilde{P}_d(l,\tfrac{\Delta\tau}{2}) &= \tilde{P}_d(l,0) + \tfrac{\Delta\tau}{2}\left[-\frac{\partial S_G}{\partial \tilde{A}_d(l,0)} - \frac{\partial S_{GF}}{\partial \tilde{A}_d(l,0)} - Re\left(\mathrm{Tr}\left(M^{-1}\frac{\partial M}{\partial \tilde{A}_d(l,0)}\right)\right)\right]
\end{aligned} \tag{41}$$

We then start a chain of molecular dynamics steps that update the gauge fields and the momenta according to equation (40). At the end of the chain, we roll back the momenta half a step using equation (42).

$$\begin{aligned}
\tilde{P}_o(l,\tau) &= \tilde{P}_o(l,\tau+\tfrac{\Delta\tau}{2}) - \tfrac{\Delta\tau}{2}\left[-\frac{\partial S_G}{\partial \tilde{A}_o(l,\tau)} - \frac{\partial S_{GF}}{\partial \tilde{A}_o(l,\tau)} - Re\left(\mathrm{Tr}\left(M^{-1}\frac{\partial M}{\partial \tilde{A}_o(l,\tau)}\right)\right)\right] \\
\tilde{P}_d(l,\tau) &= \tilde{P}_d(l,\tau+\tfrac{\Delta\tau}{2}) - \tfrac{\Delta\tau}{2}\left[-\frac{\partial S_G}{\partial \tilde{A}_d(l,\tau)} - \frac{\partial S_{GF}}{\partial \tilde{A}_d(l,\tau)} - Re\left(\mathrm{Tr}\left(M^{-1}\frac{\partial M}{\partial \tilde{A}_d(l,\tau)}\right)\right)\right]
\end{aligned} \tag{42}$$

Next, we evaluate the Hamiltonian for the configurations at the start of the molecular dynamics chain and at the end and accept the end configuration with probability

$$P = \begin{cases} 1 & : \quad \text{if } H^{\text{end}} < H^{\text{start}} \\ e^{-\left(H^{\text{end}} - H^{\text{start}}\right)} & : \quad \text{if } H^{\text{end}} > H^{\text{start}} \end{cases}$$

If we accept the end configuration, we store it, generate a new set of momenta from the Gaussian distribution and repeat the molecular dynamics chain, starting with the half step forward in the momenta. If we reject the end configuration, we store the start configuration, generate a new set of momenta and start a new molecular dynamics chain from the start configuration.

After a period of thermalization, the stored set of gauge configurations will become representative of the contributions to the path integral.

We chose the parameters for the simulations so as to achieve a reasonable sampling of phase space in a reasonable length of time. The complex had dimensions 6x6 and the fermion field was massless. Each molecular dynamics chain had a duration of 0.2 in simulation time and comprised 20 steps, giving $\Delta\tau = 0.01$. To reach an acceptable level of thermalization, this configuration was run for 140 Monte Carlo tests and the whole algorithm took roughly 90 hours to complete on Trinity College's IITAC cluster [79].

Figure 22 shows the value of the gauge action for a typical calculation. We considered thermalization to have taken place when the random variation in the gauge action was significantly greater than the deviation from horizontal caused by the transient curve. With these parameters, we judged thermalization to have taken place after 80 Metropolis steps. This left us only 60 reliable configurations to use in our calculations, so we ran three of these processes simultaneously.

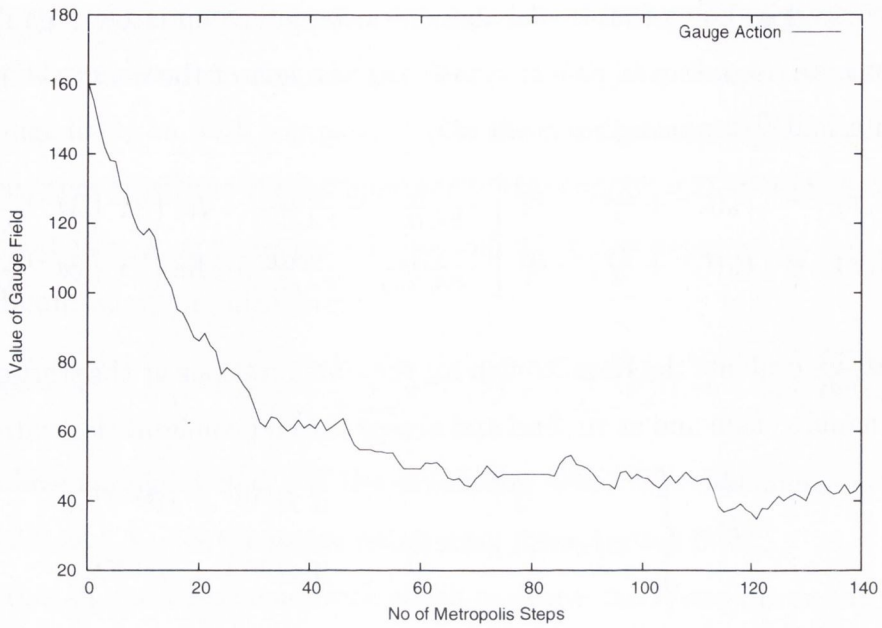

Figure 22: A plot of the gauge action after each Metropolis step. The plateau represents the thermalized gauge field with $e = 0.89$.

For a coupling constant of $e = 0.89$, the three simulations yielded 180 thermalized gauge configurations which we found to have an acceptance rate of 92%.

8 Review of the Schwinger Model

Before we use this computational framework to calculate phenomenological quantities, we will first devote a chapter to familiarising ourselves with the underlying Schwinger model and its properties.

The Schwinger model is named in honour of Julian Schwinger who studied the properties of $U(1)$ gauge fields in one space and one time dimension, showing that mass was dynamically generated by the gauge field [14]. In his original work [14] both the space and time dimensions were continuous and the fermion field was taken to be massless.

This arrangement can be described as a $1+1$ dimensional model. However, Schwinger wasn't the first to use $1+1$ dimensional models. Thirring had previously used them to study a purely fermionic interacting theory [13], but such was the interest surrounding Schwinger's result that the model came to be associated with his name.

One of the reasons that the model is of great interest is that the reduced dimensionality sometimes permits the calculation of quantities that cannot be calculated in four space-time dimensions. Thus, it provides an environment comparable to four dimensions, in which to study fermionic field theory. Several studies have analytically calculated the properties of the model [81][82][83][84]

In our case, we have chosen to use the Schwinger model because its dimension and gauge group are much less computationally demanding than higher dimensional models. This allows us to perform calculations in a manageable amount of time on single processor supercomputing facilities.

For our calculations, we use one time dimension and one space dimension. Both dimensions are discrete and we include a single flavour of massless fermion field with $U(1)$ symmetry. We use Euclidean space, in which we can describe the discrete $1+1$ dimensional theory as a discrete two dimensional theory.

In the subsequent sections, we shall use our implementation of the Schwinger model to calculate the static quark potential and to consider the chiral condensate. In this section, we shall outline some of the established results regarding the static

quark potential.

8.1 Static Fermion Potential

Iso and Murayama [85] studied the static fermion potential for the Schwinger model in the continuum and Dilger [86] and Joos and Azakov [87] studied the geometric description of the continuous Schwinger model. In the geometric cases, the fermion fields were represented using a Dirac-Kähler algebra, making them more in keeping with the geometric description that we have used.

Both Dilger [86] and Joos and Azakov [87] showed that in the continuum of two Euclidean dimensions (one spatial, one temporal), with dynamical fermions

$$V(R) = \frac{\pi m}{4}\left(1 - e^{-mR}\right) - \frac{\pi m\left(\cosh mR - 1\right)}{2\left(e^{mL_1} - 1\right)} \tag{43}$$

where $m^2 = \frac{2e^2}{\pi}$ and L_1 is the spatial extension of the space-time.

The second term in equation (43) describes the effect of the finite extent of the space. In the limit $mL_1 \to \infty$, this term goes to zero. Iso and Murayama [85] attained this same result in this limit. If we look at the potential in the the small R limit, subsequent to $mL_1 \to \infty$, we have $V(R) \to \frac{1}{2}e^2R + O(R^2)$.

This is intuitively sound. Leaving aside screening for a moment, the force exerted by the potential is constant in the Schwinger model due to its single spatial dimension. Consequently, the potential must grow linearly with separation between the fermion and antifermion. In the unquenched case, the creation of virtual fermion pairs acts so as to screen the fermion and antifermion from one another. This reduces the force at large separation.

A plot of the potential described in equation (43) is shown in Figure 23 for the parameters $e = 0.89$ and $L_1 = 6$. The plot shows the potential for the quenched case, both with and without finite extent effects, in which we expect no screening. It also shows the unquenched case, both with and without finite extent effects, in which we expect to see screening. We can see that the influence of the screening is much more dramatic than that of the finite spatial extent.

In the lattice case, it has been shown explicitly by Rothe [19] (pages 111-115), that the quenched calculation leads to a potential proportional to R, where R is

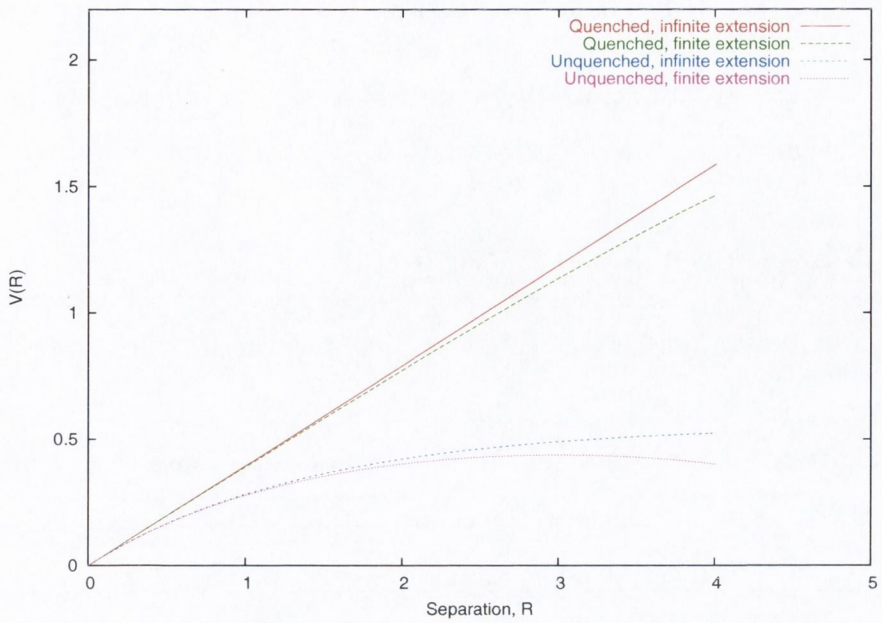

Figure 23: The static quark potential for $e = 0.89$ and $L_1 = 6$ with the linear, unscreened potential in the limit of infinite spatial extent (red), the unscreened potential with finite spatial extent (green), the screened potential with infinite extent (blue) and the screened potential with finite extent(pink).

the separation. In [88], Potvin compares the screened, analytical potential to the potential calculated using ensemble projector Monte Carlo methods and obtains good agreement, observing both a linear regime at low R and a screened regime at high R. In [89], the authors study a strategy for addressing the computational cost associated with including dynamical fermions in these calculations. Their calculations show good agreement with the predicted values in the quenched case and their attempt at recreating the dynamical behaviour shows a degree of screening comparable to the expected result in the unquenched case.

The formulation proposed in Section 7 uses dynamical fermions so we expect to see a potential that is close to linear for small R, but that shows screening as R grows. As such, we anticipate a potential that is consistent with the unquenched curves in Figure 23.

9 Computational Results

Here we shall review the calculations of the static quark potential and we shall consider the calculation of the chiral condensate.

9.1 The Static Fermion Potential

The standard approach is to calculate the gauge invariant correlation function between two fermions a finite distance R apart, at Euclidean time $t = 0$ and the same two fermions at a later time, $t = T$. The fermions are taken to be infinitely heavy and are therefore static. As T becomes large, the ground state of this arrangement dominates, which is determined by the interaction potential.

In practice, we proceed by taking a rectangular loop around a group of lattice plaquettes of dimensions TxR, and we calculate the phase incurred by passing around the loop. We average over all the loops of the same size and dimension from the lattice and we calculate an expectation value for the phase from an ensemble of gauge configurations.

If we were able to take the extent of the loop in the time direction to be infinitely large, we would find that the ensemble average for the phase becomes: $< W(A) > \rightarrow F(R)e^{-V(R)T}$, where $V(R)$ is the potential as a function of the separation between the fermions, R. In the infinitely heavy case, $V(R)$ is the ground state of the system. In practise, we must use a finitely sized loop and we are particularly interested in values of T large enough for the ground state to dominate, but small enough that the behaviour $F(R)e^{-V(R)T}$ dominates over the noise in the ensemble average.

To find this window in T, we calculate the following quantity

$$\ln\left(\frac{< W(T) >}{< W(T+1) >}\right) \tag{44}$$

across a range of T, for a fixed value of R. We then identify the region in which this becomes independent of T, with small enough error bars to determine an acceptably accurate value. The plots of the quantity in equation (44) should fall off to a level value, for increasing T, before the error bars become large. The position of this

plateau tells us the value of $V(R)$ for a given R. To determine the shape of the potential, we must study this for several values of R.

9.1.1 Our Parameters

We present here results from calculations performed for two values of e. In the first case, $e = 0.89$, as in Vranas' paper [72]. In the second, we chose $e = 1.3$. The calculations were performed for a massless fermion, on a 6x6 complex with a molecular dynamics chain of length 0.2 divided into 20 steps of 0.01. This yielded an acceptance rate of 92%.

9.1.2 Thermalization

Figure 22 in Section 7.8, shows the value of the gauge action as one calculation progressed. We used the gauge action as an indicator of when thermalization had been achieved.

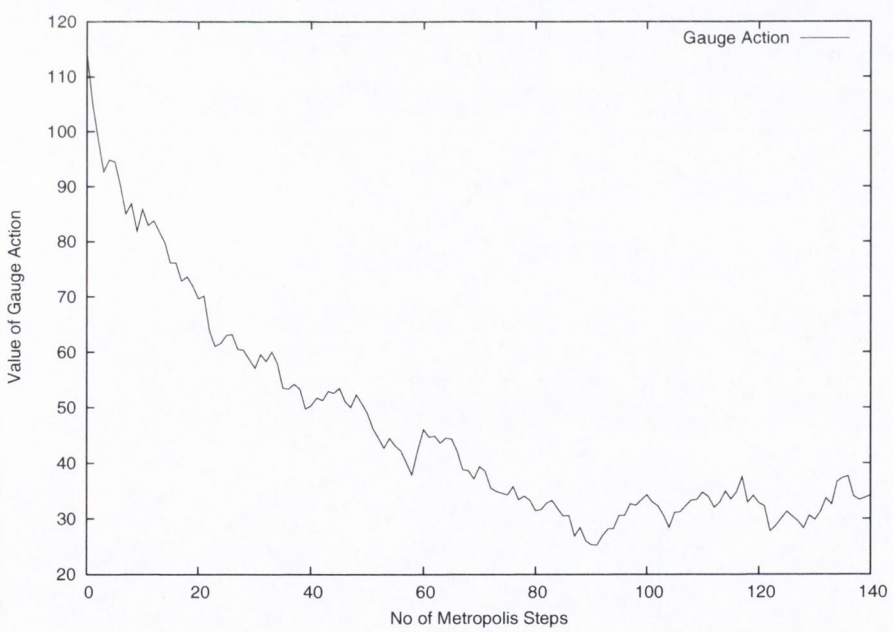

Figure 24: A plot of the gauge action after each Metropolis step. The plateau represents the thermalized gauge field with $e = 1.3$.

Each calculation ran for roughly 90 hours and involved 140 Metropolis tests. As

described in Section 7.8, we deemed thermalization to have taken place when the noise obscured any trend in the value of the action. We judged that this was achieved after 80 Metropolis steps, leaving us with 60 thermalized gauge configurations. To generate a larger set of thermalized gauge configurations, we ran three such calculations simultaneously for each set of parameters.

In Figure 22, $e = 0.89$. Figure 24 shows an equivalent plot for the case where $e = 1.3$. In this case also, 80 Metropolis steps proved to be a suitable threshold for thermalization and we used three calculations to generate 140 thermalized configurations.

9.1.3 The Potential at $e = 0.89$

We start by looking at the quantity in equation (44). With $R = 1$, we produced the plot in Figure 25. As T increases, the error bars start off small and increase in size, as we would anticipate from the decreased signal-to-noise ratio. At $T = 1$, the value of equation (44) is 0.384 ± 0.013. With $e = 0.89$, the value of $\frac{e^2 R}{2}$ is 0.396, so the plateau agrees with the expected result.

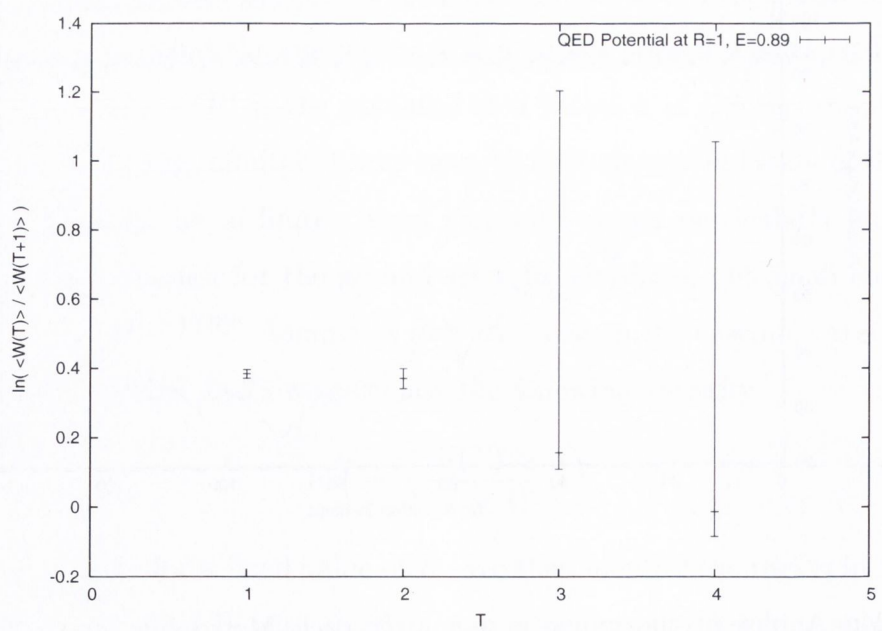

Figure 25: The static fermion potential at $R = 1$ and $e = 0.89$.

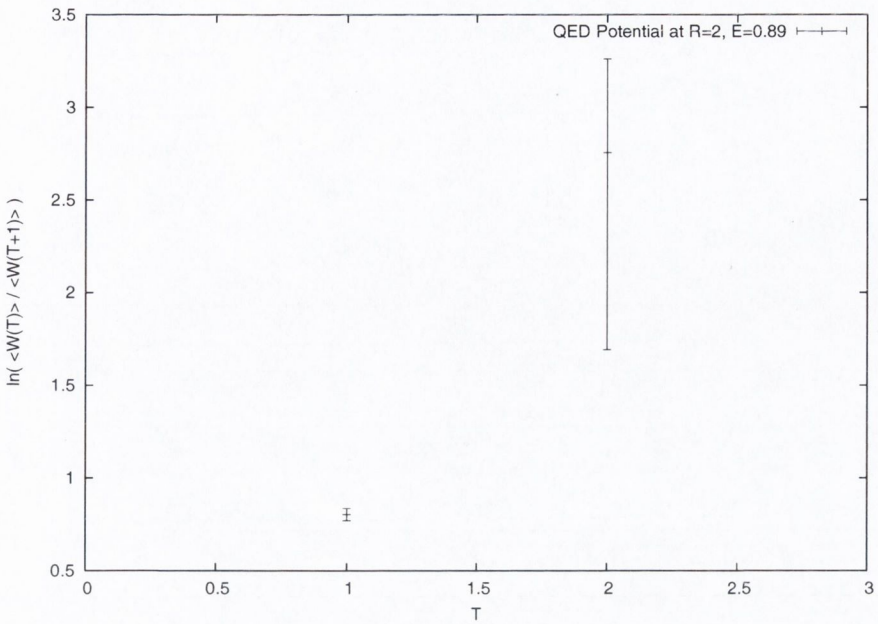

Figure 26: The static fermion potential at $R = 2$ and $e = 0.89$.

Figure 26 corresponds to the $R = 2$ case and here the results are less clear. We were only able to generate data points at $T = 1$ and $T = 2$. At $T = 3$, equation (44) requires Wilson loops with an extension in the time dimension of four and this takes the expression $e^{-V(R)T}$ too close to zero. When the ensemble averages go to close too zero, the noise can easily send the mean to zero or below, resulting in the ln function becoming singular.

Whilst the second data point in this plot is a standard deviation away from the expected result, the first point follows it closely. At $R = 2$, we expect $\frac{e^2 R}{2}$ to be 0.792. The first data point is located at $0.804(+0.032, -0.033)$, which agrees well.

At $R = 3$ and $R = 4$, we also found that some of the points succumbed to the noise problem. At $R = 3$, we were only able to obtain a value for the $T = 1$ data point: $1.258(+0.078, -0.084)$. The theoretical result is 1.188, so again there is agreement.

At $R = 4$, $T = 1$ was also the only data point with non-singular errors. We obtained $1.463(+0.157, -0.187)$. The theoretical result is 1.584, so these values are also in agreement.

These results are summarized in the Table 1 and in the plot of $V(R)$ at $e = 0.89$

Table 1: Static quark potential data points at $e = 0.89$.

R	$\ln\left(\frac{<W(1)>}{<W(2)>}\right)$	$+\Delta$	$-\Delta$	Theor. Val.
1	0.384	0.013	0.013	0.396
2	0.804	0.032	0.033	0.792
3	1.258	0.078	0.084	1.188
4	1.463	0.157	0.187	1.584

in Figure 27.

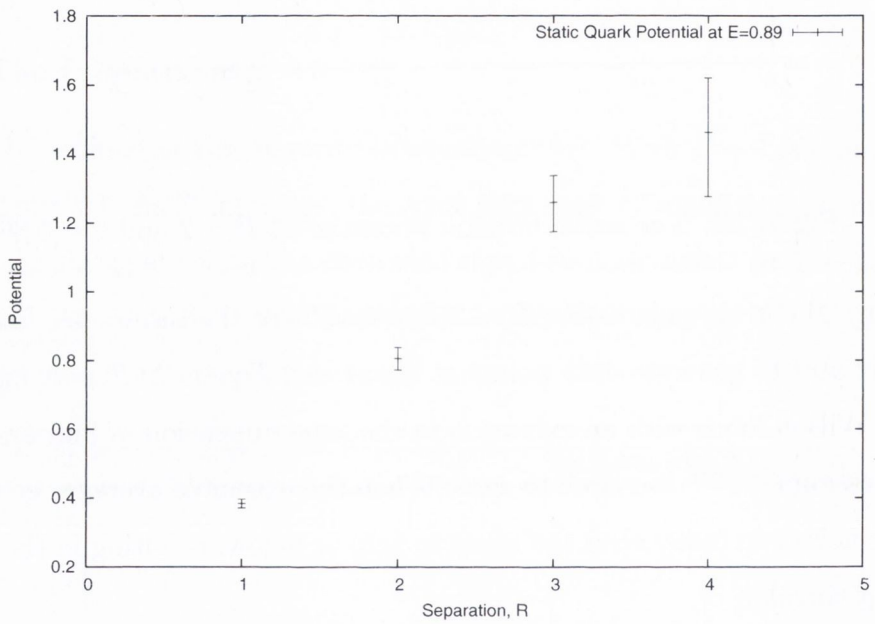

Figure 27: The static quark potential calculated at $e = 0.89$.

We interpolated the points from Figure 27 with cubic splines to produce a smooth representative function. Combining the interpolating function and the analytical expression plotted in Figure 23 gives us Figure 28

The interpolating function agrees well with the linear form of the quenched analytical result and at large R, it shows a small deviation from the linear form, suggesting either screening of the potential by the dynamical fermions or finite volume effects. However these deviations are within one standard deviation of the linear form, so it cannot be ruled out that they are attributable to noise in the ensemble of gauge

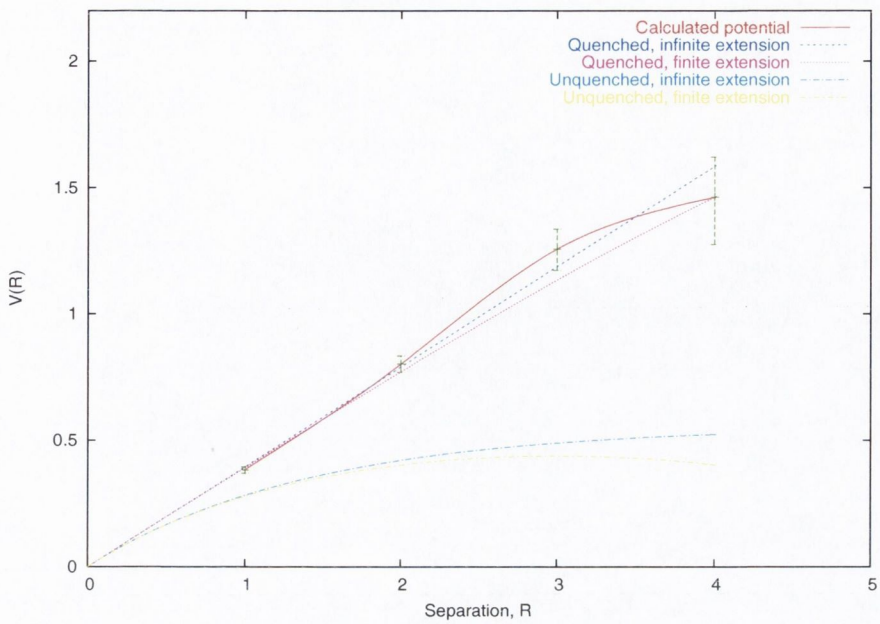

Figure 28: The analytic predictions for the static fermion potential at $e = 0.89$ together with the results from our calculation.

configurations.

To determine the statistical validity of the deviations, a greater number of gauge configurations would have to be obtained to reduce the error bars and to allow measurements on data points at greater R. In the latter case, more configurations would improve the signal-to-noise ratio, reducing the influence of the noise.

9.1.4 The Potential at $e = 1.3$

In increasing e, we encounter the same signal-to-noise problems as when we increased R. Consequently, the range of data points that we can access decreases. As we move up to $e = 1.3$, we find that only $R = 1$ provides us with a range of values of T. Figure 29 shows this range. The $T = 2$ data point is errant, but the remaining data points follow the predicted pattern.

The $T = 1$ data point is $0.888(+0.056, -0.060)$. At $R = 1$, the analytical value of the potential is 0.845, which is comfortably in agreement. For each subsequent value of R, we only have one data point. These are summarized in the Table 2 and are

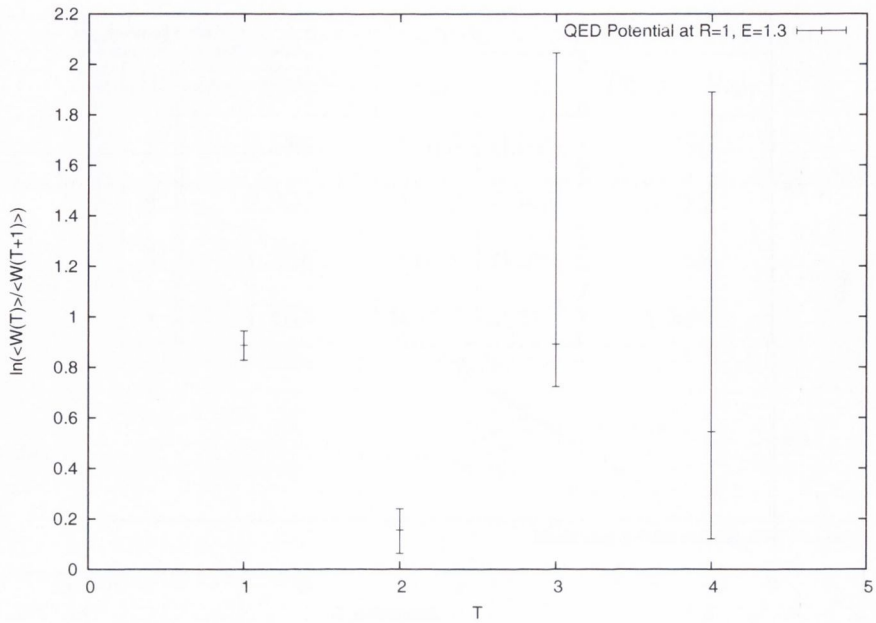

Figure 29: The static fermion potential at $R = 1$ and $e = 1.3$.

Table 2: The static quark potential data points at $e = 1.3$.

R	$\ln\left(\frac{<W(1)>}{<W(2)>}\right)$	$+\Delta$	$-\Delta$	Theor. Val.
1	0.888	0.056	0.060	0.845
2	1.659	0.213	0.271	1.690
3	2.274	0.499	1.040	2.535

plotted in Figure 30.

In Figure 31, we see the four potentials predicted by equation (43) for $e = 1.3$. The potential for the quenched, infinite spatial extent case is shown in red and the potential for the quenched, finite spatial extent case (with $L_1 = 6$) is shown in green. The blue and violet plots show the unquenched potentials for infinite and finite extent, respectively.

In Figure 32, we compare these predictions with the potential calculated and shown in Figure 30. As in the $e = 0.89$ case, we use cubic splines to obtain a smooth function that is representative of the data points. As before, we see some agreement between the predictions and the numerically generated potential. The calculated

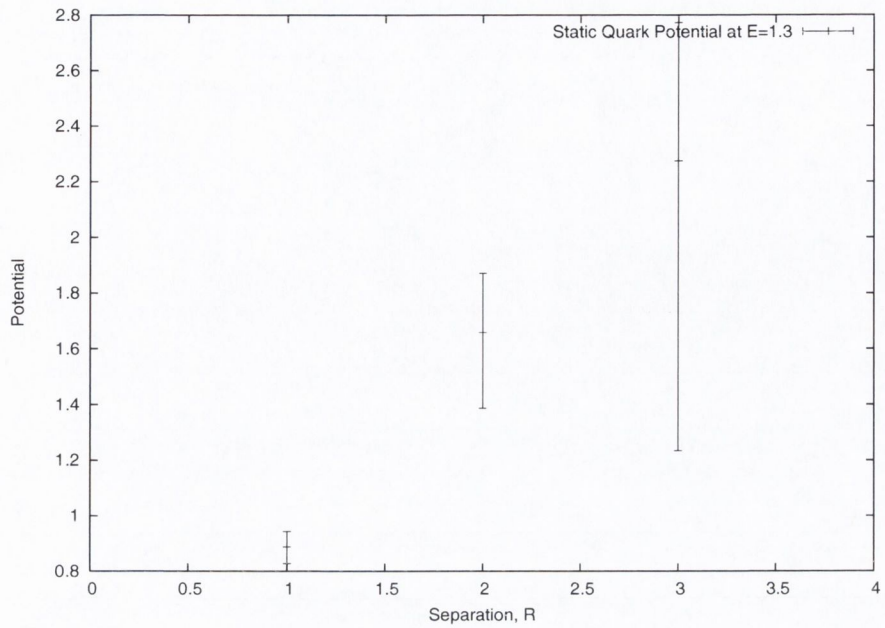

Figure 30: The static quark potential calculated at $e = 1.3$.

potential agrees broadly with the quenched predictions, although it suggests deviation for increasing R. This deviation would be consistent with either the screening effects of the dynamical fermions or with the finite volume effects. As in the $e = 0.89$ case, the deviation is within one standard deviation of the the quenched predictions, so we cannot be certain that it is not a figment of noise in the ensemble.

9.1.5 Discussion

The calculated potential in both cases agrees with the quenched predictions. This is surprising as the simulation uses dynamical fermions and so we would expect to see a screened potential that more resembled the unquenched plots.

In both cases, we see some deviation from the quenched predictions, but it is small, lying within one standard deviation of the data point. It is possible that the deviation is produced by noise in the ensemble, but the consistency between both plots would suggest that this is a systematic result.

The deviation of the interpolated calculated potential is significantly larger than the deviation shown by the quenched finite spatial extent case from the quenched

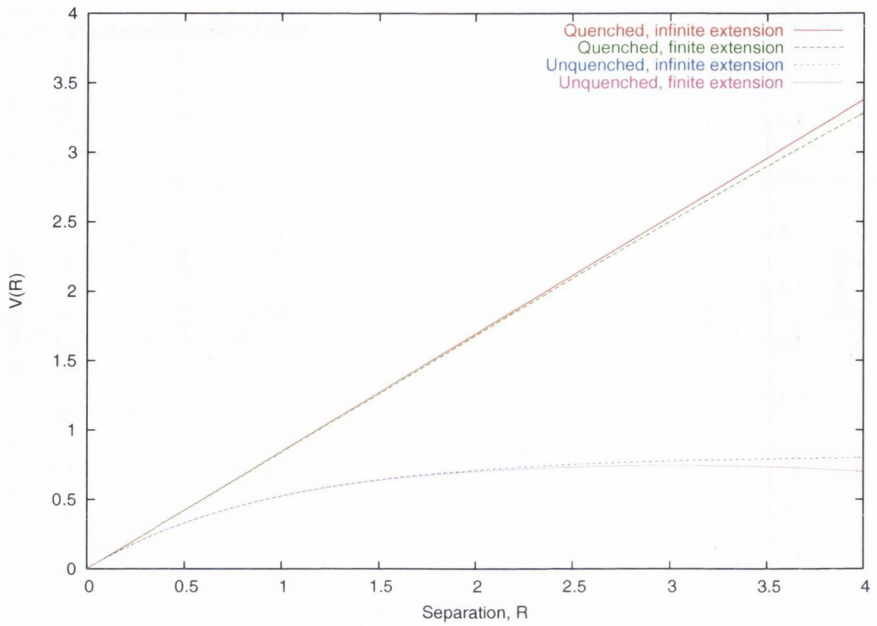

Figure 31: The static quark potential for $e = 1.3$ and $L_1 = 6$ with the linear, unscreened potential in the limit of infinite spatial extent (red), the unscreened potential with finite spatial extent (green), the screened potential with infinite extent (blue) and the screened potential with finite extent(pink).

infinite extent case. This would suggest that the deviation of the calculated potential from the quenched result is due to screening effects, rather than finite spatial extent effects. However, the size of the error bars at each points do not permit us to draw hard conclusions here.

To investigate this further, a greater number of gauge configurations would have to be generated, in order to reduce the size or the error bars and to allow measurements to be made at higher R, where the deviation would be greater, if it is not an artifact of the noise.

9.2 The Topological Charge

In Figure 18, we see that in standard lattice field theory, there are free energy hills that are likely to impede the transitions of the system between configurations with different topological charge in a Hybrid Monte Carlo calculation. In Figure 19, we

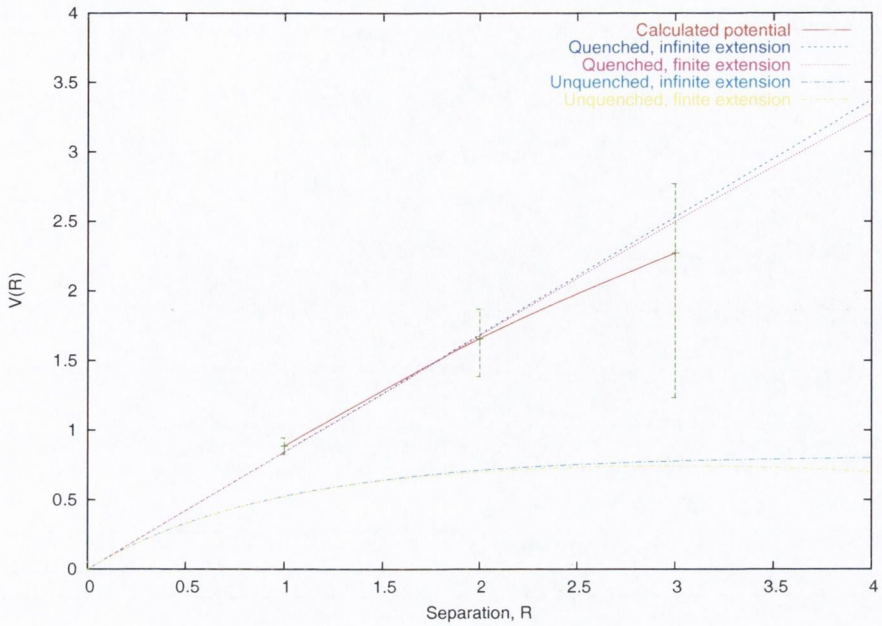

Figure 32: The analytic predictions for the static fermion potential at $e = 1.3$ together with the result of from our calculation.

see that these hills do not appear in the geometric discretization. Using these sets of gauge field configurations, we calculated the topological charge, using the definition in equation (32), in order to see how the configurations were distributed.

We calculated the topological charge for sets of gauge configurations generated with $e = 1.3$, $e = 1.5$ and $e = 1.7$ and the results are shown in Figures 33, 34 and 35, respectively.

In the limit of a large number of distributions, the curves should become Gaussian. In our case, where the number of configurations is limited to 180, we can see that the system visits states of non-zero topological charge liberally enough to suggest that there does not appear to be barriers impeding the transition between states of differing topological charge. The number of configurations is too few to show that the underlying distribution is Gaussian, but the distributions shown would not be incompatible with this.

With a larger data set, we would be able to infer the topological susceptibility of

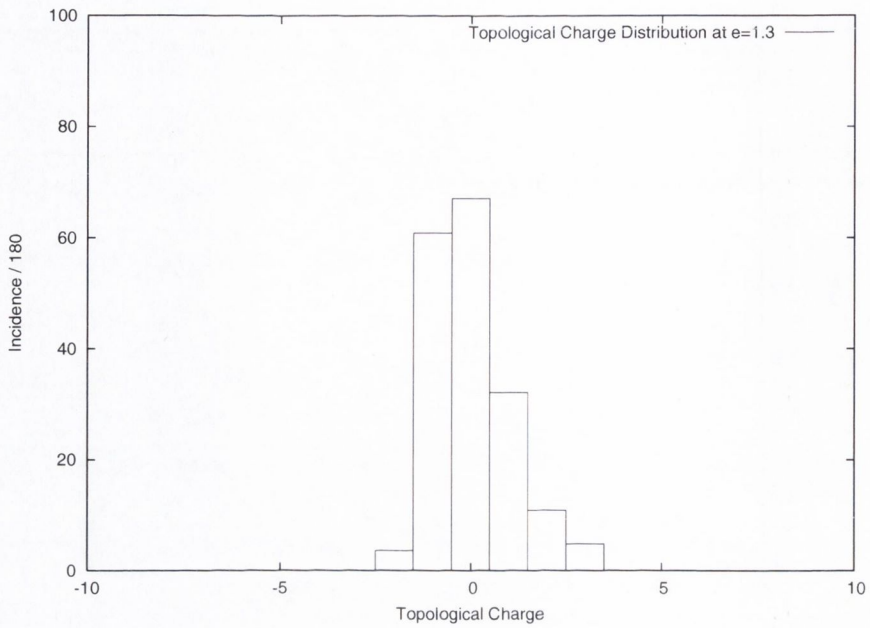

Figure 33: The topological charge distribution for $e = 1.3$.

the vacuum which is calculated from the variance of the distribution [92]

$$\chi = \frac{< Q^2 >}{V}$$

where V is the volume of the system.

9.3 The Chiral Condensate

In [87], Joos and Azakov describe analytical calculations showing the limiting behaviour of the chiral condensate with respect to the extension of the lattice in the time dimension.

We had hoped that a calculation of the chiral condensate for our formulation would compare to the theoretical values as well as the static fermion potential calculation had done. Unfortunately, this proved not to be the case.

The reason is the lack of hermiticity in the Dirac operator. In a conventional lattice QCD calculation, the chiral condensate, $< \bar{\Psi}\Psi >$, is evaluated by calculating the ensemble average of $\mathrm{Tr}\,(M^{-1})$, where M is the Dirac operator. This quantity is guaranteed to be real because of the γ_5-hermiticity of M. In our case, the lack of

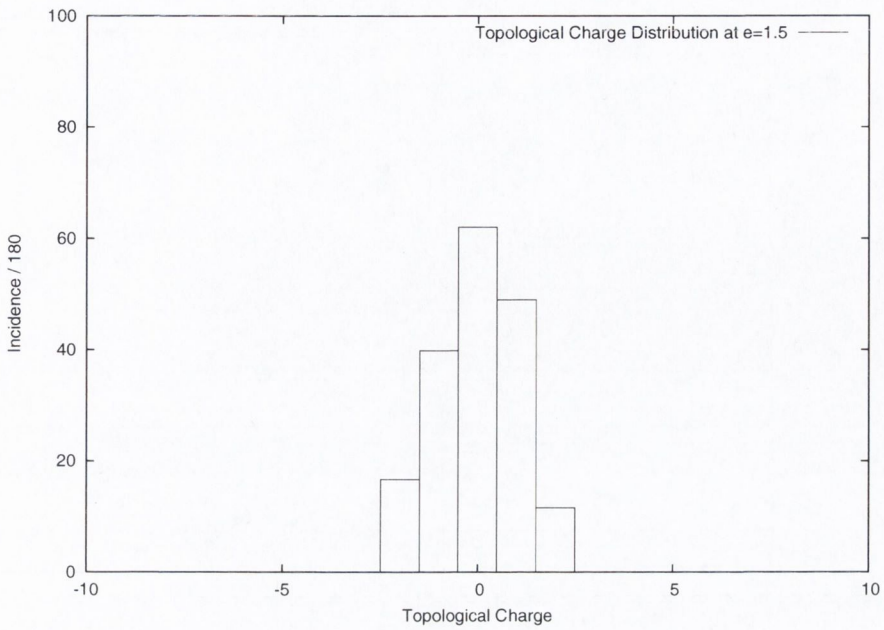

Figure 34: The topological charge distribution for $e = 1.5$.

a hermiticity property means that the eigenvalues can be complex and so $\mathrm{Tr}\,(M^{-1})$ can be complex.

This left us with the question of how to make $\mathrm{Tr}\,(M^{-1})$ real. Using the product $M^{\dagger}M$ is inadvisable as this represents a different combination of propagating fields to that represented by the product $< \bar{\Psi}\Psi >$. Instead we chose to drop the imaginary component on the grounds that preliminary simulations showed that the imaginary part of $< \bar{\tilde{\phi}}, \tilde{\phi} >$ was significantly smaller in magnitude than the real part. For example, on a simulation of a 5x5 complex, using 140 Metropolis steps, $Re\left(< \bar{\tilde{\phi}}, \tilde{\phi} >\right) = 2514.6$ and $Im\left(< \bar{\tilde{\phi}}, \tilde{\phi} >\right) = -352.5$. Whilst the imaginary figures were not negligible, they were not dominant either and for that reason, we thought that dropping might not affect the data significantly.

Unfortunately, this proved not to be the case. The values for $Re\left(< \bar{\tilde{\phi}}, \tilde{\phi} >\right)$ that we obtained had standard deviations that were several orders of magnitude too large to admit any meaningful comparison with the theoretical values. In the example where $Re\left(< \bar{\tilde{\phi}}, \tilde{\phi} >\right) = 2514.6$, we found that $\sigma = 8036.7$.

This still leaves an open question of how to construct a fermion propagator with

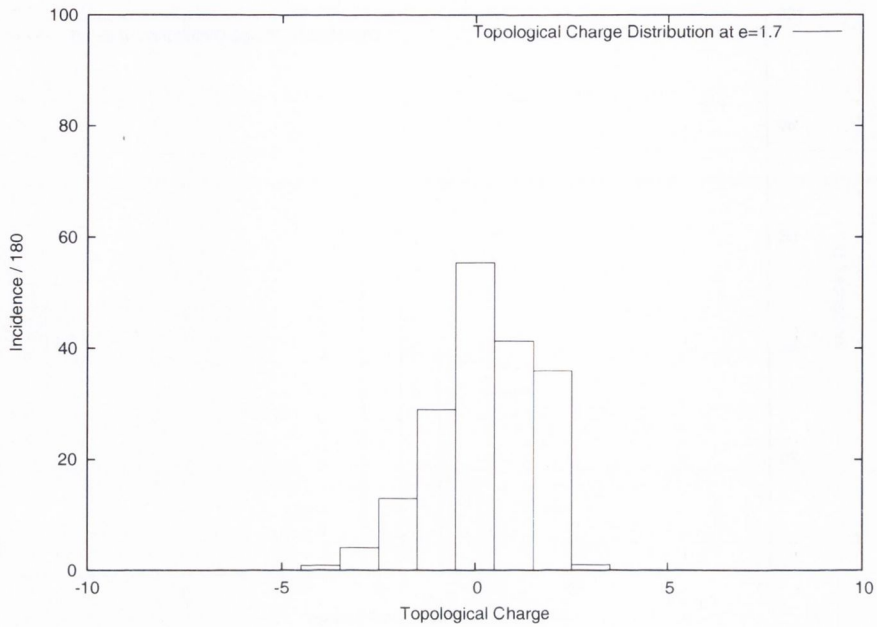

Figure 35: The topological charge distribution for $e = 1.7$.

a real trace in this formulation.

9.4 Autocorrelation

The Hybrid Monte Carlo algorithm achieves its computational efficiency by sampling richly from the configurations with high probability. Each new configuration is determined from the previous configuration using molecular dynamics and a Metropolis test. This invites the question of whether there is a high degree of autocorrelation within the generated sequence of gauge field configurations.

Autocorrelation can be tested using any observable and we shall use the gauge action, defined in section 6.3.2. We use the definition for autocorrelation provided by Sokal [94] and used in [95] [96]. For a general observable, X_i with n components and mean $\bar{X}$

$$A(t) = \frac{1}{n - |t|} \sum_{i=1}^{n-|t|} (X_i - \bar{X})(X_{i+|t|} - \bar{X})$$

A plot of the autocorrelation function for the gauge action is shown in Figure 36 for $e = 0.89$.

We can see here that, at low t, the autocorrelation is high, as expected. However,

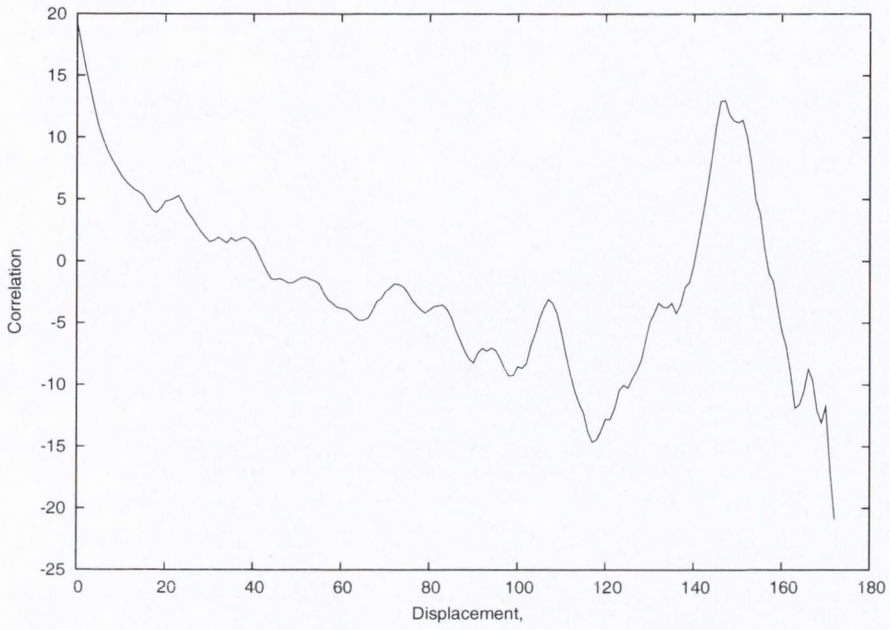

Figure 36: The autocorrelation of the gauge action measured against the displacement in simulation time.

as t increases the autocorrelation quickly falls away, reaching zero after approximately 40 Monte Carlo steps. As t continues to increase, there is a period of low amplitude oscillation before the value of the autocorrelation becomes more erratic. The erratic behaviour is expected at high t because the number of components used in the sum is small, making the value of the autocorrelation more sensitive to noise.

In our calculations, we use 180 gauge configurations and we can here see that the autocorrelation has hampered, but not prevented us from representatively sampling the configuration space.

10 Future Work

The work that we have presented here is largely developmental. We have shown how to construct and use an Abelian field theory within the geometric discretization framework to numerically calculate analytically known quantities. We have also proposed an original scheme for isolating the flavour and chiral components of Dirac-Kähler fermions. Both of these topics could be extended in a range of ways.

The gauge theory is an Abelian theory and it would be interesting to generalise it to non-Abelian gauge groups. It would also be of interest to compare it to other non-compact $U(1)$ formulations [75][90] for performance and accuracy.

One unusual feature of this description is the lack of hermiticity present in the Dirac-Kähler operator. It would be of great interest to analyse the implications of this for the formulation. The substitution $\sqrt{\det(M^\dagger M)}$ partially addresses this and it resembles both the quarter-root trick used in staggered fermion calculations [73][91] and the denominator of the Overlap Dirac operator in equation (5), but it is different enough that the degree of locality is not clear from the definition. This would be worth further study.

The lack of a hermiticity property also has consequences for the lattice Feynman rules. As we saw in Section 9.3, a non-hermitian Dirac-Kähler operator leads to a non-hermitian fermion propagator. This is an important issue that deserves to be addressed in future work.

We saw agreement between the analytical values for the static fermion potential and our calculated values. However, the error bars were smaller at lower e. It would be valuable to test this agreement at greater accuracy by performing more calculations at lower values of e. This would also allow us to further investigate the screening and finite volume effects in the static fermion potential by allowing us to extend the calculated potential to higher values of R.

The description that we have proposed for isolating the components of Dirac-Kähler fermions using multiple complexes has much potential for development and could have some bearing on the quarter-root trick of staggered fermions [73][91]. In the four dimensional version, we used eight complexes, but only four were needed to

separate the different flavours. In a free field calculation, there would be a separate action for each complex. The total action would then be the sum of four terms: $S = S_o + S_d + S_e + S_t$. Integrating the fermion fields for each complex separately would mean that the determinant in the path integral was a product of four separate determinant, one for each complex.

To generalise this to the gauged case, would require us to study how effectively we could project out the gauge fields so that we could isolate those that associate with just one flavour.

Naturally, it would be of interest to try to rewrite these ideas in the conventional Dirac basis. The ideas behind the multiple complex approach are inspired by discrete differential geometry, but there is no reason, in principle, why the same ideas cannot be applied to the standard staggered fermion formulation.

Whether these ideas bear fruit or not, it would be nonetheless valuable to try using the multiple complex system to perform lattice gauge calculations, just as we have done for original geometric discretization formulation. This would require redesigning the code and algorithms that we have used to calculate the results in Section 9, but the adjustments would be a manageable project.

11 Conclusions

The work in this thesis mostly relates to the construction and use of an Abelian gauge theory in the geometric discretization formulation of discrete differential geometry when used to represent Dirac-Kähler fermions. However, the first result that we obtained was a definition for a wedge product that admitted a local equation of motion for the fermion field, but not a local action.

Our first development of the geometric discretization formulation was to show that, in two space-time dimensions, we could use combinations of the original and dual complexes to separate out either the chiral components of the free fermion fields or the flavour components. To enable us to isolate both the chiral and flavour components simultaneously, we were required to introduce another pair of complexes and to adjust the Hodge star definition so that it mapped in a suitable way between the four complexes.

Having done this for two dimensions, we studied the same idea in four dimensions. We found that we could isolate the chiral components using just the original and dual complexes, but to isolate each of the four degenerate flavours, we needed to introduce two new structures of complex and a new operator. The first complex was defined to have simplices complementary to the original complex in two of the four space-time dimensions, but not in the remaining two. The simplices of the second complex were complementary to the simplices of the first complex in all four dimensions. The operator mapped differential forms to their complement in two of the four dimensions. As in the two dimensional case, we needed to introduce a second set of all the complexes and modify the operators appropriately to be able to isolate the chiral and flavour components simultaneously.

In the next section of the thesis, we constructed an Abelian field theory for the Dirac-Kähler formulation. We introduced a set of gauge transforms, an invariant gauge action and, because the theory is non-compact, a gauge fixing term for the Lorentz gauge. We defined a topological charge for the theory and compared it to established results analytically. We also looked at a specific topological gauge configuration and showed how the gauge transformation defining the topology for

the discrete formulation converged on the continuum definition for large complexes.

We then set about constructing a computational framework for the Abelian gauge theory so that we could test it, numerically, against analytical results. The framework used the Hybrid Monte Carlo algorithm to generate an ensemble of gauge fields on both the dual and original complexes.

We used Wilson loops on the configurations generated to calculate the static potential and showed that the potential produced by our formulation agreed with the analytic results.

Our final result was to study the topological charge of ensembles of gauge configurations and to show that the system appears to move liberally into regions of non-zero topological charge with a distribution consistent with the Gaussian shaped gauge action.

A An Alternative Definition for the Wedge Product

In this section, we show that it is possible to define a wedge product within the framework introduced by Becher and Joos [45] that allows Leibnitz' rule to be satisfied and that admits a local Clifford algebra.

Leibnitz' rule describes the derivative of the product of a pair of functions and it is desirable to have the same relationship on the complex as in the continuum. In the Dirac basis, on the lattice, the derivative is a finite difference operator and the functions are vectors or scalars found at the vertices of the lattice. In discrete differential geometry, the derivative is the exterior derivative and the functions are linear combinations of discrete differential forms. The product between the functions is taken using the discrete wedge product and the exterior derivative also contains a discrete wedge product between a discrete 1-form and the function on which it operates. The definition of the discrete wedge product determines which terms are non-zero and so it has a subtle but critical role in defining the properties of the product and the exterior derivative. In the Dirac basis, its role would be played by Dirac delta functions between lattice sites.

Here, we modify the definition of the wedge product, which affects the definition of the product between functions and the definition of the exterior derivative, so that it allows Leibnitz' rule to be fulfilled. The definition for the wedge product is local, but when we use it to define the Hodge star operator, which is necessary to define an inner product, we find that we cannot construct a local operator, with the consequence that the action retains its non-locality. The modification is subtle and to interpret it in the Dirac basis would require the introduction of non-trivial Dirac delta-functions between lattice points in both the finite difference derivative operator and in the product between functions.

This appendix is organised as follows. Firstly, we introduce the notation used by Becher and Joos in their paper. We then use locality and Leibnitz' rule as constraints on an undefined wedge product and find the form it must take in order to

satisfy these constraints. We subsequently provide examples of this definition on one dimensional and two dimensional complexes to show that it allows Leibnitz' rule to be satisfied. We then consider the role of this wedge product definition in axial gauge transformations. Finally, we consider the associated Hodge star operator and the inner product.

The construction

Becher and Joos divided the 2D Euclidean lattice into squares with a length of side of twice the lattice spacing. From each square, the simplices at the bottom left corner, the bottom edge, the left edge and the whole square, represent different discrete differential forms, with the same coordinate.

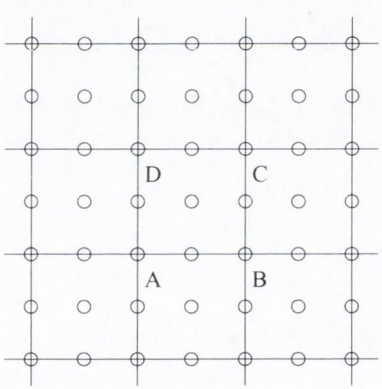

Figure 37: The lattice divided for Becher and Joos formulation.

From the square $ABCD$, in Figure 37, the simplices A, AB, AD and $ABCD$ each represent a different discrete differential form, taking the coordinate of the point A as their coordinates. Thus

$d^{A,\emptyset}$ is represented by the simplex $[A]$

$d^{A,1}$ is represented by the simplex $[AB]$

$d^{A,2}$ is represented by the simplex $[AD]$

$d^{A,12}$ is represented by the simplex $[ABCD]$

An arbitrary function can be written as $\Phi = \sum_{x,H} \phi(x,H) d^{x,H}$, where the sum over H is a sum over all simplices on the complex, for each coordinate x.

We start the derivation by writing Leibnitz' rule as

$$d(\Phi\tilde{\wedge}\Theta) - (d\Phi)\tilde{\wedge}(\Theta) - (\mathcal{A}\Phi)\tilde{\wedge}(d\Theta) = 0$$

where the wedge product $\tilde{\wedge}$ is undefined and the two arbitrary fields are

$$\Phi = \textstyle\sum_{x,H} \phi(x,H) d^{x,H} \qquad\qquad \Theta = \textstyle\sum_{y,K} \theta(y,K) d^{y,K}$$

The product between Φ and Θ is

$$\Phi\tilde{\wedge}\Theta = \sum_{x,H}\sum_{y,K} \phi(x,H)\theta(y,K) d^{x,H}\tilde{\wedge}d^{y,K}$$

and applying the exterior derivative to this, we have

$$d(\Phi\tilde{\wedge}\Theta) = \sum_{z,\mu}\sum_{x,H}\sum_{y,K} \partial_\mu\Big(\phi(x,H)\theta(y,K)\Big) d^{z,\mu}\tilde{\wedge}d^{x,H}\tilde{\wedge}d^{y,K}$$

where ∂_μ is as yet undefined. Applying the exterior derivative to the two fields individually yields

$$d\Phi = \textstyle\sum_{z,\mu}\sum_{x,H} \partial_\mu\Big(\phi(x,H)\Big) d^{z,\mu}\tilde{\wedge}d^{x,H} \qquad d\Theta = \textstyle\sum_{z,\mu}\sum_{y,K} \partial_\mu\Big(\theta(y,K)\Big) d^{z,\mu}\tilde{\wedge}d^{y,K}$$

After inserting these expressions into Leibnitz' rule, we have

$$\sum_{z,x,y,H,K,\mu} \Big[\partial_\mu\Big(\phi(x,H)\theta(y,K)\Big) d^{z,\mu}\tilde{\wedge}d^{x,H}\tilde{\wedge}d^{y,K} - \theta(y,K)\Big(\partial_\mu\phi(x,H)\Big) d^{z,\mu}\tilde{\wedge}d^{x,H}\tilde{\wedge}d^{y,K}$$

$$-(-1)^h \phi(x,H)\Big(\partial_\mu\theta(y,K)\Big) d^{x,H}\tilde{\wedge}d^{z,\mu}\tilde{\wedge}d^{y,K}\Big] = 0$$

where h is the number of members of the set H.

If the Clifford algebra is to behave locally, the wedge must use the forms on its left and right to construct a form with the same coordinate as the one on its right, but of higher dimension. The resulting form will correspond to a simplex that is centred around a lattice site further from the origin, along at least one axis, than the lattice site centred in the simplex corresponding to the form on the right hand side of the wedge. For example, in Figure 37, $(\sum_y d^{y,2})\tilde{\wedge}d^{A,1}$ must have a product with coordinate A, if we are to be able to have $e^2\lrcorner(\sum_y d^{y,2})\tilde{\wedge}d^{A,1} = d^{A,1}$. Therefore, the product $(\sum_y d^{y,2})\tilde{\wedge}d^{A,1}$ must be proportional to $d^{A,12}$ which corresponds to a simplex

centred on a lattice site further along the 2 axis than the lattice site at the centre of the simplex corresponding to $d^{1,x}$.

Consequently, the requirement that the square of the Clifford product behaves locally means that the exterior derivative must contain a forward derivative: $(T_{e_\mu}-1)$. Applying the forward derivatives to Leibnitz' rule, we have

$$\sum_{z,x,y,H,K,\mu}\Big[\Big(\phi(x+e_\mu,H)\theta(y+e_\mu,K)-\phi(x,H)\theta(y,K)\Big)d^{z,\mu}\tilde{\wedge}d^{x,H}\tilde{\wedge}d^{y,K}$$

$$-\theta(y,K)\Big(\phi(x+e_\mu,H)-\phi(x,H)\Big)d^{z,\mu}\tilde{\wedge}d^{x,H}\tilde{\wedge}d^{y,K}$$

$$-(-1)^h\phi(x,H)\Big(\theta(y+e_\mu,K)-\theta(y,K)\Big)d^{x,H}\tilde{\wedge}d^{z,\mu}\tilde{\wedge}d^{y,K}\Big]=0$$

The second terms of the first and second lines cancel, leaving us with

$$\sum_{z,x,y,H,K,\mu}\Big[\Big(\phi(x+e_\mu,H)\theta(y+e_\mu,K)-\theta(y,K)\phi(x+e_\mu,H)\Big)d^{z,\mu}\tilde{\wedge}d^{x,H}\tilde{\wedge}d^{y,K} \quad (45)$$

$$-(-1)^h\Big(\phi(x,H)\theta(y+e_\mu,K)-\phi(x,H)\theta(y,K)\Big)d^{x,H}\tilde{\wedge}d^{z,\mu}\tilde{\wedge}d^{y,K}\Big]=0$$

In order for Leibnitz' rule to be satisfied, the remaining terms must cancel. If the θ field is constant across the complex, the first and second terms will cancel with each other and the third and fourth terms will also cancel with each other. However, we are interested in a result for arbitrary fields, so instead we define the wedge so that the first and third terms cancel with each other and the second and fourth terms cancel.

If we choose the $\tilde{\wedge}$ to be

$$\begin{array}{rcll} d^{x,H}\tilde{\wedge}d^{y,K} & = & \epsilon_{H,K}d^{y,H\cup K}\delta^{x,y+e_K} & \text{for } H\cap K=\emptyset \\ & & 0 & \text{otherwise} \end{array} \quad (46)$$

the first and third terms become

$$\sum_{y,H,K,\mu}\Big(\phi(y+e_K+e_\mu,H)\theta(y+e_\mu,K)\epsilon_{\mu HK}d^{y,\mu\cup H\cup K}$$

$$-(-1)^h\phi(y+e_k+e_\mu,H)\theta(y+e_\mu,K)\epsilon_{H\mu K}d^{y,\mu\cup H\cup K}\Big)$$

If we rewrite $\epsilon_{H\mu K}$ as $(-1)^h\epsilon_{\mu HK}$, we can see that the two terms cancel.

The second and fourth terms of equation (45) are

$$\sum_{z,x,y,H,K,\mu} \Big[\Big(-\theta(y,K)\phi(x+e_\mu,H) \Big) d^{z,\mu} \tilde{\wedge} d^{x,H} \tilde{\wedge} d^{y,K} \tag{47}$$

$$-(-1)^h \Big(-\phi(x,H)\theta(y,K) \Big) d^{x,H} \tilde{\wedge} d^{z,\mu} \tilde{\wedge} d^{y,K} \Big] = 0$$

Applying the same definition for $\tilde{\wedge}$, we have

$$\sum_{y,H,K,\mu} \Big[\Big(-\theta(y,K)\phi(y+e_K+e_\mu,H) \Big) \epsilon_{\mu HK} d^{y,\mu\cup H\cup K} \tag{48}$$

$$-(-1)^h \Big(-\phi(y+e_K+e_\mu,H)\theta(y,K) \Big) \epsilon_{H\mu K} d^{y,\mu\cup H\cup K} \Big]$$

By rewriting $\epsilon_{H\mu K}$ as $(-1)^h \epsilon_{\mu HK}$ we can see that these terms also cancel.

A.1 Example in 1d

To demonstrate this definition, we show how it satisfies Leibnitz' rule in one dimension.

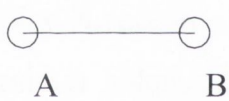

Figure 38: A one dimensional complex.

In Figure 38, we have three simplices: $[A]$, $[B]$ and $[AB]$ corresponding to $d^{A,\emptyset}$, $d^{B,\emptyset}$ and $d^{A,1}$, respectively. We define two fields on this complex with

$$\begin{aligned} \Phi &= \phi(A,\emptyset)d^{A,\emptyset} + \phi(B,\emptyset)d^{B,\emptyset} + \phi(A,1)d^{A,1} \\ \Theta &= \theta(A,\emptyset)d^{A,\emptyset} + \theta(B,\emptyset)d^{B,\emptyset} + \theta(A,1)d^{A,1} \end{aligned}$$

Using the wedge product $d^{x,H} \tilde{\wedge} d^{y,K} = \epsilon_{HK} d^{y,H\cup K} \delta^{x,y+e_K}$, the product between these fields is

$$\Phi \tilde{\wedge} \Theta = \phi(A,\emptyset)\theta(A,\emptyset)d^{A,\emptyset} + \phi(B,\emptyset)\theta(B,\emptyset)d^{B\emptyset} + \phi(B,\emptyset)\theta(A,1)d^{A,1}$$

The exterior derivative of this expression is

$$\begin{aligned} d(\Phi\tilde{\wedge}\Theta) &= \textstyle\sum_{y,\mu} d^{y,\mu}\tilde{\wedge}(T_{e_\mu}-1)(\Phi\tilde{\wedge}\Theta) \\ &= d^{A,1}\tilde{\wedge}(T_{e_1}-1)(\Phi\tilde{\wedge}\Theta) \\ &= \Big(\phi(B,\emptyset)\theta(B,\emptyset)-\phi(A,\emptyset)\theta(A,\emptyset)\Big)d^{A,1}\tilde{\wedge}d^{A,\emptyset} \\ &= \Big(\phi(B,\emptyset)\theta(B,\emptyset)-\phi(A,\emptyset)\theta(A,\emptyset)\Big)d^{A,1} \end{aligned} \tag{49}$$

with all other terms going to zero.

Now we look at the two terms $(d\Phi)\tilde{\wedge}\Theta$ and $(\mathcal{A}\Phi)\tilde{\wedge}(d\Theta)$.

$$\begin{aligned} d\Phi &= \textstyle\sum_{y,\mu} d^{y,\mu}\tilde{\wedge}(T_{e_\mu}-1)\Phi \\ &= d^{A,1}\tilde{\wedge}(T_{e_1}-1)\Phi \\ &= \Big(\phi(B,\emptyset)-\phi(A,\emptyset)\Big)d^{A,1}\tilde{\wedge}d^{A,\emptyset} \\ &= \Big(\phi(B,\emptyset)-\phi(A,\emptyset)\Big)d^{A,1} \\ d\Theta &= \Big(\theta(B,\emptyset)-\theta(A,\emptyset)\Big)d^{A,1} \end{aligned}$$

For the first of the two terms, we have

$$\begin{aligned} (d\Phi)\tilde{\wedge}\Theta &= \Big(\Big(\phi(B,\emptyset)-\phi(A,\emptyset)\Big)d^{A,1}\Big) \\ &\quad \tilde{\wedge}\Big(\theta(A,\emptyset)d^{A,\emptyset}+\theta(B,\emptyset)d^{B,\emptyset}+\theta(A,1)d^{A,1}\Big) \\ &= \Big(\phi(B,\emptyset)\theta(A,\emptyset)-\phi(A,\emptyset)\theta(A,\emptyset)\Big)d^{A,1} \end{aligned}$$

For the second of the two terms, we have

$$\begin{aligned} (\mathcal{A}\Phi)\tilde{\wedge}(d\Theta) &= \mathcal{A}\Big(\phi(A,\emptyset)d^{A,\emptyset}+\phi(B,\emptyset)d^{B,\emptyset}+\phi(A,1)d^{A,1}\Big) \\ &\quad \tilde{\wedge}\Big(\theta(B,\emptyset)-\theta(A,\emptyset)\Big)d^{A,1} \\ &= \Big(\phi(A,\emptyset)d^{A,\emptyset}+\phi(B,\emptyset)d^{B,\emptyset}-\phi(A,1)d^{A,1}\Big) \\ &\quad \tilde{\wedge}\Big(\theta(B,\emptyset)-\theta(A,\emptyset)\Big)d^{A,1} \\ &= \Big(\phi(B,\emptyset)\theta(B,\emptyset)-\phi(B,\emptyset)\theta(A,\emptyset)\Big)d^{A,1} \end{aligned}$$

Adding these terms together we have

$$\begin{aligned} (d\Phi)\tilde{\wedge}\Theta+(\mathcal{A}\Phi)\tilde{\wedge}(d\Theta) &= \Big(\phi(B,\emptyset)\theta(A,\emptyset)-\phi(A,\emptyset)\theta(A,\emptyset)\Big)d^{A,1} \\ &+ \Big(\phi(B,\emptyset)\theta(B,\emptyset)-\phi(B,\emptyset)\theta(A,\emptyset)\Big)d^{A,1} \\ &= \Big(\phi(B,\emptyset)\theta(B,\emptyset)-\phi(A,\emptyset)\theta(A,\emptyset)\Big)d^{A,1} \end{aligned}$$

which is the same as the last line of equation (49).

A.2 Example in 2d

To demonstrate that the exterior derivative satisfies Leibnitz' rule in less trivial contexts, we shall apply it to a two dimensional complex.

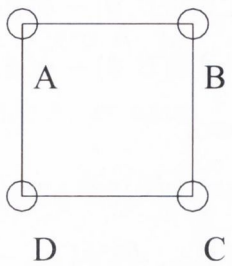

Figure 39: A two dimensional complex.

In Figure 39, the complex comprises nine simplices. Four simplices are zero dimensional: $[A]$, $[B]$, $[C]$ and $[D]$ which correspond to $d^{A,\emptyset}$, $d^{B,\emptyset}$, $d^{C,\emptyset}$ and $d^{D,\emptyset}$, respectively. Four are one dimensional: $[AB]$, $[BC]$, $[DC]$ and $[AD]$ correspond to $d^{A,1}$, $d^{C,2}$, $d^{D,1}$ and $d^{D,2}$. Finally there is the two dimensional simplex $[ABCD]$ corresponding to $d^{D,12}$.

The two fields Φ and Θ are

$$\begin{aligned}
\Phi &= \phi(A,\emptyset)d^{A,\emptyset} + \phi(B,\emptyset)d^{B,\emptyset} + \phi(C,\emptyset)d^{C,\emptyset} + \phi(D,\emptyset)d^{D,\emptyset} \\
&\quad +\phi(A,1)d^{A,1} + \phi(C,2)d^{C,2} + \phi(D,1)d^{D,1} + \phi(D,2)d^{D,2} \\
&\quad +\phi(D,12)d^{D,12} \\
\Theta &= \theta(A,\emptyset)d^{A,\emptyset} + \theta(B,\emptyset)d^{B,\emptyset} + \theta(C,\emptyset)d^{C,\emptyset} + \theta(D,\emptyset)d^{D,\emptyset} \\
&\quad +\theta(A,1)d^{A,1} + \theta(C,2)d^{C,2} + \theta(D,1)d^{D,1} + \theta(D,2)d^{D,2} \\
&\quad +\theta(D,12)d^{D,12}
\end{aligned}$$

Using the product of equation (46), the product between Φ and Θ is

$$\begin{aligned}
\Phi\tilde{\wedge}\Theta &= \phi(A,\emptyset)\theta(A,\emptyset)d^{A,\emptyset} + \phi(B,\emptyset)\theta(B,\emptyset)d^{B,\emptyset} + \phi(C,\emptyset)\theta(C,\emptyset)d^{C,\emptyset} \\
&\quad +\phi(D,\emptyset)\theta(D,\emptyset)d^{D,\emptyset} + \phi(D,12)\theta(D,\emptyset)d^{D,12} + \phi(B,\emptyset)\theta(D,12)d^{D,12} \\
&\quad +\phi(A,1)\theta(D,2)d^{D,12} - \phi(C,2)\theta(D,1)d^{D,12} + \phi(A,\emptyset)\theta(D,2)d^{D,2} \\
&\quad +\phi(B,\emptyset)\theta(A,1)d^{A,1} + \phi(B,\emptyset)\theta(C,2)d^{C,2} + \phi(C,\emptyset)\theta(D,1)d^{D,1} \\
&\quad +\phi(A,1)\theta(A,\emptyset)d^{A,1} + \phi(C,2)\theta(C,\emptyset)d^{C,2} + \phi(D,1)\theta(D,\emptyset)d^{D,1} \\
&\quad +\phi(D,2)\theta(D,\emptyset)d^{D,2}
\end{aligned}$$

Applying the exterior derivative to this, we have

$$
\begin{aligned}
d(\Phi\tilde{\wedge}\Theta) &= \textstyle\sum_{y,\mu} d^{y,\mu}\tilde{\wedge}(T_{e_\mu}-1)(\Phi\tilde{\wedge}\Theta) \\
&= \Big(\phi(B,\emptyset)\theta(B,\emptyset)-\phi(A,\emptyset)\theta(A,\emptyset)\Big)d^{A,1} \\
&\quad +\Big(\phi(B,\emptyset)\theta(B,\emptyset)-\phi(C,\emptyset)\theta(C,\emptyset)\Big)d^{C,2} \\
&\quad +\Big(\phi(C,\emptyset)\theta(C,\emptyset)-\phi(D,\emptyset)\theta(D,\emptyset)\Big)d^{D,1} \\
&\quad +\Big(\phi(A,\emptyset)\theta(A,\emptyset)-\phi(D,\emptyset)\theta(D,\emptyset)\Big)d^{D,2} \\
&\quad +\Big(\phi(B,\emptyset)\theta(C,2)-\phi(A,\emptyset)\theta(D,2)\Big)d^{D,12} \\
&\quad -\Big(\phi(B,\emptyset)\theta(A,1)-\phi(C,\emptyset)\theta(D,1)\Big)d^{D,12} \\
&\quad -\Big(\phi(A,1)\theta(A,\emptyset)-\phi(D,1)\theta(D,\emptyset)\Big)d^{D,12} \\
&\quad +\Big(\phi(C,2)\theta(C,\emptyset)-\phi(D,2)\theta(D,\emptyset)\Big)d^{D,12}
\end{aligned}
\tag{50}
$$

Now we build the terms $(d\Phi)\tilde{\wedge}\Theta$ and $(\mathcal{A}\Phi)\tilde{\wedge}(d\Theta)$. For the former, we have

$$
\begin{aligned}
d\Phi &= \textstyle\sum_{y,\mu} d^{y,\mu}\tilde{\wedge}(T_{e_\mu}-1)\Phi \\
&= \Big(\phi(B,\emptyset)-\phi(A,\emptyset)\Big)d^{A,1}+\Big(\phi(B,\emptyset)-\phi(C,\emptyset)\Big)d^{C,2} \\
&\quad +\Big(\phi(C,\emptyset)-\phi(D,\emptyset)\Big)d^{D,1}+\Big(\phi(A,\emptyset)-\phi(D,\emptyset)\Big)d^{D,2} \\
&\quad +\Big(\phi(C,2)-\phi(D,2)\Big)d^{D,12}-\Big(\phi(A,1)-\phi(D,1)\Big)d^{D,12} \\
(d\Phi)\tilde{\wedge}\Theta &= \Big(\phi(B,\emptyset)-\phi(A,\emptyset)\Big)\theta(A,\emptyset)d^{A,1}+\Big(\phi(B,\emptyset)-\phi(C,\emptyset)\Big)\theta(C,\emptyset)d^{C,2} \\
&\quad +\Big(\phi(C,\emptyset)-\phi(D,\emptyset)\Big)\theta(D,\emptyset)d^{D,1}+\Big(\phi(A,\emptyset)-\phi(D,\emptyset)\Big)\theta(D,\emptyset)d^{D,2} \\
&\quad +\Big(\phi(B,\emptyset)-\phi(A,\emptyset)\Big)\theta(D,2)d^{D,12}-\Big(\phi(B,\emptyset)-\phi(C,\emptyset)\Big)\theta(D,1)d^{D,12} \\
&\quad +\Big(\phi(C,2)-\phi(D,2)\Big)\theta(D,\emptyset)d^{D,12}-\Big(\phi(A,1)-\phi(D,1)\Big)\theta(D,\emptyset)d^{D,12}
\end{aligned}
$$

For the latter, we have

$$
\begin{aligned}
d\Theta &= \textstyle\sum_{y,\mu} d^{y,\mu}\tilde{\wedge}(T_{e_\mu}-1)\Theta \\
&= \Big(\theta(B,\emptyset)-\theta(A,\emptyset)\Big)d^{A,1}+\Big(\theta(B,\emptyset)-\theta(C,\emptyset)\Big)d^{C,2} \\
&\quad +\Big(\theta(C,\emptyset)-\theta(D,\emptyset)\Big)d^{D,1}+\Big(\theta(A,\emptyset)-\theta(D,\emptyset)\Big)d^{D,2} \\
&\quad +\Big(\theta(C,2)-\theta(D,2)\Big)d^{D,12}-\Big(\theta(A,1)-\theta(D,1)\Big)d^{D,12} \\
(\mathcal{A}\Phi)\tilde{\wedge}(d\Theta) &= \phi(B,\emptyset)\Big(\theta(B,\emptyset)-\theta(A,\emptyset)\Big)d^{A,1}+\phi(B,\emptyset)\Big(\theta(B,\emptyset)-\theta(C,\emptyset)\Big)d^{C,2} \\
&\quad +\phi(C,\emptyset)\Big(\theta(C,\emptyset)-\theta(D,\emptyset)\Big)d^{D,1}+\phi(A,\emptyset)\Big(\theta(A,\emptyset)-\theta(D,\emptyset)\Big)d^{D,2} \\
&\quad -\phi(A,1)\Big(\theta(A,\emptyset)-\theta(D,\emptyset)\Big)d^{D,12}+\phi(C,2)\Big(\theta(C,\emptyset)-\theta(D,\emptyset)\Big)d^{D,12} \\
&\quad +\phi(B,\emptyset)\Big(\theta(C,2)-\theta(D,2)\Big)d^{D,12}-\phi(B,\emptyset)\Big(\theta(A,1)-\theta(D,1)\Big)d^{D,12}
\end{aligned}
$$

In the sum $(d\Phi)\tilde{\wedge}\Theta + (\mathcal{A}\Phi)\tilde{\wedge}(d\Theta)$, we see that many terms cancel, leaving us with

$$\begin{aligned}(d\Phi)\tilde{\wedge}\Theta + (\mathcal{A}\Phi)\tilde{\wedge}(d\Theta) \;=\; & \Big(\phi(B,\emptyset)\theta(B,\emptyset) - \phi(A,\emptyset)\theta(A,\emptyset)\Big)d^{A,1} \\ & +\Big(\phi(B,\emptyset)\theta(B,\emptyset) - \phi(C,\emptyset)\theta(C,\emptyset)\Big)d^{C,2} \\ & +\Big(\phi(C,\emptyset)\theta(C,\emptyset) - \phi(D,\emptyset)\theta(D,\emptyset)\Big)d^{D,1} \\ & +\Big(\phi(A,\emptyset)\theta(A,\emptyset) - \phi(D,\emptyset)\theta(D,\emptyset)\Big)d^{D,2} \\ & +\Big(\phi(B,\emptyset)\theta(C,2) - \phi(A,\emptyset)\theta(D,2)\Big)d^{D,12} \\ & -\Big(\phi(B,\emptyset)\theta(A,1) - \phi(C,\emptyset)\theta(D,1)\Big)d^{D,12} \\ & -\Big(\phi(A,1)\theta(A,\emptyset) - \phi(D,1)\theta(D,\emptyset)\Big)d^{D,12} \\ & +\Big(\phi(C,2)\theta(C,\emptyset) - \phi(D,2)\theta(D,\emptyset)\Big)d^{D,12}\end{aligned}$$

which is the same as the right hand side of equation (50).

A.3 Transforming the Spinor

One of the contexts in which this wedge has the potential to be useful is that of transforms. In the 2D continuum, in the Dirac basis, the $U_V(1)$ and $U_A(1)$ symmetries are implemented on the spinor with the transforms $\psi(x) \to e^{i\alpha(x)}\psi(x)$ and $\psi(x) \to e^{i\alpha(x)\sigma_3}\psi(x)$, respectively. In the Dirac-Kähler basis, this becomes $\Phi(x) \to e^{i\alpha(x)}\Phi(x)$ and $\Phi(x) \to e^{i\alpha(x)(-idx^1\vee dx^2\vee)}\Phi(x)$ which reduces to $\Phi(x) \to e^{\alpha(x)dx^1\vee dx^2\vee}\Phi(x)$. The term $e^{i\alpha(x)(-idx^1\vee dx^2\vee)}$ can be rewritten as $\cos(\alpha(x)) + \sin(\alpha(x))dx^1 \vee dx^2\vee$.

On the complex, it would also be desirable to have the same transformation: $\Phi(x) \to e^{i\alpha(x)(-idx^1\vee dx^2\vee)}\Phi(x)$. However, the definition of the wedge that Becher and Joos settled on in [45] does not facilitate this because $e^\mu \lrcorner \sum_y d^{y,\mu}\wedge$ and $\sum_y d^{y,\mu}\wedge e^\mu \lrcorner$ are proportional to the translation operators so every pair of consecutive terms in the power series expansion of $e^{i\alpha(x)(-i\sum_y d^{y,1}\vee\sum_z d^{z,2}\vee)}$ is proportional to a different number of translation operators.

For example,

$$e^{i\alpha(x)(-i\sum_y d^{y,1}\vee\sum_z d^{z,2}\vee)} = 1 + i\alpha(x)(-i\sum_y d^{y,1}\vee\sum_z d^{z,2}\vee) \tag{51}$$

$$-\frac{1}{2}\alpha^2(x)(-i\sum_y d^{y,1}\vee\sum_z d^{z,2}\vee)^2 - i\frac{1}{3!}\alpha^3(x)(-i\sum_y d^{y,1}\vee\sum_z d^{z,2}\vee)^3$$

$$+\frac{1}{4!}\alpha^4(x)(-i\sum_y d^{y,1}\vee\sum_z d^{z,2}\vee)^4+i\frac{1}{5!}\alpha^5(x)(-i\sum_y d^{y,1}\vee\sum_z d^{z,2}\vee)^5-.....$$

When we simplify the above expression using the definition for the wedge selected by Becher and Joos, it becomes

$$e^{i\alpha(x)(-i\sum_y d^{y,1}\vee\sum_z d^{z,2}\vee)}=1+i\alpha(x)(-i\sum_y d^{y,1}\vee\sum_z d^{z,2}\vee)$$

$$-\frac{1}{2}\alpha^2(x)(T_{-e_1}T_{-e_2})-i\frac{1}{3!}\alpha^3(x)(-i\sum_y d^{y,1}\vee\sum_z d^{z,2}\vee)(T_{-e_1}T_{-e_2})$$

$$+\frac{1}{4!}\alpha^4(x)(T^2_{-e_1}T^2_{-e_2})+i\frac{1}{5!}\alpha^5(x)(-i\sum_y d^{y,1}\vee\sum_z d^{z,2}\vee)(T^2_{-e_1}T^2_{-e_2})-.....$$

However, when we expand (51) using the wedge definition from equation (46), it becomes

$$e^{i\alpha(x)(-i\sum_y d^{y,1}\vee\sum_z d^{z,2}\vee)}=1+i\alpha(x)(-i\sum_y d^{y,1}\vee\sum_z d^{z,2}\vee)$$

$$-\frac{1}{2}\alpha^2(x)-i\frac{1}{3!}\alpha^3(x)(-i\sum_y d^{y,1}\vee\sum_z d^{z,2}\vee)$$

$$+\frac{1}{4!}\alpha^4(x)+i\frac{1}{5!}\alpha^5(x)(-i\sum_y d^{y,1}\vee\sum_z d^{z,2}\vee)-.....$$

which is free of the translation operators and so can be written as $\cos(\alpha(x))+sin(\alpha(x))dx^1\vee dx^2\vee$.

A.4 Implications

Changing the definition of the wedge product has implications for many other operators and operations within differential geometry. In the continuum, the Hodge star is defined with the requirement that $dx^H\wedge(*dx^H)=dx^N$ in n dimensional space, where dx^N is an ordered n-form containing all the components of the space. The inner product takes advantage of this relation to build an orientated integral over all of the space: $(\Phi,\Theta)=\int\Phi\wedge(*\Theta)$.

On the complex, it would be desirable to have the same properties. The definition for the wedge chosen by Becher and Joos facilitates this: $d^{x,H}\tilde{\wedge}(*d^{x,H})=d^{x,N}$, where $*$ is naturally defined to be $*d^{x,H}=\epsilon_{H,\mathcal{C}H}d^{x+e_H,\mathcal{C}H}$ and $\mathcal{C}H$ is the complement of H in the n-dimensional space. However, equation (46) leads instead to $d^{x,H}\tilde{\wedge}(*d^{x,H})=$

$d^{x-e_{CH},N}$, where the natural definition of $*$ is $*d^{x,H} = \epsilon_{H,\mathcal{C}H} d^{x-e_{CH},\mathcal{C}H}$. Using this naively in the inner product, we have

$$\begin{aligned}(\phi(x,H)d^{x,H}, \theta(x,H)d^{x,H}) &= \phi(x,H)\theta(x,H)d^{x,H}\tilde{\wedge}d^{x-e_{CH},\mathcal{C}H} \\ &= \phi(x,H)\theta(x,H)d^{x-e_{CH},N}\end{aligned}$$

This has the undesirable property that the field and the resulting n-form belong to different coordinates. So, whilst we have gained something in terms of locality with the exterior derivative, it would appear that we have lost something with the Hodge star and the inner product.

It might be possible to resolve this issue by modifying the inner product in such a way that the fields and resulting n-form have the same coordinate and that the inner product retains the same continuum limit. However, as it is not central to this thesis, we shall not pursue its development. The emphasis of this thesis is on work using the GD formalism.

B 4D Flavour Projection

In this appendix, we want to prove relationships between γ_5^T and the Hodge star and between $\spadesuit$ and $\gamma_1\gamma_2$. The notation for Z, $\mathcal{B}$, $\mathcal{A}$ and ρ follows on from the paper of Becher and Joos [45].

B.1 The Hodge Star and γ_5

In section 4.2, we saw that the differential description of the fermion fields was achieved by taking the product $\Phi(x) = \sum_{ab} \psi_b^{(b)} Z_{ab}$, where $\Phi(x)$ was a combination of differential forms, ψ was the 4×4 matrix, comprising Dirac spinors, and Z was a matrix of differential forms relating them.

In 4D, Z is defined as

$$Z = \sum_H (-1)^{\binom{h}{2}} \gamma_H^T dx^H$$

where dx^H denotes the various ordered differential forms of dimension h. We use Euclidean γ_μ and we have that $\gamma_5 = -\gamma_1\gamma_2\gamma_3\gamma_4$. From the definition for $\Phi(x)$, we can show that applying γ_5^T to the right hand side of Z is equivalent to applying γ_5 to the right hand side of $\psi(x)$ in the definition for $\Phi(x)$.

$$\begin{aligned} \left[\sum_H (-1)^{\binom{h}{2}} \gamma_H^T dx^H\right] \gamma_5^T &= -\left[\sum_H (-1)^{\binom{h}{2}} \gamma_H^T dx^H\right] \gamma_4^T \gamma_3^T \gamma_2^T \gamma_1^T \\ &= -\sum_H (-1)^{\binom{h}{2}} \rho_{1234,H} \gamma_{\mathcal{C}H}^T dx^H \\ &= -\sum_H (-1)^{\binom{4-h}{2}} \rho_{1234,\mathcal{C}H} \gamma_H^T dx^{\mathcal{C}H} \end{aligned} \tag{52}$$

where $\mathcal{C}H$ is the ordered complement of H and 4 is the dimension of the space. $\rho_{A,B}$ is defined to be equal to $(-1)^r$ where r is defined to be the number of pairs (a, b) with $a \in A$ and $b \in B$ where $a > b$.

When we apply the Hodge star to Z, we have

$$* \left[(-1)^{\binom{h}{2}} \gamma_H^T dx^H\right] = \sum_H (-1)^{\binom{h}{2}} \rho_{H,\mathcal{C}H} \gamma_H^T dx^{\mathcal{C}H} \tag{53}$$

By expanding the definition of $\binom{h}{2}$ and $\binom{4-h}{2}$, we can show that $(-1)^{\binom{4-h}{2}}(-1)^h = (-1)^{\binom{h}{2}}$. We can also show from the definition of $\rho_{A,B}$ that $\mathcal{B}dx^{\mathcal{C}H} = (-1)^{\binom{4-h}{2}} dx^{\mathcal{C}H} = \rho_{\mathcal{C}H,\mathcal{C}H} dx^{\mathcal{C}H}$ and that $\rho_{\mathcal{C}H,\mathcal{C}H} + \rho_{H,\mathcal{C}H} = \rho_{1234,\mathcal{C}H}$. Including these results, we have that

$$\mathcal{B} * \mathcal{A} \left[(-1)^{\binom{h}{2}} \gamma_H^T dx^H\right] = \sum_H (-1)^{\binom{4-h}{2}} \rho_{1234,\mathcal{C}H} \gamma_H^T dx^{\mathcal{C}H}$$

which is minus the last line of equation (52). Finally, we can take advantage of $(-1)^{\binom{4-h}{2}}(-1)^h = (-1)^{\binom{h}{2}}$ again to show that $\mathcal{B} * \mathcal{A} = *\mathcal{B}$ giving

$$- * \mathcal{B} Z = Z \gamma_5^T$$

Now we look at left multiplying Z by γ_5^T, which is the same as $\gamma_5 \psi(x)$ according to the definition for $\Phi(x)$.

$$\begin{aligned} \gamma_5^T \left[\textstyle\sum_H (-1)^{\binom{h}{2}} \gamma_H^T dx^H \right] &= -\gamma_4^T \gamma_3^T \gamma_2^T \gamma_1^T \left[\textstyle\sum_H (-1)^{\binom{h}{2}} \gamma_H^T dx^H \right] \\ &= -\textstyle\sum_H (-1)^{\binom{h}{2}} \rho_{H,1234} \gamma_{\mathcal{C}H}^T dx^H \\ &= -\textstyle\sum_H (-1)^{\binom{4-h}{2}} \rho_{\mathcal{C}H,1234} \gamma_H^T dx^{\mathcal{C}H} \end{aligned} \tag{54}$$

Using $\rho_{H,\mathcal{C}H} = (-1)^{h(4-h)} \rho_{\mathcal{C}H,H} = (-1)^h \rho_{\mathcal{C}H,H}$ and $(-1)^{\binom{4-h}{2}}(-1)^h = (-1)^{\binom{h}{2}}$, we can rewrite equation (53) as

$$* \left[(-1)^{\binom{h}{2}} \gamma_H^T dx^H \right] = \sum_H (-1)^{\binom{4-h}{2}} \rho_{\mathcal{C}H,H} \gamma_H^T dx^{\mathcal{C}H}$$

And finally taking advantage of $(-1)^{\binom{4-h}{2}} = \rho_{\mathcal{C}H,\mathcal{C}H}$ and $\rho_{\mathcal{C}H,H} + \rho_{\mathcal{C}H,\mathcal{C}H} = \rho_{\mathcal{C}H,1234}$, we have

$$\mathcal{B} * \left[\sum_H (-1)^{\binom{h}{2}} \gamma_H^T dx^H \right] = \sum_H (-1)^{\binom{4-h}{2}} \rho_{\mathcal{C}H,1234} \gamma_H^T dx^{\mathcal{C}H}$$

which is minus the last line of equation (54). Because $(-1)^{\binom{4-h}{2}} = (-1)^{\binom{h}{2}}(-1)^h$, we can rewrite $\mathcal{B}*$ as $*\mathcal{B}\mathcal{A}$ giving

$$- * \mathcal{B}\mathcal{A} Z = \gamma_5^T Z$$

B.2 $\gamma_1\gamma_2$ and ♠

We are only interested in the right application of $\gamma_1\gamma_2$ to $\psi(x)$, because $\gamma_1\gamma_2$ is used only in the context of flavour separation.

$$\begin{aligned} \left[\textstyle\sum_H (-1)^{\binom{h}{2}} \gamma_H^T dx^H \right] \gamma_2^T \gamma_1^T &= \textstyle\sum_H (-1)^{\binom{h}{2}} \rho_{12,H_{12}} \gamma_{(\mathcal{C}H_{12})H_{34}}^T dx^H \\ &= \textstyle\sum_H (-1)^{\binom{2-h_{12}}{2}+h_{34}} \rho_{12,\mathcal{C}H_{12}} \gamma_H^T dx^{(\mathcal{C}H_{12})H_{34}} \end{aligned} \tag{55}$$

where we have split H into $H_{12}H_{34}$, H_{12} containing all the components of H in the $\{1,2\}$ subspace and H_{34} containing all the components in the $\{3,4\}$ subspace. Our

operator $\spadesuit$ is defined through

$$\spadesuit\left[\sum_H (-1)^{\binom{h}{2}}\gamma_H^T dx^H\right] = \sum_H (-1)^{\binom{h}{2}}\rho_{H_{12},\mathcal{C}H_{12}}\gamma_H^T dx^{(\mathcal{C}H_{12})H_{34}}$$

To complete the relationship, we define the operators $\mathcal{B}_{12}dx^H = (-1)^{\binom{h_{12}}{2}}dx^H = \rho_{H_{12},H_{12}}dx^H$ where h_{12} is the dimension of H_{12} and $\mathcal{A}_{12}dx^H = (-1)^{h_{12}}dx^H$. We can show that $(-1)^{\binom{h_{12}+h_{34}}{2}} = -(-1)^{h_{12}}(-1)^{\binom{2-h_{12}+h_{34}}{2}}$ which gives us

$$-\spadesuit\mathcal{A}_{12}\left[(-1)^{\binom{h}{2}}\gamma_H^T dx^H\right] = \sum_H (-1)^{\binom{2-h_{12}+h_{34}}{2}}\rho_{H_{12},\mathcal{C}H_{12}}\gamma_H^T dx^{(\mathcal{C}H_{12})H_{34}}$$

Finally we have that,

$$-\mathcal{B}_{12}\spadesuit\mathcal{A}_{12}\left[(-1)^{\binom{h}{2}}\gamma_H^T dx^H\right] = \sum_H (-1)^{\binom{2-h_{12}+h_{34}}{2}}\rho_{12,\mathcal{C}H_{12}}\gamma_H^T dx^{(\mathcal{C}H_{12})H_{34}}$$

which is the same as the last line of equation (55). We note that we can write $-\mathcal{B}_{12}\spadesuit\mathcal{A}_{12}$ as $\spadesuit\mathcal{B}_{12}$

B.3 Flavour Commutation Relations

The flavour projection operators are defined to be

$$P^{(b)} = \frac{1}{4}(1 + i\alpha_b\spadesuit\mathcal{B}_{12})(1 + \beta_b * \mathcal{B})$$

To show that the Dirac-Kähler operator commutes with this expression, we must show that it commutes with each of the operators $*\mathcal{B}$ and $\spadesuit\mathcal{B}_{12}$. All that differs between the complex and the continuum formulations is the domain of integration, which we have addressed in the body of the thesis, so it is enough to show that they commute in the continuum.

Starting with the former

$$[d - \delta, *\mathcal{B}]\, f(x)dx^H = [dx^\mu \vee \partial_\mu, *\mathcal{B}]\, f(x)dx^H = (\partial_\mu f(x))\, [dx^\mu\vee, *\mathcal{B}]\, dx^H$$

So we need to prove that $dx^\mu \vee *\mathcal{B}dx^H = *\mathcal{B}(dx^\mu \vee dx^H)$. The left hand side is

$$\rho_{H,\mathcal{C}H}(-1)^{\binom{h}{2}}\rho_{\mu,\mathcal{C}H}(dx^{\mathcal{C}H\cup\mu} + dx^{\mathcal{C}H/\mu})$$

The right hand side is

$$\rho_{\mu,H}\left((-1)^{\binom{h-1}{2}}\rho_{H/\mu,\mathcal{C}H\cup\mu}dx^{\mathcal{C}H\cup\mu}+(-1)^{\binom{h+1}{2}}\rho_{H\cup\mu,\mathcal{C}H/\mu}dx^{\mathcal{C}H/\mu}\right)$$

where $\mathcal{C}$ denotes complementarity in 4D.

In the case where $\mu \in H$, we relate the two terms containing $dx^{\mathcal{C}H\cup\mu}$. If they are equivalent, then we have

$$\rho_{H,\mathcal{C}H}(-1)^{\binom{h}{2}}\rho_{\mu,\mathcal{C}H}=\rho_{\mu,H}(-1)^{\binom{h-1}{2}}\rho_{H/\mu,\mathcal{C}H\cup\mu}$$

An expansion of $\binom{h-1}{2}$ gives $(-1)^{\binom{h-1}{2}}=(-1)^{\binom{h}{2}}(-1)^{1-h}$. The equality becomes

$$\begin{aligned}\rho_{H,\mathcal{C}H}\rho_{\mu,\mathcal{C}H} &= \rho_{\mu,H}(-1)^{h+1}\rho_{H/\mu,\mathcal{C}H\cup\mu}\\ &= \rho_{\mu,H}(-1)^{h+1}\rho_{H,\mathcal{C}H\cup\mu}\rho_{\mu,\mathcal{C}H\cup\mu}\\ &= \rho_{\mu,H}(-1)^{h+1}\rho_{H,\mathcal{C}H}\rho_{H,\mu}\rho_{\mu,\mathcal{C}H\cup\mu}\\ &= \rho_{\mu,H}(-1)^{h+1}\rho_{H,\mathcal{C}H}\rho_{H,\mu}\rho_{\mu,\mathcal{C}H}\rho_{\mu,\mu}\end{aligned}$$

We know that $\rho_{\mu,\mu}=1$ and we can factor out some of the terms to reach

$$1=\rho_{\mu,H}(-1)^{h+1}\rho_{H,\mu}$$

When $\mu \in H$, we have that $\rho_{\mu,H}\rho_{H,\mu}=(-1)^{h-1}$ and so the right hand side equals 1.

For the case where $\mu \notin H$, we must compare the coefficients from the terms containing $dx^{\mathcal{C}H/\mu}$. We want to prove the equivalence of

$$\rho_{H,\mathcal{C}H}(-1)^{\binom{h}{2}}\rho_{\mu,\mathcal{C}H}=(-1)^{\binom{h+1}{2}}\rho_{H\cup\mu,\mathcal{C}H/\mu}\rho_{\mu,H}$$

By expanding $\binom{h+1}{2}$, we can show that $(-1)^{\binom{h+1}{2}}=(-1)^{\binom{h}{2}}(-1)^{h}$. The equality is now

$$\begin{aligned}\rho_{H,\mathcal{C}H}\rho_{\mu,\mathcal{C}H} &= (-1)^{h}\rho_{H\cup\mu,\mathcal{C}H/\mu}\rho_{\mu,H}\\ &= (-1)^{h}\rho_{H,\mathcal{C}H/\mu}\rho_{\mu,\mathcal{C}H/\mu}\rho_{\mu,H}\\ &= (-1)^{h}\rho_{H,\mathcal{C}H}\rho_{H,\mu}\rho_{\mu,\mathcal{C}H/\mu}\rho_{\mu,H}\\ &= (-1)^{h}\rho_{H,\mathcal{C}H}\rho_{H,\mu}\rho_{\mu,\mathcal{C}H}\rho_{\mu,\mu}\rho_{\mu,H}\end{aligned}$$

Using $\rho_{\mu,\mu}=1$, we can simplify the equality to

$$1=(-1)^{h}\rho_{H,\mu}\rho_{\mu,H}$$

When $\mu \notin H$, we have that $\rho_{H,\mu}\rho_{\mu,H} = (-1)^h$, which completes the proof of the commutation of $*\mathcal{B}$ with $d - \delta$.

For the second operator, we proceed in a similar fashion. We want to prove that

$$dx^\mu \vee \spadesuit\mathcal{B}_{12}dx^H = \spadesuit\mathcal{B}_{12}dx^\mu \vee dx^H \tag{56}$$

It is easiest to divide this proof into two halves. In the first, we will assume that $\mu \in \{1,2\}$. In the second, we will assume that $\mu \in \{3,4\}$.

When $\mu \in \{1,2\}$, the left hand side of equation (56) is

$$(-1)^{\binom{h_{12}}{2}}\rho_{H_{12},\mathcal{C}H_{12}}\rho_{\mu,\mathcal{C}H_{12}}\left(dx^{\mathcal{C}H_{12}H_{34}\cup\mu} + dx^{\mathcal{C}H_{12}H_{34}/\mu}\right)$$

The right hand side is

$$\rho_{\mu,H_{12}}\left((-1)^{\binom{h_{12}+1}{2}}\rho_{H_{12}\cup\mu,\mathcal{C}H_{12}/\mu}dx^{\mathcal{C}H_{12}H_{34}/\mu} + (-1)^{\binom{h_{12}-1}{2}}\rho_{H_{12}/\mu,\mathcal{C}H_{12}\cup\mu}dx^{\mathcal{C}H_{12}H_{34}\cup\mu}\right)$$

Comparing the cases where $\mu \in H_{12}$, we want to check that the following equality holds true.

$$\rho_{\mu,H_{12}}(-1)^{\binom{h_{12}-1}{2}}\rho_{H_{12}/\mu,\mathcal{C}H_{12}\cup\mu} = (-1)^{\binom{h_{12}}{2}}\rho_{H_{12},\mathcal{C}H_{12}}\rho_{\mu,\mathcal{C}H_{12}}$$

By expanding $\binom{h_{12}-1}{2}$, we can show that $(-1)^{\binom{h_{12}-1}{2}} = (-1)^{\binom{h_{12}}{2}}(-1)^{1-h_{12}}$. Inserting this (and swapping left for right), we have for the equality

$$\rho_{H_{12},\mathcal{C}H_{12}}\rho_{\mu,\mathcal{C}H_{12}} = \rho_{\mu,H_{12}}(-1)^{1-h_{12}}\rho_{H_{12}/\mu,\mathcal{C}H_{12}\cup\mu}$$

We can rearrange some of the terms on the right as follows

$$\begin{aligned}\rho_{H_{12},\mathcal{C}H_{12}}\rho_{\mu,\mathcal{C}H_{12}} &= \rho_{\mu,H_{12}}(-1)^{1-h_{12}}\rho_{H_{12},\mathcal{C}H_{12}\cup\mu}\rho_{\mu,\mathcal{C}H_{12}\cup\mu} \\ &= \rho_{\mu,H_{12}}(-1)^{1-h_{12}}\rho_{H_{12},\mu}\rho_{H_{12},\mathcal{C}H_{12}}\rho_{\mu,\mathcal{C}H_{12}}\rho_{\mu,\mu}\end{aligned}$$

We can use $\rho_{\mu,\mu} = 1$ and factor out some common terms to reduce the expression to

$$1 = \rho_{\mu,H_{12}}(-1)^{1-h_{12}}\rho_{H_{12},\mu}$$

In the case where $\mu \in H_{12}$, we have that $\rho_{\mu,H_{12}}\rho_{H_{12},\mu} = (-1)^{h_{12}-1}$, so the equivalence holds.

For $\mu \in \mathcal{C}H_{12}$, the equivalence that we are seeking to prove is

$$\rho_{\mu,H_{12}}(-1)^{\binom{h_{12}+1}{2}}\rho_{H_{12}\cup\mu,\mathcal{C}H_{12}/\mu} = (-1)^{\binom{h_{12}}{2}}\rho_{H_{12},\mathcal{C}H_{12}}\rho_{\mu,\mathcal{C}H_{12}}$$

We can show that $(-1)^{\binom{h_{12}+1}{2}} = (-1)^{\binom{h_{12}}{2}}(-1)^{h_{12}}$, which reduces this expression to (again, we swap left and right hand sides)

$$\rho_{H_{12},\mathcal{C}H_{12}}\rho_{\mu,\mathcal{C}H_{12}} = \rho_{\mu,H_{12}}(-1)^{h_{12}}\rho_{H_{12}\cup\mu,\mathcal{C}H_{12}/\mu}$$

After further expansion, we have

$$\begin{aligned}
\rho_{H_{12},\mathcal{C}H_{12}}\rho_{\mu,\mathcal{C}H_{12}} &= \rho_{\mu,H_{12}}(-1)^{h_{12}}\rho_{H_{12},\mathcal{C}H_{12}/\mu}\rho_{\mu,\mathcal{C}H_{12}/\mu} \\
&= \rho_{\mu,H_{12}}(-1)^{h_{12}}\rho_{H_{12},\mathcal{C}H_{12}}\rho_{H_{12},\mu}\rho_{\mu,\mathcal{C}H_{12}/\mu} \\
&= \rho_{\mu,H_{12}}(-1)^{h_{12}}\rho_{H_{12},\mathcal{C}H_{12}}\rho_{H_{12},\mu}\rho_{\mu,\mathcal{C}H_{12}}\rho_{\mu,\mu}
\end{aligned}$$

Using $\rho_{\mu,\mu} = 1$ and cancelling some common expressions, this becomes

$$1 = \rho_{\mu,H_{12}}(-1)^{h_{12}}\rho_{H_{12},\mu}$$

Because $\mu \in \mathcal{C}H_{12}$, we have $\rho_{\mu,H_{12}}\rho_{H_{12},\mu} = (-1)^{h_{12}}$, so this equivalence holds.

In the case where $\mu \in \{3,4\}$, for the left hand side of equation (56) we have

$$(-1)^{\binom{h_{12}}{2}}\rho_{H_{12},\mathcal{C}H_{12}}\rho_{\mu,(\mathcal{C}H_{12})H_{34}}\left(dx^{(\mathcal{C}H_{12})H_{34}\cup\mu} + dx^{(\mathcal{C}H_{12})H_{34}/\mu}\right)$$

For the right hand side, we have

$$(-1)^{\binom{h_{12}}{2}}\rho_{\mu,H_{12}H_{34}}\rho_{H_{12}\mathcal{C}H_{12}}\left(dx^{(\mathcal{C}H_{12})H_{34}/\mu} + dx^{\mathcal{C}H_{12}H_{34}\cup\mu}\right)$$

If we equate the coefficients for the case $\mu \in H_{34}$, we have

$$\rho_{\mu,H_{12}H_{34}}(-1)^{\binom{h_{12}}{2}}\rho_{H_{12},\mathcal{C}H_{12}} = (-1)^{\binom{h_{12}}{2}}\rho_{H_{12}\mathcal{C}H_{12}}\rho_{\mu,\mathcal{C}H_{12}H_{34}}$$

which simplifies to

$$\rho_{\mu,H_{12}H_{34}} = \rho_{\mu,\mathcal{C}H_{12}H34}$$

In the case where $\mu \in \{3,4\}$, it is the case that $\rho_{\mu,H_{12}} = \rho_{\mu,\mathcal{C}H_{12}}$, so we can equate these two terms. An identical argument follows for the case $\mu \in \mathcal{C}H_{34}$.

C Mathematical Identities

Here, we prove the identity in equation (39).

$$\begin{aligned}
\frac{\partial}{\partial \tilde{A}(l,\tau)} \ln \sqrt{\det(M^\dagger M)} &= \frac{1}{2} \frac{\partial}{\partial \tilde{A}(l,\tau)} \ln \left(\det(M^\dagger M)\right) \\
&= \frac{1}{2} \mathrm{Tr} \frac{\partial}{\partial \tilde{A}(l,\tau)} \left(\ln \left(M^\dagger M\right)\right) \\
&= \frac{1}{2} \mathrm{Tr}, \left((M^\dagger M)^{-1} \frac{\partial}{\partial \tilde{A}(l,\tau)} (M^\dagger M)\right) \\
&= \frac{1}{2} \mathrm{Tr} \left((M^\dagger M)^{-1} \frac{\partial M^\dagger}{\partial \tilde{A}(l,\tau)} M\right) + \frac{1}{2} \mathrm{Tr} \left((M^\dagger M)^{-1} M^\dagger \frac{\partial M}{\partial \tilde{A}(l,\tau)}\right) \\
&= \frac{1}{2} \mathrm{Tr} \left(M^{-1} M^{\dagger -1} \frac{\partial M^\dagger}{\partial \tilde{A}(l,\tau)} M\right) + \frac{1}{2} \mathrm{Tr} \left(M^{-1} M^{\dagger -1} M^\dagger \frac{\partial M}{\partial \tilde{A}(l,\tau)}\right) \\
&= \frac{1}{2} \mathrm{Tr} \left(M^{\dagger -1} \frac{\partial M^\dagger}{\partial \tilde{A}(l,\tau)}\right) + \frac{1}{2} \mathrm{Tr} \left(M^{-1} \frac{\partial M}{\partial \tilde{A}(l,\tau)}\right) \\
&= \frac{1}{2} \mathrm{Tr} \left(\frac{\partial M^*}{\partial \tilde{A}(l,\tau)} M^{*-1}\right) + \frac{1}{2} \mathrm{Tr} \left(M^{-1} \frac{\partial M}{\partial \tilde{A}(l,\tau)}\right) \\
&= \frac{1}{2} \mathrm{Tr} \left(M^{*-1} \frac{\partial M^*}{\partial \tilde{A}(l,\tau)}\right) + \frac{1}{2} \mathrm{Tr} \left(M^{-1} \frac{\partial M}{\partial \tilde{A}(l,\tau)}\right) \\
&= Re \left(\mathrm{Tr} \left(M^{-1} \frac{\partial M}{\partial \tilde{A}(l,\tau)}\right)\right)
\end{aligned}$$

where we have made use of the properties $\mathrm{Tr}\,(ABC) = \mathrm{Tr}\,(CAB)$ and $\mathrm{Tr}\left(A^T\right) = \mathrm{Tr}\,(A)$.

References

[1] S Chandrasekharan, Phys Rev D **60**, 074503 (1999), hep-lat/9805015

[2] J Kogut and L Susskind, Phys Rev D **11**, 395 (1975)

[3] T Banks, J Kogut and L Susskind, Phys Rev D **13**, 1043 (1976)

[4] L Susskind, Phys Rev D **16**, 3031 (1977)

[5] D H Adams, Phys Rev Lett **78**, 4155 (1997), hep-th/9704150

[6] D H Adams, hep-th/9612009

[7] J M Rabin, Nucl Phys B **201**, 315 (1982)

[8] Discrete exterior calculus with applications to flows and spinors, PhD Thesis, Vivien de Beaucé, 2004

[9] Extending Geometric Discretization, PhD Thesis, Samik Sen, 2001

[10] S Duane, A D Kennedy, B J Pendleton, D Roweth, Phys Lett B **195**, 216 (1987)

[11] W Lucha, F F Schoberl and D Gromes, Phys Rep **200**, 127 (1991)

[12] S Watterson and J Sexton, PoS LAT2005 **277** (2006), hep-lat/0510052

[13] W Thirring, Ann Phys **3**, 91 (1958)

[14] J S Schwinger, Phys Rev **128**, 2425 (1962)

[15] Quantum Field Theory, F Mandl & G Shaw, John Wiley & Sons (1993)

[16] Quantum Field Theory: A Modern Introduction, M Kaku, Oxford University Press (1993)

[17] Relativistic Quantum Mechanics, J Bjorken & S D Drell, McGraw-Hill education (1964)

[18] K G Wilson, Phys Rev D **10**(8), 2445 (1974)

[19] Lattice Gauge Theories: An Introduction, Heinz J Rothe, 2ed, World Scientific (1998)

[20] R Gupta, *Scaling, the Renormalization Group and Improved Lattice Actions*, Quantum Fields on the Computer, ed Michael Creutz, World Scientific (1992)

[21] Gauge Theory of Elementary Particle Physics, T P Cheng and L F Li, Oxford Science Publications (1984)

[22] Quantum Fields on the Computer, ed Michael Creutz, World Scientific (1992)

[23] R Gupta, Les Houches 1997, Probing the Standard Model of Particle Interactions Pt 2, 83, hep-lat/9807028

[24] H B Nielsen and M Ninomiya, Nuclear Physics B **185**, 20 (1981)

[25] H B Nielsen and M Ninomiya, Nuclear Physics B **193**, 173 (1981)

[26] S D Drell, M Weinstein and S Yankielowicz, Phys Rev D **14**, 1627 (1976)

[27] J P Costella, hep-lat/0207008

[28] D B Kaplan, Phys Lett B **288**, 342 (1992), hep-lat/9206013

[29] C G Callan Jr and J A Harvey, Nucl Phys B **250**, 427 (1985)

[30] V Furman and Y Shamir, Nucl Phys B **439**, 54 (1995), hep-lat/9405004

[31] K Hashimoto et al, Proc Sci (Lattice 2005), **093**, hep-lat/0510079

[32] D Galletley *et al*, Proc Sci (Lattice 2005), **363**, hep-lat/0510050

[33] P H Ginsparg and K G Wilson, Phys Rev D **25**, 2649 (1982)

[34] A Borici, Nucl Phys Proc Suppl **83**, 771 (2000), hep-lat/9909057

[35] A Borici, Dubna 1999 - Lattice Fermions and structure of the vacuum,41 (1999), hep-lat/9912040

[36] A P Balachandran, S Vaidya, Int J Mod Phys A **16**, 17 (2001), hep-th/9910129

[37] A P Balachandran, T R Govindarajan and B Ydri, Mod Phys Lett A **15**, 1279 (2000), hep-th/9911087

[38] A P Balachandran, X Martin and D O'Connor, Int J Mod Phys A **16**, 2577 (2001), hep-th/0007030

[39] J Medina, W Bietenholz, F Hofheinz and D O'Connor, Proc Sci (Lattice 2005), **263**, hep-lat/0509162

[40] S Hands, Phys Lett B **195**, 448 (1987)

[41] S Hands and R D Kenway, Nucl Phys B **276**, 429 (1986)

[42] Differential Forms with Applications to the Physical Sciences, H Flanders, Dover Publications (1989)

[43] Differential Forms and Connections, R W R Darling, Cambridge University Press (1994)

[44] E Kähler, Rend Mat Ser V **21**, 425 (1962)

[45] P Becher and H Joos, Z Phys C **15**, 343 (1982)

[46] H Neuberger, Phys Lett B **417**, 141 (1998), hep-lat/9707022

[47] H Neuberger, Phys Lett B **427**, 353 (1998), hep-lat/9801031

[48] H Neuberger, Phys Rev D **57**, 5417 (1998), hep-lat/9710089

[49] R Narayanan and H Nerberger, Nucl Phys B **443**, 305 (1995), hep-th/9411108

[50] R Narayanan and H Neuberger, Nucl Phys B **412**, 574 (1994), hep-lat/9307006

[51] S O Wilson, math.GT/0505227

[52] I Kanamori and N Kawamoto, Nucl Phys Proc Suppl **129**, 877 (2004), hep-lat/0309120

[53] I Kanamori and N Kawamoto, Int J Mod Phys A **19**, 695 (2004), hep-th/0305094

[54] N Kawamoto, T Tsukioka and H Umetsu, Int J Mod Phys A **16**, 3867 (2001), hep-th/0010254

[55] A Dimakis, F Müller-Hoissen and T Striker, J Phys A **26**, 1927 (1993)

[56] A Dimakis, F Müller-Hoissen and T Striker, Phys Lett B **300**, 141 (1993)

[57] A Dimakis and F Müller-Hoissen, J Phys A **27**, 3159 (1994)

[58] Some Aspects of Topological Field Studies, PhD Thesis, David H Adams, 1997

[59] D Adams, hep-th/9612009

[60] D Adams, Phys Rev Lett **78**, 4155 (1997), hep-th/9704150

[61] D Adams, Sa Sen, Si Sen and J Sexton, Nucl Phys Proc Suppl **63**, 492 (1998)

[62] V de Beaucé and Sa Sen, hep-th/0305125

[63] V de Beaucé, Sa Sen and J C Sexton, Nucl Phys Proc Suppl **129**, 468, hep-lat/0309167

[64] V de Beaucé and Si Sen, hep-th/0403206

[65] S Sen, hep-th/0307166

[66] Sa Sen, Si Sen, J Sexton and D Adams, Phys Rev E **61**, 3174 (2000), hep-th/0001030

[67] V de Beaucé, PoS LAT2005 **276** (2006), hep-lat/0510028

[68] V de Beaucé and Si Sen, hep-th/0610065

[69] B Czech, hep-th/0701263

[70] K Fujikawa, Phys Rev Lett **42**, 1979 (1979)

[71] J Smit and J C Vink, Nucl Phys B **286**, 485 (1987)

[72] P Vranas, Phys Rev D **57**, 1415 (1998), hep-lat/9705023

[73] F Maresca and M Peardon, hep-lat/0411029

[74] K E Cahill, Phys Lett B **304**, 307 (1993), hep-lat/9301010

[75] K E Cahill, Phys Lett B **365**, 239 (1996), hep-lat/9805010

[76] M Gockeler *et al*, Nucl Phys B **487**, 313 (1997), hep-lat/9605035

[77] R Fiore, P Giudice, D Giuliano, D Marmottini, A Papa and P Sodano, Proc Sci (Lattice 2005), **243**, hep-lat/0509183

[78] R Fiore, P Giudice, D Giuliano, D Marmottini, A Papa and P Sodano, Phys Rev D **72**, 094508 (2005), Erratum-ibid D **72**: 119902 (2005), Erratum-ibid D **72**: 119905 (2005), hep-lat/0506020

[79] Trinity Centre for High Performance Computing, Lloyd Building, Trinity College, Dublin. http://www.tchpc.tcd.ie

[80] Parallel Computer Centre, Queens University Belfast, 7 College Park East, Belfast. http://www.pcc.qub.ac.uk

[81] J H Lowenstein and J A Swieca, Ann Phys **68**, 172 (1971)

[82] N S Manton, Ann Phys **159**, 220 (1985)

[83] J B Kogut and L Susskind, Phys Rev D **11**, 3594 (1975)

[84] S Coleman, Ann Phys **101**, 239 (1976)

[85] S Iso and H Murayama, Prog Theor Phys **84**, 142 (1990)

[86] H Dilger, Nucl Phys B **434**, 321 (1995)

[87] H Joos and S I Azakov, Helv Phys Acta **67**, 723 (1994)

[88] J Potvin, Phys Rev D **32**, 2070 (1985)

[89] A C Irving and J C Sexton, Nucl Phys Proc Suppl **47**, 679 (1996), hep-lat/9508032

[90] H Neuberger, Phys Rev D **63**, 014503, 2001, hep-lat/0002032

[91] D H Adams, hep-lat/0411030

[92] L Del Debbio, H Panagopoulos and E Vicari, JHEP **0409**, 028 (2004), hep-th/0407068

[93] H Dilger, Int J Mod Phys C **6**, 123 (1995), hep-lat/9408017

[94] A Sokal, Monte Carlo Methods in Statistical Mechanics: Foundations and New Algorithms, in Cours de Troisième Cycle de la Physique en Suisse Romande (Lausanne, June 1989)

[95] T Draper, C Nenkov and M Peardon, Nucl Phys Proc Suppl **53**, 997 (1997)

[96] B Jegerlehner, Nucl Phys B **465**, 487 (1996)